2013

Optimization of biomass fast pyrolysis for the production of monomers

Dustin Lee Dalluge
Iowa State University

Optimization of biomass fast pyrolysis for the production of monomers

by

Dustin Lee Dalluge

A dissertation submitted to the graduate faculty

in partial fulfillment of the requirements for the degree of

DOCTOR OF PHILOSOPHY

Co-Majors: Mechanical Engineering; Biorenewable Resources and Technology

Program of Study Committee:
Robert Brown, Major Professor
Song-Charng Kong
Terry Meyer
Laura Jarboe
Young-Jin Lee

Iowa State University
Ames, Iowa
2013

DEDICATION

To my parents, Steve and Jane Dalluge. For all of their love, support, and time dedicated to making me who I am and inspiring me to always do my best.

NOMENCLATURE

AAEM – Alkali and alkaline earth metal

BFB – Bubbling Fluidized Bed

DI – Deionized (water)

FID – Flame Ionization Detector

GC – Gas Chromatography

HPLC – High Performance Liquid Chromatography

NCG – Non-condensable gas

MMB-Moles of Side Chain per Mole of Benzene Moiety

MS-Mass Spectrometer

PY - Micropyrolyzer

SLPM – Standard Liters per Minute

SF# - Stage Fraction (numbered according to position in the system)

TABLE OF CONTENTS

ACKNOWLEDGEMENTS

I would like to express my deepest gratitude to my major professor, Dr. Robert C. Brown, for the opportunities, guidance, mentorship, and wisdom. The dynamics of Dr. Brown's group and abundance of opportunities have provided an excellent research environment, which has helped my research career to thrive.

I would also like to thank my graduate committee consisting of Dr. Song-Charng Kong, Dr. Terry Meyer, Dr. Laura Jarboe, and Dr. Young-Jin Lee. Numerous discussions about research projects and the feedback provided during my qualifiers and preliminary exam helped guide me to complete this work.

I am grateful to the Phillips 66 Company and the United States Department of Energy for their generous funding of my research projects. I'm also thankful for all of their discussions and feedback throughout the process of completing these projects

I am very thankful for all the help, guidance, and discussions with staff at the Center for Sustainable Environmental Technologies (CSET), in particular Ryan Smith, Patrick Johnston, Marjorie Rover, Xianglan Bai, and Lysle Whitmer. I would also like to thank previous CSET staff members Sam Jones, Justinus Satrio, Sunitha Sadula, Doug Bull, and Satya Jujjuri for all of their help and guidance in the beginning of my research career.

I would also like to thank the many faculty and staff at Iowa State University who have offered me a tremendous amount of guidance and direction throughout my

time at Iowa State. In particular I would like to thank the Directors of Graduate Education from both the Mechanical Engineering Department and Biorenewable Resources and Technology Program, Dr. Pranav Shrotria and Dr. Jackie Baughman. I would also like to thank the Department of Mechanical Engineering staff for help on so many occasions, in particular Amy Carver and Deborah Schroeder.

I would like to thank Dr. Jackie Baughman, Dr. Tristan Brown, and Dr. Raj Raman for the opportunity to assist with teaching several sections of the BRT 501 class. The opportunity to teach a portion of a graduate level course really helped me to reflect on my communication skills and test my own knowledge.

I am grateful to all of my colleagues at CSET for all of the valuable discussions and help with completion of projects. I would especially like to thank Jared Brown, Cody Ellens, Randy Kasperbauer, Mark Mba Wright, Pushkaraj Patwardhan, AJ Sherwood-Pollard, and Lysle Whitmer who were senior members of the group at the time I started and helped to lay the foundation for my research. I'm also thankful to the many colleagues that I was fortunate to meet and work with throughout my time at CSET, including: Catie Brewer, Karl Broer, Yong Choi, Nick Creager, Tannon Daugaard, Bernardo Del Campo, Kwang Ho Kim, Najeeb Kuzhiyil, Kaige Wang, and Patrick Woolcock. The discussions and friendships were much appreciated.

I was fortunate to have the assistance of several very talented undergraduate research assistants throughout my time at Iowa State. I am especially grateful to Jordan Donner, Ben Franzen, Preston Gable, Robbie Hable, Nate Hamlett, Trevor Heithoff, Eric Larson, Steven Laskowski, Nick Miller, William Paisley, Chris Quinnett, John Sievert,

and Sean Smith. Without their assistance and dedication, much of this work would not have been possible.

I've also had the privilege and opportunity to work with numerous other groups and collaborators at Iowa State that have resulted in several co-authored papers. In particular I have had a multitude of discussion with Dr. Young-Jin Lee and several of his group members, including Carolyn Hutchinson, Paul Cole, and my wife Erica Dalluge (Smith). Their wealth of knowledge has helped me to learn so much about many of the analytical techniques necessary for this work and further applications of analytical techniques to my own work.

I would like to extend my gratitude to the many friends, mentors, and teachers that helped me through my first few years in the engineering program at North Iowa Area Community College (NIACC). The small class sizes, knowledgeable staff, and affordability of NIACC really gave me a good start before finishing up my B.S. at Iowa State.

I would also like to thank all my teachers and mentors throughout grade school at St. Ansgar Community Schools, in particular Devin Schwiesow, Susan LeMaster, and Cindy Fell, who helped me to develop my interests, scientific foundation, and the discipline necessary to do this work.

I would also like to greatly thank all my family and friends. My parents, Steve and Jane Dalluge, have been the most influential to me in encouraging me to always do my best, to inspire me to go after things I love, and who helped me develop the work ethic that has made this work possible. My siblings, Zach, Sara, and Sawyer have also

been great inspiration to me and have helped me to want to set a good example for them and show them what is possible if they put their mind to it. My grandparents, Larry and Carol Dalluge and Ruth Hollatz, have also been a major influence in my life. Their loving words and encouragement have helped me to get to where I am.

My wife, Erica, really deserves a big thank you. Her love, encouragement, and time throughout the process, while she was still working on her own dissertation, have been very much appreciated.

I would also like to thank all of my friends, old and new, who have stuck with me throughout my graduate career. I'd like to thank them for the time spent outside of work de-stressing and for understanding the times I wasn't able to spend with them while I have been working on my dissertation.

Lastly, I would like to thank God for blessing me with the skills necessary to complete this work. I thank Him for unveiling to me a small portion of His creation and I pray that I might better understand it and use it to serve His will. "For what can be known about God is plain to them, because God has shown it to them. For His invisible attributes, namely, His eternal power and divine nature, have been clearly perceived, ever since the creation of the world, in the things that have been made. So they are without excuse." Romans 1:19-20 ESV

ABSTRACT

Fast pyrolysis is a promising method for producing advanced biofuels and chemicals from lignocellulosic biomass. The process will however require further optimization to produce fuels and chemicals at a price competitive to conventional fossil fuel-derived products. Research in this dissertation focuses on both pre- and post-processes for optimizing fast pyrolysis to produce increased yields of valuable anhydrosugars and phenolic monomers.

The concept of alkali and alkaline earth metal (AAEM) passivation using sulfuric acid had only previously been demonstrated in batch micropyrolyzer trials. A bench-scale, continuous-flow auger pyrolyzer was used in this work to demonstrate AAEM passivation on both woody and herbaceous feedstocks. Passivation of AAEMs in red oak and switchgrass increased total sugars by more than 105% and 260%, respectively. Light oxygenates simultaneously decreased by nearly 50% from each feedstock. The synchronous increase in sugars and decrease in light oxygenates provides evidence of the hypothesis that AAEM passivation prevents pyranose ring fragmentation and promotes glycosidic bond cleavage in holocellulose. An undesirable consequence of AAEM passivation was an increase in biochar from both lignin and carbohydrates. Demonstration of the enhanced production of sugars from AAEM passivated feedstocks in a continuous auger pyrolyzer at the kilogram scale is an important step in determining the feasibility of using fast pyrolysis to produce sugars from lignocellulosic biomass.

Lignin-derived biochar increased from AAEM passivated feedstocks which led to suspicions that thermally active AAEMs catalyze lignin pyrolysis. Effect of thermally active AAEMs on lignin pyrolysis was therefore investigated in more detail. Experimental results indicated that sodium was the most active AAEM on lignin pyrolysis in which it increased overall volatile aromatic monomers by over 16% compared to the control. Alkali metals as a group both increased char and decreased alkenyl side chains amongst volatile aromatics. Alkenyl side chains are known to result from the cleavage of certain bonds within the lignin structure. Therefore AAEMs are predicted to catalyze the cleavage of linkages within the lignin structure during pyrolysis.

The rate at which pyrolysis vapors are cooled in bio-oil collection equipment has been noted to have an influence on bio-oil composition, however prior to this research has never been quantified. A novel cold-gas quench system was developed that utilizes liquid nitrogen to quickly quench pyrolysis products, which produced a more than seven fold increase in cooling rate compared to a conventional shell and tube condenser. The increased cooling rate and elimination of radial temperature gradients in the quench system increased levoglucosan yield from cellulose by 23% compared to the conventional system.

CHAPTER 1

GENERAL INTRODUCTION

Biomass as an Energy Source

Renewable energy and sustainable energy production are top priorities for the nation to help provide national, economic, and environmental security. Biomass is renewable in that it can be regrown on an annual basis anywhere water, soil, nutrients and sun light are available. Similar to other renewable energy sources, biomass utilizes solar energy as its primary energy source. Biomass however offers the distinct advantage of storing captured solar energy in chemical bonds, whereas many of the other renewable energy technologies generate electricity for immediate use.

In 2011 the United States imported approximately 45% of its annual petroleum supply [1] from which petroleum accounted for more than 36% of total U.S. energy consumption [2]. Dependence on such imports puts the U.S. at great economic disadvantage. In 2011 alone the U.S. imported more than 4.165 billion barrels of petroleum at a total cost of $421.4 billion [3]. Many of the countries from which petroleum is imported are not friendly to the U.S. and payment to them may be in direct disinterest to national security. Retaining assets domestically could also provide a major boost to the U.S. economy in terms of both sales and job growth within both the energy and agricultural sectors.

The U.S. Department of Energy's *Billion Ton Study* looked at scenarios from which the U.S. could produce up to one billion tons of biomass annually with the

potential to displace up to 30% of the U.S. petroleum consumption, or equivalently reducing the amount of imported petroleum by 67% [4]. Replacing up to 67% of imported petroleum with home grown biomass would be a major step toward energy independence for the U.S. Technology developed to displace petroleum with biomass-derived products could also be deployed to other countries and provide a much more renewable and sustainable energy future for the world as a whole.

Biomass also offers the ability to reduce atmospheric carbon dioxide concentration. Utilizing photosynthesis biomass scavenges carbon dioxide from the atmosphere as it grows. Carbon is accumulated in the biomass structure and oxygen is released back to the atmosphere. Therefore, use of biomass as a fuel essentially closes the carbon cycle which in turn helps to mitigate concern of increasing atmospheric carbon dioxide concentration. The process of recycling carbon leads to what is known as a carbon-neutral fuel. Carbon-negative fuels can also be produced by utilizing biomass processing co-products, such as biochar. Combustion of fuels derived from biomass releases carbon dioxide, however carbon sequestered in co-products is not returned to the atmosphere. The process therefore results in a negative net carbon balance [5]. Displacement of fossil fuels with carbon-negative biofuels could therefore offset carbon emissions coming from fossil fuels and provide a much higher level of environmental security.

One major disadvantage of biomass is its low bulk density which leads to prohibitively high costs associated with transporting biomass feedstock long distances. As a result, the optimum biorefinery size is expected to be much smaller than that of a

typical petroleum refinery. Wright et al. [6-9] and You et al. [10] studied optimum biorefinery size in effort to determine the distance biomass feedstocks can economically be transported. In several scenarios a distributed model is investigated which utilizes smaller satellite plants to first densify biomass before it is transported to a central facility for final processing. Wright et al. [11] found that fast pyrolysis of Midwest cornstover in a distributed model could produce gasoline and diesel fuel equivalents at a price of $2-$3 per gallon. Models predicting that biofuels from fast pyrolysis can be produced at a similar price to that of petroleum derived fuels are a major step in developing fast pyrolysis into a commercial process. However, in practice, optimization of the fast pyrolysis process is required to produce biofuels at a price competitive with petroleum-derived fuels.

Many pathways exist for the conversion of biomass to fuels and chemicals. Conversion pathways are typically split into two general platforms; the biochemical platform and the thermochemical platform. The biochemical platform employs the use of microorganisms or enzymes for the key conversion step while the thermochemical platform utilizes heat, chemicals and/or catalysts. Examples of biochemical processes are anaerobic digestion for production of biogas and fermentation for production of ethanol. Examples of thermochemical processes include fast pyrolysis for production of bio-oil, hydrothermal processing for production of bio-crude, and gasification for production of either synthesis gas or producer gas. Hybrid processing utilizes conversion steps from both platforms and includes processes such as bio-oil fermentation for production of alcohols and syngas fermentation for production of

alcohols or hydrocarbons. Hence, there are many approaches to produce biofuels and further process optimization is essential to determining which approach will be the most competitive with petroleum-derived products.

Biomass Anatomy

Biomass consists of three major components: cellulose, hemicellulose, and lignin. Cellulose and hemicellulose are collectively called holocellulose and the collection of all three components is commonly referred to as lignocellulose. Cellulose is a homogeneous polysaccharide composed of repeating glucose units that are bound via β (1-4) linkages, as shown in Figure 1. Hemicellulose is a heterogeneous polysaccharide consisting of a variety of pentoses and hexoses. Hemicellulose also has many different linkage types between sugar monomers which gives it a much more amorphous structure, as shown in Figure 2. Monosaccharides resulting from the depolymerization of holocellulose offer advantages since they can be directly upgraded to liquid fuels and chemicals through aqueous phase processing [12], or fermented via microorganisms using hybrid processing [13]. In either case, holocellulose must first be depolymerized to monosaccharides.

Lignin makes up the remaining ~30 wt. % of the lignocellulosic biomass [15]. Lignin has a much higher carbon-to-oxygen ratio than the holocellulose which gives it energy content similar to that of certain bituminous coals [16]. Several types of carbon-carbon and carbon-oxygen bonds link phenolic moieties in lignin giving it an amorphous

structure. Plant lignins are classified as H-, G-, or S- lignin depending on if they have zero, one or two methoxyl side chains per phenolic moiety, respectively. Herbaceous

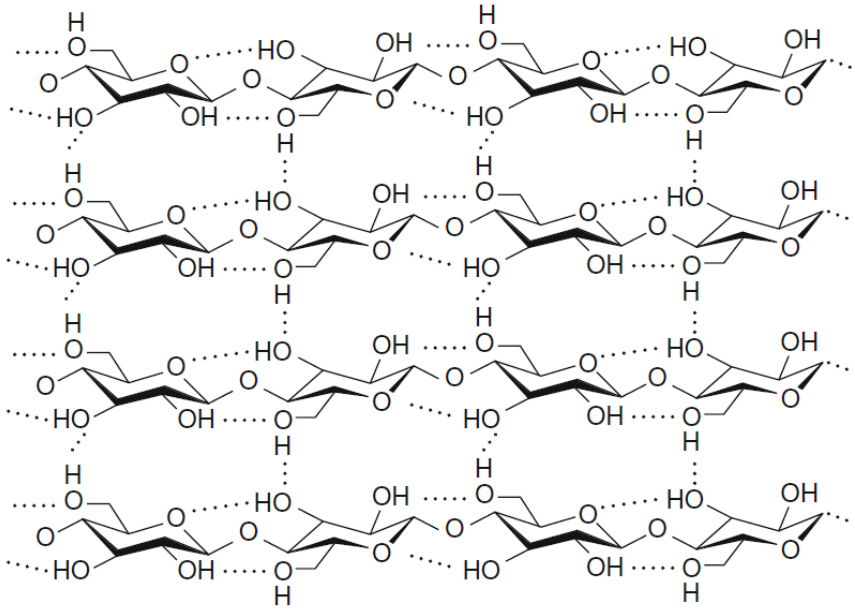

Figure 1: Cellulose structure [14]

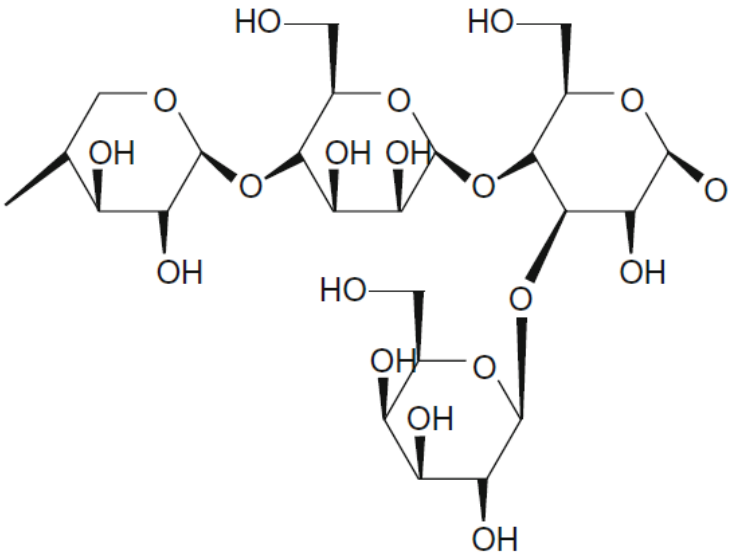

Figure 2: Hemicellulose Structure [14]

crops typically contain more H-lignin, softwoods contain more G-lignin, and hardwoods contain more S-lignin [17]. Figure 3 shows an example of a typical softwood lignin structure.

Although beneficial in keeping the plant living, the recalcitrance of lignin presents several challenges to conversion of the biomass to fuels and chemicals. For instance, biochemical conversion of cellulosic feedstocks leaves nearly all of the lignin unconverted [18] where it is then commonly used in low value applications, such as combustion for process heat. Thermochemical processes offer the advantage of converting much more of the lignin into more valuable products. Fast pyrolysis, for example, converts over 20 wt. % of the lignin into phenolic monomers, around 40 wt. % to biochar, and the remainder is split between phenolic oligomers and light products [19, 20]. Phenolic monomers, being the most valuable lignin products, are commonly used in industry for precursor chemicals and also make good candidates for upgrading to fuels [21]. Additionally, the tarry phenolic oligomers are finding niche applications such as in the production of bio-asphalt [22] or for use in binders, resins, and polymers [23]. Therefore it is desirable to convert a higher percentage of the lignin to phenolic monomers; however co-products, such as phenolic oligomers, are also more valuable than simply combusting the lignin for process heat.

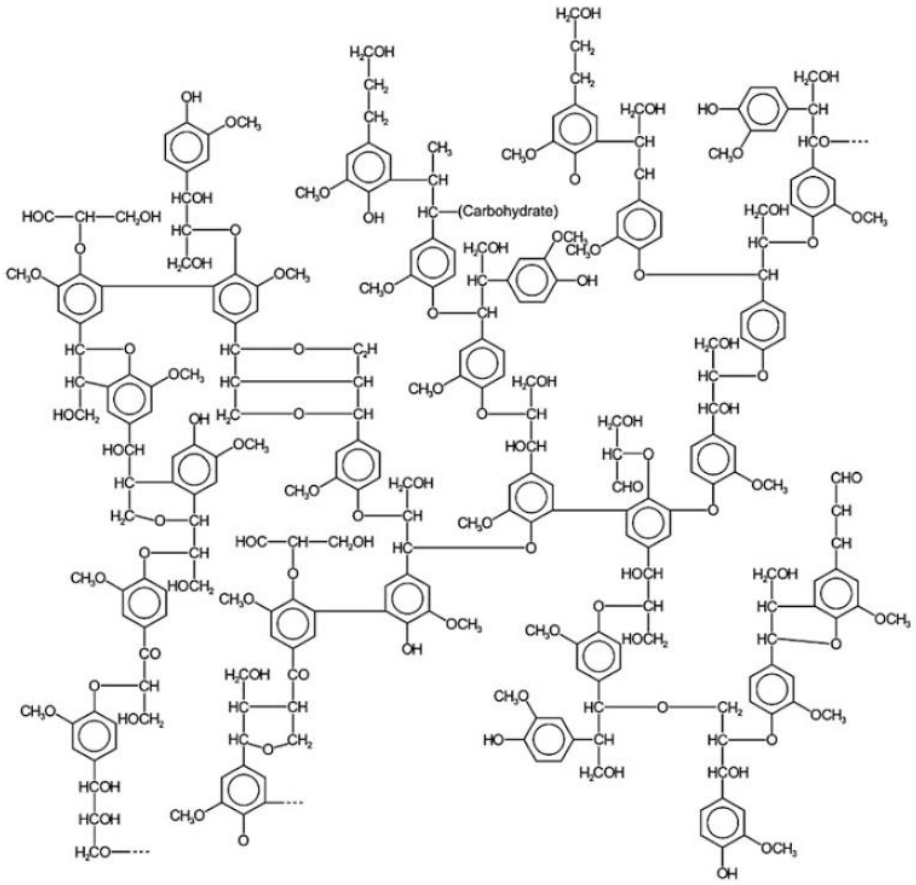

Figure 3: Typical Softwood Lignin Structure [24]

Fast Pyrolysis Overview

Fast pyrolysis is the process in which organic materials are decomposed by rapidly heating to moderate temperatures (400-600°C) in the absence of oxygen to produce solids, liquids and gases. The liquids, known as bio-oil, can account for up to 78% of the total mass for short residence times (0.5-2.0 s) and rapid quenching at the end of the process [25]. Besides the liquids, fast pyrolysis also produces a solid carbonaceous residue, known as biochar, and non-condensable gases (NCGs).

Biochar has potential value as a soil amendment since it retains most of the biomass mineral, increases moisture availability, builds soil organic matter, enhances nutrient recycling, and reduces leaching of nutrients [5]. Details of biochar soil application have been the subject of several researchers and are discussed elsewhere [26-29]. Biochar has several other applications including its use as fuel, activated carbon, and as a carbon sequestration agent [30].

Non-condensable gases resulting from fast pyrolysis are composed of predominately carbon monoxide and carbon dioxide, with lesser quantities of hydrogen, methane, and light hydrocarbons. Since fast pyrolysis is performed in the absence of an oxidizer, the gases produced retain some heating value and therefore may be combusted to produce process heat. Non-condensable gases or their combustion products can also be used to provide an oxidizer free gas stream for recycling during the fast pyrolysis process. Recycling of NCGs eliminates the need to separate oxygen from air or having large reservoirs of inert gas to provide the oxygen free atmosphere.

Several types of reactors exist that are capable of achieving conditions essential to production of bio-oil from fast pyrolysis, which include high heat transfer rate and low residence time of condensable vapors. Both a bubbling fluidized bed reactor (BFB) and an auger reactor were used in this work and will be described in more detail throughout subsequent chapters.

The BFB reactor has many advantages for use in biomass pyrolysis. For one, the BFB reactor is known to produce very high heat transfer rates due to approximately 90% of the heat transfer occurring via conduction from the fluidizing media to the

biomass [31]. The BFB reactor requires relatively high sweep gas flow rates in order to maintain proper reactor hydrodynamics, which also offers the advantage of providing a short vapor residence time. High heat transfer rates and short residence time of vapors in the BFB reactor help it to produce high bio-oil yield. Bubbling fluidized bed reactors are also used in several other industrial applications and therefore the technology is relatively mature. Thus scaling up a BFB reactor for biomass fast pyrolysis should be fairly straight forward.

The BFB reactor also has several disadvantages. Many of the disadvantages arise due to the sensitive hydrodynamic conditions required for proper operation. One in particular is the sensitivity to feedstock particle size to properly fluidize without elutriating before pyrolysis is complete. If the operating conditions aren't just right, the small particles can quickly elutriate from the bed before completely pyrolyzing or large particles can accumulate in the bed which eventually leads to defluidization. Size reduction and screening the feedstock to a precise size range can be a major upfront cost in biomass preprocessing. Additionally, discarding particles that are too small will prevent utilization of the entire feedstock.

Another disadvantage of the BFB reactor is the large quantity of inert gas required for proper operation. Inert gas used in the process must be both heated to reaction temperature and then cooled during the condensation process. Heating and cooling large volumes of inert gas will lead to higher energy input compared to reactors utilizing less gas. High ratio of inert gas to biomass, as is used in the BFB reactor, will

also produce a dilute exhaust stream that will provide little heating value to supplement energy inputs.

The auger reactor has several advantages over the BFB reactor such as less sensitivity to feedstock particle size and lower inert gas requirements. Because the reactor requires less inert gas, the ratio of inert gas-to-biomass is also lower, which results in an exhaust gas with a much higher heating value than the non-condensable gases from the BFB reactor. Combustion of the exhaust gas will therefore be capable of supplying a significant amount of process heat. The auger reactor is also capable of higher energy efficiency than the BFB reactor due to less heating and cooling required for a lower inert gas flow. The auger reactor produces similar heat transfer rates as the BFB reactor due to obtaining most of its heat transfer via direct conduction between heat carrier material and the biomass. Therefore, the auger reactor can produce similar bio-oil yields as the BFB reactor, as shown by Brown [32]; however requires fewer inputs.

The auger reactor also has its own disadvantages. One major limitation is that an auger reactor has not yet been demonstrated at any size larger than pilot scale. Therefore much higher risk is involved in demonstrating the first commercial scale auger reactor. Additional mechanical complexity compared to the BFB reactor will also likely lead to higher maintenance and operating costs. Therefore many questions about the auger reactor and its capabilities must be answered before it is likely to gain support at the commercial scale.

Several other reactor types exist and are summarized by Venderbosch and Prins [33], Bridgwater [31, 34] and on the PyNe website (www.pyne.co.uk), all of which provide additional information for BFB and auger reactors.

Dissertation Organization

As summarized throughout *Chapter 1*, fast pyrolysis offers several advantages for production of fuels and chemicals from biomass. The process will however require further optimization to produce fuels and chemicals at a price competitive to conventional fossil fuel-derived products. Fast pyrolysis can produce an abundance of carbohydrate-derived monomers, many of which can be upgraded utilizing approaches such aqueous phase processing to produce hydrocarbons or hybrid processing to produce ethanol. Phenolic monomers coming from fast pyrolysis of lignin require less deoxygenation compared to carbohydrates and therefore require less expensive upgrading technology. Hence, it is important to look holistically at improving the yield of both carbohydrate and lignin derived products while simplifying the processing.

Work in this dissertation is summarized into three chapters in addition to the introduction and conclusions. *Chapter 2* focuses on improving the yield of carbohydrate monomers by passivation of the alkali and alkaline earth metals (AAEMs) to thermally stable salts. Alkali and alkaline earth metal passivation was demonstrated to drastically improve the yield of carbohydrate monomers; however, the yield of lignin-derived compounds was considerably reduced. The decrease in lignin-derived material coincided with an increase in char. The simultaneous passivation of AAEMs and

decrease in lignin-derived products in the bio-oil led to the hypothesis that thermally active AAEMs also affect the depolymerization of lignin to phenolic monomers. Review of the literature provided mixed results as to the effect of AAEMs on lignin, so an extensive investigation was performed and is the focus of *Chapter 3*.

Chapter 2 and *Chapter 3* focused on variables prior to pyrolysis for improving the yield of carbohydrate and phenolic monomers. Observations also suggested that post-processing operations, including the method in which the bio-oil was collected, can have a significant impact on the resulting bio-oil composition. *Chapter 4* therefore focuses on development and testing of a new type of bio-oil collection system and its capacity to improve the yield of monomeric carbohydrates.

Chapter 5 summarizes some general conclusions and recommendations from each of the prior chapters. Several suggestions for future work are also discussed in *Chapter 5.*

Lastly, four appendices are attached at the end of this dissertation. *Appendix A* and *Appendix B* give detailed mass balance and bio-oil composition data for the work with red oak and switchgrass, respectively, discussed in *Chapter 2*. *Appendix C* consists of a short literature review that supplements the work with AAEM effect on lignin pyrolysis covered in *Chapter 3*. *Appendix D* provides a list of definitions and calculations used for summarizing mass balance and bio-oil composition data.

References

1. U.S. Energy Information Administration. *How dependent are we on foreign oil?* 2012 November 4, 2012]; Available from: http://www.eia.gov/energy_in_brief/foreign_oil_dependence.cfm.

2. U.S. Energy Information Administration. *Annual Energy Review 2011*. 2011 November 4, 2012]; Available from: http://www.eia.gov/totalenergy/data/annual/pdf/aer.pdf.

3. Jackson, J.K., *U.S. trade deficit and the impact of changing oil prices*, 2012, Congressional Research Service (CRS) Reports and Issue Briefs.

4. U.S. Department of Energy, *U.S. Billion-Ton Update: Biomass Supply for a Bioenergy and Bioproducts Industry*, R.D. Perlack and B.J.S. (Leads), Editors. 2011: Oak Ridge, TN. p. 227.

5. Laird, D.A., *The Charcoal Vision: A Win–Win–Win Scenario for Simultaneously Producing Bioenergy, Permanently Sequestering Carbon, while Improving Soil and Water Quality.* Agron. J., 2008. **100**(1): p. 178-181.

6. Wright, M. and R.C. Brown, *Establishing the optimal sizes of different kinds of biorefineries.* Biofuels, Bioproducts and Biorefining, 2007. **1**(3): p. 191-200.

7. Wright, M.M., R.C. Brown, and A.A. Boateng, *Distributed processing of biomass to bio-oil for subsequent production of Fischer-Tropsch liquids.* Biofuels, Bioproducts and Biorefining, 2008. **2**(3): p. 229-238.

8. Wright, M.M., D.E. Daugaard, J.A. Satrio, and R.C. Brown, *Techno-economic analysis of biomass fast pyrolysis to transportation fuels.* Fuel, 2010. **89, Supplement 1**: p. S2-S10.

9. Wright, M.M., J.A. Satrio, R.C. Brown, D.E. Daugaard, and D.D. Hsu, *Techno-Economic Analysis of Biomass Fast Pyrolysis to Transporation Fuels*, 2010, National Renewable Energy Laboratory: Golden, Colorado.

10. You, F. and B. Wang, *Life Cycle Optimization of Biomass-to-Liquid Supply Chains with Distributed–Centralized Processing Networks.* Industrial & Engineering Chemistry Research, 2011. **50**(17): p. 10102-10127.

11. Wright, M.M., *Techno-economic, location, and carbon emission analysis of thermochemical biomass to transportation fuels*, in *Department of Mechanical Engineering*2010, Iowa State University: Ames, Iowa.

12. Huber, G.W. and J.A. Dumesic, *An overview of aqueous-phase catalytic processes for production of hydrogen and alkanes in a biorefinery.* Catalysis Today, 2006. **111**(1–2): p. 119-132.

13. Jarboe, L.R., W. Zhiyou, C. DongWon, and R.C. Brown, *Hybrid thermochemical processing: fermentation of pyrolysis-derived bio-oil.* Applied Microbiology & Biotechnology, 2011. **91**(6): p. 1519-1523.

14. Kalia, S., B. Kaith, and I. Kaur, *Cellulose Fibers: Bio-and Nano-Polymer Composites.*

15. U.S. Department of Energy, *Biomass Feedstock Composition and Property Database*, 2006, Energy Efficiency and Renewable Energy - Biomass Program.

16. Boateng, A.A., P.J. Weimer, H.G. Jung, and J.F.S. Lamb, *Response of Thermochemical and Biochemical Conversion Processes to Lignin Concentration in Alfalfa Stems †.* Energy & Fuels, 2008. **22**(4): p. 2810-2815.

17. Simoneit, B.R., W. Rogge, M. Mazurek, L. Standley, L. Hildemann, and G. Cass, *Lignin pyrolysis products, lignans, and resin acids as specific tracers of plant classes in emissions from biomass combustion.* Environmental Science & Technology, 1993. **27**(12): p. 2533-2541.

18. Wyman, C.E., *What is (and is not) vital to advancing cellulosic ethanol.* Trends in Biotechnology, 2007. **25**(4): p. 153-157.

19. Patwardhan, P.R., R.C. Brown, and B.H. Shanks, *Understanding the Fast Pyrolysis of Lignin.* ChemSusChem, 2011. **4**(11): p. 1629-1636.

20. Piskorz, J., P. Majerski, D. Radlein, and D.S. Scott, *Conversion of lignins to hydrocarbon fuels.* Energy & Fuels, 1989. **3**(6): p. 723-726.

21. Stewart, D., *Lignin as a base material for materials applications: Chemistry, application and economics.* Industrial Crops and Products, 2008. **27**(2): p. 202-207.

22. Williams, R.C., J. Satrio, M.R. Rover, R.C. Brown, and S. Teng. *Utilization of Fractionated Bio-Oil in Asphalt*. in *The 38th Annual Rocky Mountain Asphalt Conference & Equipment Show*. 2011. Denver, Colorado.

23. Sukhbaatar, B., P.H. Steele, and M.G. Kim, *Use of Lignin Separated from Bio-oil in Oriented STrand Board Binder Phenol-Formaldehyde Resins.* BioResources, 2009. **4**(2): p. 789-804.

24. Potumarthi, R., R.R. Baadhe, and S. Bhattacharya, *Fermentable Sugars from Lignocellulosic Biomass: Technical Challenges*, in *Biofuel Technologies*2013, Springer. p. 3-27.

25. Brown, R.C., *Biorenewable resources : engineering new products from agriculture*. 1st ed2003, Ames, Iowa: Iowa State Press. xii, 286 p.

26. Brewer, C., R. Unger, K. Schmidt-Rohr, and R. Brown, *Criteria to Select Biochars for Field Studies based on Biochar Chemical Properties.* BioEnergy Research, 2011. **4**(4): p. 312-323.

27. Brewer, C.E., K. Schmidt-Rohr, J.A. Satrio, and R.C. Brown, *Characterization of biochar from fast pyrolysis and gasification systems.* Environmental Progress & Sustainable Energy, 2009. **28**(3): p. 386-396.

28. Deal, C., C.E. Brewer, R.C. Brown, M.A.E. Okure, and A. Amoding, *Comparison of kiln-derived and gasifier-derived biochars as soil amendments in the humid tropics.* Biomass and Bioenergy, 2012. **37**: p. 161-168.

29. Unger, R., R. Killorn, and C. Brewer, *Effects of Soil Application of Different Biochars on Selected Soil Chemical Properties.* Communications in Soil Science and Plant Analysis, 2011. **42**(19): p. 2310-2321.

30. Lehmann, J. and S. Joseph, *Biochar for environmental management : science and technology*2009, London ; Sterling, VA: Earthscan. xxxii, 416 p.

31. Bridgwater, A.V., *Principles and practice of biomass fast pyrolysis processes for liquids.* Journal of Analytical and Applied Pyrolysis, 1999. **51**(1–2): p. 3-22.

32. Brown, J.N., *Development of a lab-scale auger reactor for biomass fast pyrolysis and process optimization usingresponse surface methodology*, 2009, Iowa State University: Ames, Iowa.

33. Venderbosch, R.H. and W. Prins, *Fast Pyrolysis*, in *Thermochemical Processing of Biomass: Conversion into Fuels, Chemicals and Power*, R.C. Brown, Editor 2011, John Wiley & Sons, Ltd. p. 124-156.

34. Bridgwater, A.V., *Renewable fuels and chemicals by thermal processing of biomass.* Chemical Engineering Journal, 2003. **91**(2–3): p. 87-102.

CHAPTER 2

CONTINUOUS PRODUCTION OF SUGARS FROM BIOMASS IN AN AUGER PYROLYZER THROUGH PASSIVATION OF ALKALI AND ALKALINE EARTH METALS

A paper prepared for submission to *Energy and Environmental Science*

Dustin Dalluge, Tannon Daugaard, Patrick Johnston, Najeeb Kuzhiyil, Mark Wright, and Robert Brown

Abstract

Achieving high yields of sugars from the fast pyrolysis of biomass is hindered by alkali and alkaline earth metals (AAEMs) inherent to biomass that fragment holocellulose to light oxygenates as opposed to the preferred pathway of depolymerization to anhydrosugars. The concept of AAEM passivation, by which the catalytic activity of AAEMs can be suppressed to enhance thermal depolymerization of lignocellulose to sugars, has been previously established at the microgram scale using batch reactors. The feasibility of increasing sugar yield via AAEM passivation has however never been demonstrated at the kilogram scale in a continuous flow reactor. The goal of this research is to demonstrate the enhanced production of sugars from AAEM passivated feedstocks in a continuous auger pyrolyzer at the kilogram scale.

As a result of AAEM passivation total sugars from red oak more than doubled, increasing from 7.8 wt. % to 15.9 wt. % of feedstock, while light oxygenates decreased by 45%, from 27.1 wt. % to 14.7 wt. % of feedstock. Similarly with AAEM passivated switchgrass the total sugars increased by 260%, from 4.5 wt. % to 16.2 wt. % of feedstock, while the light oxygenates decreased by 48%, from 20.0 wt. % to 10.5 wt. % of feedstock. An undesirable outcome of AAEM passivation was an increase in

biochar yield, increasing by 66% and 30% for red oak and switchgrass, respectively. Loss of lignin-derived phenolic compounds can explain 67% and 38% of the increase in char for red oak and switchgrass, respectively. The remaining 33% char increase for red oak (3.1 wt. % char) and 62% char increase for switchgrass (4.0 wt. % char) must be attributable to carbonization of carbohydrate.

Introduction

Sugars can be readily converted into biofuels, but sugars derived from starch and sugar crops have limited availability for fuels production. In principle, more plentiful supplies of sugars can be obtained from cellulosic biomass [1, 2]. Although enzymatic and acid hydrolysis have received most of the attention for the production of sugars from cellulose; purely thermal processes are also possible. In particular, fast pyrolysis can depolymerize cellulose to anhydrosugars such as levoglucosan (LG) [3, 4]. Practical exploitation of thermally converting cellulose to anhydrosugars has been stymied by the presence of alkali and alkaline earth metals (AAEMs) inherent to most lignocellulosic biomass. Alkali and alkaline earth metals dramatically decrease the yield of anhydrosugars by catalyzing pyranose and furanose ring fragmentation leading to increased yields of less desirable light oxygenates such as aldehydes and carboxylic acids [3, 5, 6].

Experiments at the microgram scale have demonstrated that fast pyrolysis of biomass pretreated with a carefully controlled quantity of sulfuric or phosphoric acid can convert almost 60% of the cellulose in lignocellulosic biomass to anhydrosugars [7]. The

pretreatment process, known as passivation, consists of adding just enough sulfuric or phosphoric acid to convert all of the AAEM cations into thermally stable sulfates or phosphates, respectively. Conversion to thermally stable salts significantly reduces the catalytic activity of the AAEM cations, which would otherwise fragment biomass carbohydrates to light oxygenates. Alkali and alkaline earth metal passivation appears to produce acid salts of AAEM cations [7], such as potassium hydrogen sulfate ($KHSO_4$), which produce a buffering effect along with passivation of AAEM cations to preferentially cleave glycosidic bonds rather than fragment pyranose rings [6, 8]. The amount of acid required for passivation is stoichiometric with respect to the AAEM content of the biomass [7]. Thus, the quantity of acid required is very small, especially for low ash content feedstocks such as red oak. For example, the red oak used in this work required only 0.4 wt. % sulfuric acid on a dry biomass basis.

Alkali and alkaline earth metal passivation requires relatively little water and subsequent drying compared to attempts to remove AAEM via washing [9-14]. Water can present a major input both in terms of operating costs and energy, therefore water use should be minimized to make the process more economically feasible. The biomass-to-water ratios used in the reviewed literature for washing or infusion of acid catalysts ranged from 1:3 to 1:25 in batch systems, whereas the ratio used in this work was as low as 1:1 for red oak. For AAEM passivation, water is used only to the extent necessary to homogeneously distribute the acid throughout the biomass. It is therefore likely that the biomass-to-water ratio could be reduced further with process optimization and improved mixing.

Alkali and alkaline earth metal passivation offers a purely thermal route to the production of sugars from lignocellulosic biomass. However, it has previously only been demonstrated with analytical pyrolysis instrumentation using microgram quantities of biomass. The objective of this study is to demonstrate the kilogram scale continuous production of sugar-rich bio-oil from fast pyrolysis of AAEM passivated lignocellulosic biomass.

Materials and Methods

Feedstock Preparation

Northern red oak (Quercus rubra) was obtained from Wood Residuals Solutions (Montello, WI). Switchgrass (Panicum virgatum) was obtained from Chariton Valley Resource Conservation and Development, Inc. (Centerville, IA). The as received feedstocks were ground using a Retsch® Type SM2000 Heavy-Duty Cutting Mill with a 750 μm screen, and sieved using a W.S. Tyler Ro-Tap® sieve shaker with screens that allowed separation of the desired size range of 300-710 μm. A portion of the prepared feedstock was set aside as the control and the remainder was AAEM passivated with sulfuric acid.

Alkali and Alkaline Earth Metal Passivation

First the ratio of biomass-to-water at which the biomass was homogeneously wetted was determined. Dry biomass was mixed with varying ratios of water and the ratio at which all of the biomass was wet, but had no pooling water, was determined the

optimum ratio. Red oak and switchgrass were uniformly wetted for mass ratios of biomass-to-water of 1:1 and 1:2, respectively.

Next the mass ratio of pure sulfuric acid-to-biomass necessary to convert all of the AAEMs in the biomass to thermally stable salts was determined based on the correlation developed by Kuzhiyil et al. [7]. The weight percentage of sulfuric acid was calculated to be 0.40 wt. % for red oak and 2.0 wt. % for switchgrass, the latter of which required more acid by virtue of its higher AAEM content.

A dilute sulfuric acid solution was prepared using the required mass of pure sulfuric acid and deionized water to achieve the proper biomass-to-water and biomass-to-sulfuric acid ratios. The dilute acid solutions were prepared using 96.7 wt. % purity sulfuric acid purchased from Fischer Scientific® and 18.2 MΩ-cm ultrapure deionized water. Accordingly, four kg of 0.4 wt. % dilute sulfuric acid solution was required to treat the four kg of red oak, while eight kg of 1.0 wt. % dilute sulfuric acid solution was required to treat the four kg of switchgrass.

Biomass and dilute acid were thoroughly mixed by hand in plastic pails until a uniform mixture was achieved. The resulting damp biomass was loaded into shallow plastic bins and dried at 40°C in an oven with an airflow of approximately five standard liters per minute (SLPM). Biomass was stirred every 6-12 hours for the entirety of the 4-5 day drying period. Once the feedstock appeared uniformly dry at 6-10% moisture it was removed from the oven and sealed in a clean plastic pail. Actual moisture content of the feedstock was measured before pyrolysis experiments.

Auger Reactor

A twin-screw auger reactor as described by Brown et al. [15] was used to conduct laboratory-scale experiments. Shakedown trials with AAEM passivated biomass were used to determine appropriate operating conditions, which were somewhat different from those described by Brown et al. [15] with untreated biomass (including a higher heat carrier to biomass ratio, lower temperature, and more sweep gas).

Stainless steel cut-wire shot from Pellets LLC (North Tonawanda, New York) was used as heat carrier and sieved to a range from 710-1000 μm prior to experiments. Heat carrier was preheated to 550°C and augered into the reactor at a rate of 10 kg/hr. The heater surrounding the twin-screw auger reactor was held at 550°C for all ensuing experiments. Before testing with biomass, the as received heat carrier was conveyed through the reactor at 550°C to remove any contaminants, such as oils or resins, that may have been deposited during manufacturing. The biomass feeder was calibrated to feed biomass to the reactor at 0.25 kg/hr., providing a heat carrier-to-biomass mass ratio of 40:1. A total of 4 SLPM of nitrogen was injected into the reactor system using an Alicat® mass flow controller. The flow was split between heat carrier preheaters, biomass feeder, and the reactor using individual rotometers. For each experiment the reactor operated continuously for two hours.

Biomass and heat carrier entered the reactor at 25°C and 550°C, respectively. Heat absorbed by the biomass from the heat carrier during pyrolysis resulted in a mixture temperature near 500°C, which is referred to as the reaction temperature. The intermeshing, twin-screws of the reactor co-rotated at 54 rpm providing a solids

residence time of approximately 10 seconds. A solids catch bin at the end of the auger collected spent heat carrier and biochar, which were subsequently separated by screening and weighed as part of the mass balance.

The pyrolysate and sweep gas were discharged from the reactor through a vapor port located 10.8 cm downstream from the heat carrier inlet. The pyrolysate and sweep gas next passed through a solids separating cyclone to remove any entrained char before entering the bio-oil collection system. A cold gas quench system as described by Dalluge et al. [16] was used to recover bio-oil. Liquid nitrogen was generated by passing gaseous nitrogen into a heat transfer coil submerged in a dewar of liquid nitrogen. The pyrolysis vapor stream entered the quench chamber at approximately 500°C and was quenched with the liquid nitrogen to 110°C before entering an electrostatic precipitator (ESP). The ESP wall temperature was heat traced to maintain 100°C in order to both help decrease viscosity of the bio-oil film to keep it flowing downward and to volatilize any condensed moisture from the bio-oil film. The bio-oil "heavy ends" that collected in the ESP were designated as stage fraction one (SF1). The remaining pyrolysis vapors passed into a shell and tube heat exchanger that maintained a wall temperature of -5°C using a water-ethylene glycol mixture. The light bio-oil product that collected in the shell and tube heat exchanger was designated as stage fraction 2 (SF2). Bio-oil fractions were analyzed separately; however results were combined for a whole bio-oil basis in the results and discussion.

Mass Balances

Mass balances on products were determined by measuring bio-oil, biochar, and non-condensable gases (NCGs). Each component of the bio-oil collection system was weighed before and after each experiment to determine the total accumulation of bio-oil.

The mixture of biochar and heat carrier collected in the solids catch bin was screened using a 710 μm sieve to separate the fine biochar and coarse shot. Although most of the biochar could be recovered by this simple procedure, AAEM passivated feedstock commonly led to an agglomerate of biochar and heat carrier that could not be separated by sieving. Therefore, a biochar burn-off procedure was developed to account for the mass of any biochar remaining with the heat carrier. The procedure involved loading the biochar and heat carrier mixture into a fixed bed reactor and heating to750°C. Air was purged through the reactor at approximately 20 SLPM throughout the procedure in order to oxidize all of the carbon. The burn-off procedure was considered complete when the monitored levels of carbon monoxide and carbon dioxide in the exhaust stream were zero. Both the volume and composition of the exhaust stream were recorded and used to determine the total mass of carbon that was combusted from the heat carrier. Carbon mass percentage in the sieved biochar was determined via ultimate analysis on a LECO TruSpec® CHNS analyzer. The calculated carbon mass resulting from carbon monoxide and carbon dioxide in the exhaust stream from the biochar burn-off procedure was then divided by the carbon mass percentage in the sieved biochar to estimate the total biochar that could not be recovered by sieving. Both the mass of

biochar from the burn-off procedure and from sieving were added together for the total mass balance.

Non-condensable gases from pyrolysis were quantified by monitoring both the concentration of individual gas species and the total volumetric gas flow from the reactor. Concentrations of NCGs in the exhaust stream were measured using a Varian® CP-4900 micro-Gas Chromatograph (microGC) interfaced with Galaxy® Chromatography software. A split line from the main exhaust line and a sampling pump were used to supply the GC with a constant flow of approximately 0.5 L/min. The microGC was programmed to sample for 30 s followed by 140 s run time for analysis. A thermal conductivity detector was used for gas detection on each channel. Channel one was setup with a Varian® Molesieve 5 Å column operating at 100°C with argon carrier gas at 151.7 kPa and was calibrated to measure helium, hydrogen, oxygen, nitrogen, methane and carbon monoxide. A Varian® PoraPLOT Q column was setup on channel two operating at 58°C with helium carrier gas at 117.2 kPa and was calibrated to measure carbon dioxide, ethylene, acetylene, and ethane. A Varian® Al2O3 column was setup on channel three operating at 60°C with helium carrier gas at 55.2 kPa and was calibrated to measure propane. All sample lines and the injectors for channels one and two operated isothermally at 110°C with a 40 ms injection time. The injector for channel three operated isothermally at 80°C with an 80 ms injection time.

Total volume of gas leaving the reactor was measured using a Ritter® TG5/4-ER-1 bar drum type gas meter. The mass of NCGs produced during the reaction was calculated using the overall gas volume and the steady-state concentrations of

NCGs. Identical microGC and volume measuring methods were used for both the pyrolysis experiments and the biochar burn-off procedure.

Bio-oil Analysis

Moisture Analysis

Bio-oil moisture content was determined using a Karl Fischer MKS-500® moisture titrator. Hydranal Working Medium K® was used as the solvent and Hydranal Composite 5 K® was used as the titrant. The instrument was calibrated using deionized water before analysis.

Water Soluble Sugars Analysis

Cellobiosan (1,6-anhydro-β-D-cellobiose), levoglucosan (1,6-anhydro-β-D-glucopyranose), galactose, and xylosan (1,4-anhydro-α-D-xylopyranose) were quantified via a water wash method followed by analysis with High Performance Liquid Chromatography (HPLC). Levoglucosan and cellobiosan standards were purchased from Carbosynth (Compton, Berkshire, UK) and had purities of ≥99.0%. Xylosan was purchased from LC Scientific, Inc. (Concord, Ontario, Canada) and had a purity of ≥97.0%. Galactose was purchased from Acrōs Organics (part of Thermo Fisher Scientific, Waltham, MA) and had a purity of ≥99.0%. All samples and standards solutions were prepared using ultrapure 18.2 MΩ-cm deionized water from a Barnstead E-Pure® system (part of Thermo Fisher Scientific, Waltham, MA).

Approximately 500 mg of bio-oil was dissolved in three mL of water, homogeneously mixed with a vortex mixer, and then centrifuged at 3500 rpm for 15 min. The supernatant was then decanted and set aside. The procedure involving adding

three mL of water, mixing, centrifuging, and decanting was performed in triplicate to ensure the water soluble sugars were fully dissolved. An additional nine mL of water was added to the accumulated supernatant to bring the total volume up to 18 mL. The resulting solution was filtered through a Whatman® 0.45 μm glass microfiber filter before analysis.

A Dionex UltiMate® 3000 HPLC system interfaced with Chromeleon® software and a Refractive Index (RI) detector was used to quantify water soluble sugars. Two Bio-Rad® Aminex HPX-87P columns were used in series for sugars separation with a guard column and Micro-guard® cartridge. The column compartment was held at 75°C for analysis. Ultrapure deionized water of 18.2 MΩ-cm purity was used as eluent at a flow rate of 0.6 mL/min. Each sugar was calibrated using a pure standard within the range of 0.5-10 mg/mL using a five point calibration.

Xylosan had exactly the same retention time as xylose with a response factor on the RI detector of just 78% that of xylose. The calibration for xylosan was performed only once using a five point calibration due to cost. The quantity of xylosan reported here was therefore based on the calibration for xylose, where the measured quantity of xylose was divided by the response factor of 0.78 to adjust the calibration to a xylosan basis. The assumption that the entire peak is xylosan is based on trials from the GC. A peak in the bio-oil from GC analysis was verified to be xylosan via injection of a standard, whereas GC analysis did not verify the presence of xylose in the sample. Therefore, the assumption that the peak solely represented xylosan seemed reasonable.

It should be noted that anhydrosugars levoglucosan and xylosan were verified to be in the bio-oil via GC analysis; however, quantification was performed via HPLC. The limited volatility of levoglucosan and xylosan in combination with the medium polar 1701 column led both anhydrosugars to have short, broad peaks that were difficult to quantify via GC. Therefore, HPLC was deemed a more consistent method of quantification.

Total Sugars Analysis via Acid Hydrolysis

Dimeric or oligomeric carbohydrates produced during pyrolysis are difficult to directly quantify. Instead, saccharides in bio-oil were hydrolyzed to glucose, xylose, and sorbitol, which were quantified and combined to give "total sugars." A 400 mM sulfuric acid solution was prepared by dissolving concentrated sulfuric acid in the appropriate measure of 18.2 MΩ-cm deionized water. Approximately 60 mg of bio-oil and 6 mL of the 400 mM sulfuric acid solution were added to a hydrolysis reactor vessel (HRV). A Teflon gasket and a cap were placed on the HRV, which was then placed in an oil bath at 125°C for 45 min. The HRV was then quickly chilled to room temperature in a freezer. After centrifuging at 3500 rpm for 15 minutes the mixture was decanted and the supernatant was filtered through a Whatman® 0.45 μm glass microfiber filter.

The oil bath was only capable of holding 12 samples per batch. Therefore, to ensure consistency between batches, a reference standard of both levoglucosan and cellobiosan (each >99% purity) were added to each batch to verify hydrolysis was complete. If either of the reference standards contained any remaining levoglucosan or cellobiosan after HPLC analysis the entire batch was rejected.

A Dionex UltiMate® 3000 HPLC system interfaced with Chromeleon® software was used for HPLC analysis. A 300 mm X 7.7 mm 8 µm particle size HyperRez XP Carbohydrate® analytical column was used for separation of the carbohydrates. A Carbohydrate H+® cartridge was used as the guard column prior to the HyperRez XP® column. The mobile phase was 18.2 MΩ-cm deionized water at a flow rate 0.2 mL/min. The column compartment was held isothermally at 55°C. Each sugar was calibrated using a pure standard within the range of 0.5-10 mg/mL using a five point calibration. Further details of the hydrolysis method are available from Johnston and Brown [17].

Water Insolubles Analysis (Lignin Oligomers)

Water insoluble content, made up of predominately lignin oligomers, was quantified by mixing bio-oil with 80°C water using a bio-oil-to-mass ratio of 80:1. The mixture was placed in a 50 mL centrifuge tube and thoroughly mixed using a vortex mixer for one minute. Each centrifuge tube was sonicated for 30 min to ensure proper mixing. Next, the mixture was centrifuged at 2500 rpm for 20 minutes. The supernatant was filtered through a Whatman® size 42 filter (size retention of 2.5 µm) to capture the water insoluble content. Both the centrifuge tube and filter paper were then dried at 50°C for 24 hours. Accumulated mass on both the filter paper and centrifuge tube were considered water insoluble content.

Volatiles Analysis via Gas Chromatography-Flame Ionization Detection (GC/FID/MS)

Due to the chemical complexity of the bio-oils, a variety of methods were used to first identify and then quantify bio-oil volatiles. Each method utilized gas

chromatography (GC) operating with the same column and conditions; however, the detector was alternately switched from a low resolution Quadrupole Mass Spectrometer (Q-MS) for identification of the majority of bio-oil compounds, to a high resolution Time of Flight Mass Spectrometer (TOF-MS) for determining molecular formula of several compounds that could not be identified with the Q-MS, and finally to a flame ionization detector (FID) for quantification of all the identified compounds. The method of Kovats retention index [18] with n-alkanes ranging from C8-C20 was used to estimate retention time changes between each of the three systems.

A 60 m Zebron ZB-1701® (7KG-G006-11) capillary column with an inner diameter of 0.25 mm, film thickness of 0.25 μm, and a stationary phase of 14% Cyanopropylphenyl and 86% Dimethylpolysiloxane was used for GC analysis. The GC injector operated isothermally at 280°C in split/splitless mode with a split ratio of 20. Ultra high purity helium (99.999%) was used as the carrier gas at a constant flow rate of 2 ml/min through the column. The GC oven was set to first hold 35°C for 3 minutes, followed by ramping at 2°C/min to 250°C, followed by ramping at 5°C/min to 280°C where it was held for 3 minutes; providing a total run time of 119.5 minutes per sample.

A Varian® 320 Q-MS coupled with a Varian® 450-GC and 8400 autosampler was used for initial peak identification. One μL of a 5 wt. % bio-oil solution in methanol was injected on the GC for peak identification samples. The mass spectrometer operated in negative electron ionization mode (EI (-)). The source temperature was set at 280°C. The filament operated at -70 eV and an emission current of 68.75 μA. The detector scanned in the range of 30-650 Da at a rate of 2 scans per second. The 2008 NIST

library was used to identify several of the compounds, whereas compounds that were not identified, or had a low probability, were compared to literature for most likely match [19, 20]. Several compounds were not identifiable via Q-MS due to the fragmentation experienced using EI (-), therefore the TOF-MS was used to determine molecular formula of several previously unknown compounds.

A GCT® GCMS which is an orthogonal TOF-MS from Waters Inc., Milford, MA was used to acquire accurate mass data (GC-TOF). The system utilized a model 6890 GC from Agilent®, Santa Clara, CA, which is equipped with a model 7683 Autoinjector also from Agilent®. The GC-TOF operated in positive chemical ionization mode (CI (+)) utilizing ammonia dopant gas in attempt to identify molecular ions without fragmentation. The source temperature was set to 120°C and operated at 30 eV and 200 μA. The detector scanned in the range of 35-650 Da at a rate of 2 scans per second. The MS achieved a resolution near 7000. Accurate mass data was acquired using a calibrant of Chloropentafluorobenzene with an exact mass of 201.9609 Da.

For FID quantification bio-oil was mixed at approximately 33 wt. % in methanol. One μL of the mixture was injected on the GC per sample. Duplicate samples of each bio-oil were analyzed in duplicate on the GC-FID, resulting in a total of four chromatograms used to achieve the averages and standard deviations.

An alternative method was employed to quantify low boiling compounds with similar retention times as the methanol solvent (acetaldehyde, acetone, methanol, ethanol, and propanol). For the alternative method the bio-oil was mixed in water rather than methanol, however the GC analysis was identical to the standard method.

A Bruker® 430-GC with a Varian® CP-8400 liquid injection autosampler interfaced with Galaxy® software was used for GC-FID analysis. The FID was set at 300°C with 25 mL/min helium makeup flow, 30 mL/min hydrogen, and 300 mL/min air flow. Calibration was performed using the method outlined by de Saint Laumer et al. [21]. A four point calibration was first attained using methyl octanoate as a standard. The relative response factor of each individual compound was calculated using the enthalpy of combustion outlined in equations 5, 10, and 15 in the de Saint Laumer et al. paper [21]. The area response for each peak was first quantified using the calibration curve of methyl octanoate. The resulting mass based on methyl octanoate was multiplied by the relative response factor for the individual peak, resulting in an adjusted mass for the individual compound. Several bio-oil compounds were injected at known concentrations and compared to the theoretical yield obtained using the response factors with good correlation.

Ion Chromatography

Approximately 100 mg of bio-oil was dissolved in a mixture of 1.5 mL methanol and 6 mL deionized water for organic acids analysis. Samples analyzed to have acid concentrations above the calibration range were diluted with 40 mL of deionized water rather than 6 mL to adjust the acid concentration within range. The sample was filtered through a Whatman® 0.45 μm glass microfiber filter before analysis.

A Dionex® ICS3000 ion chromatography system with a conductivity detector and an Anion Micromembrane Suppressor (AMMS-ICE 300®) was used for organic acids analysis. The Dionex® system was interfaced with Chromeleon® software

version 6.8. Tetrabutylammonium hydroxide in water at a concentration of five mM was used to regenerate the suppressor at a flow rate of 4-5 mL/min. A mixture of 1.0 mM heptaflourobutyric acid in water was used for the eluent at a flow rate of 0.120 mL/min at 19°C. An IonPac® ICE-AS1 4x50 mm guard column in series with an IonPac® ICE-AS1 4x250 mm analytical column were used for separation. Standards of acetate, propionate, formate and glycolate were purchased from Inorganic Ventures to calibrate the instrument. The concentrated standard was certified at 200.0 ± 1.3 mg/L for all acids and was diluted down with 18.2 MΩ-cm ultrapure deionized water to concentrations of 10, 25, 67, 100, 200 mg/L to achieve a five point linear calibration.

Results and Discussion

Pyrolysis experiments were performed in duplicate for each feedstock. Error bars in the figures indicate standard deviation of the duplicate trials. The Student T-test was used to compare the mean value from each treatment and the p-values are reported in *Appendix A and Appendix B.* A p-value of less than 0.05 indicates a statistically significant difference at a 95% confidence interval, whereas a p-value of 0.10 or less indicates a statistically significant difference in the means at a 90% confidence interval, and so on.

Bio-oil

As shown in Figure 1, bio-oil mass yield from red oak decreased by 8% after AAEM passivation; from 57.9 wt. % to 53.0 wt. % of feedstock. Conversely, with AAEM passivated switchgrass the bio-oil yield increased by 4%; from 54.3 wt. % to

56.7 wt. % of feedstock. The increase from switchgrass, however, showed little statistical significance. It should be noted that the sum of all subsequent bio-oil analyses accounted for 68.8 wt. %, 82.2 wt. %, 72.3 wt. %, and 76.7 wt. % of the total bio-oil, respectively, for red oak, AAEM passivated red oak, switchgrass and AAEM passivated switchgrass.

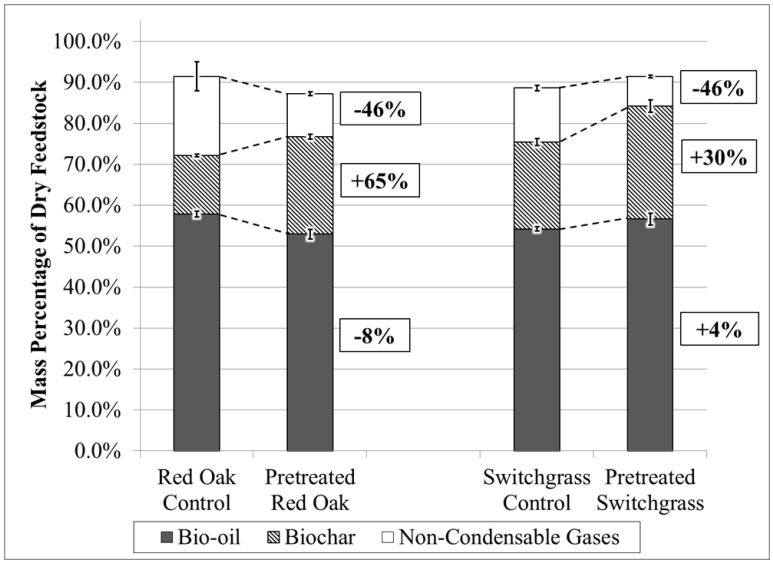

Figure 1: Mass balance comparison for control and AAEM passivated feedstocks.

Carbohydrate Products

Anhydrosugars

Anhydrosugars from pyrolysis of AAEM passivated feedstock considerably increased for both red oak and switchgrass, both at 95% confidence. As shown in Figure 2, the sugar yield from AAEM passivated red oak increased by 180% compared to the control, from 6.1 wt. % to 17.0 wt. % of feedstock. Similarly with AAEM passivated switchgrass the sugar yield increased by 198% compared to the control, from 4.4 wt. % to 13.1 wt. % of feedstock. All individual anhydrosugars except for xylosan

increased significantly with AAEM passivation. Levoglucosan made the greatest contribution to the increase as a result of AAEM passivation, increasing by 316% from red oak and 388% from switchgrass.

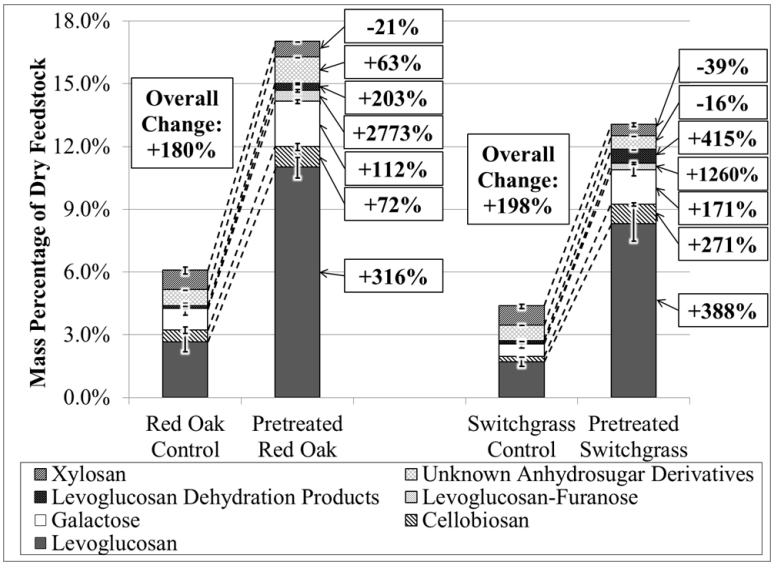

Figure 2: Sugar yield from control and AAEM passivated feedstocks.

Compounds labeled as levoglucosan dehydration products consisted of 1,4:3,6-dianhydro-a-D-glucopyranose (singly dehydrated levoglucosan) and levoglucosenone (doubly dehydrated levoglucosan). Levoglucosan dehydration products from red oak increased with AAEM passivation, from 0.11 wt. % to 0.33 wt. % of feedstock. For switchgrass the increase was more drastic, increasing from 0.13 wt. % to 0.67 wt. % of feedstock. Although both 1,4:3,6-dianhydro-a-D-glucopyranose and levoglucosenone are generally low in yield, they are useful to look at since they result from the dehydration of levoglucosan and therefore give some indication as to the fate of biomass carbohydrates from pyrolysis [22]. The increase in levoglucosan dehydration products of over 200% and over 400% from AAEM passivated red oak and switchgrass,

respectively, is likely due to acid catalyzed dehydration during pyrolysis. The more dramatic increase in levoglucosan dehydration products from switchgrass correlates with an increased amount of acid used for passivation.

Mass spectra of the compounds labeled as "Unknown Anhydrosugar Derivatives" suggested they have similar structure to other anhydrosugars; however, their molecular formula found via GC-TOF was not consistent with conventional anhydrosugars. Unknown anhydrosugar derivatives yield increased slightly with AAEM passivation of red oak. The control red oak produced 0.8 wt. % unknown anhydrosugar derivatives whereas the AAEM passivated red oak produced 1.3 wt. %. Alkali and alkaline earth metal passivation of switchgrass led to a slight reduction in unknown anhydrosugar derivatives; decreasing from 0.8 wt. % of feedstock from the control to 0.6 wt. % of feedstock from AAEM passivated switchgrass.

The molecular formula of the unknown anhydrosugar derivatives, which was found from the molecular ion via GC-TOF, suggests several may be glycosides with various functionality attached to an anhydrosugar backbone, similar to those found by Smith et al. [23]. Chaiwat et al. [24] suggests that treatment of polysaccharides with acid leads to cross-linking within the cellulose and hemicellulose structure. Depolymerization of cross-linked sugars may then produce several sugar fragments that aren't common in the native biomass. Detailed structural analysis of the unknown anhydrosugar derivatives is outside the scope of this paper, however, the molecular formula of each compound found using GC-TOF is shown in *Appendix A* and *Appendix B*. Each of unknown anhydrosugar derivatives is labeled as "Carbohydrate

Derivative #" where the # is replaced by the numbers 2-16. It should be noted that several unknown peaks appeared in HPLC analysis that were not quantified which are likely some of the unidentified anhydrosugars found via GC analysis.

Total Sugars

Bio-oil carbohydrates were hydrolyzed to glucose, xylose, or sorbitol for the purpose of determining total sugar content. In this section the sugars are labeled by their hydrolysis products; e.g. all saccharides that are hydrolyzed to form glucose are termed "glucose hydrolysable sugars." The sum of all the glucose, xylose, and sorbitol hydrolysable sugars is termed "total sugars." As shown in Figure 3, the yield of total sugars was 15.9 wt. % of feedstock from AAEM passivated red oak, a 105% increase over the control while the yield of total sugars from AAEM passivated switchgrass was 16.2 wt. % of feedstock, a remarkable 259% increase over the control.

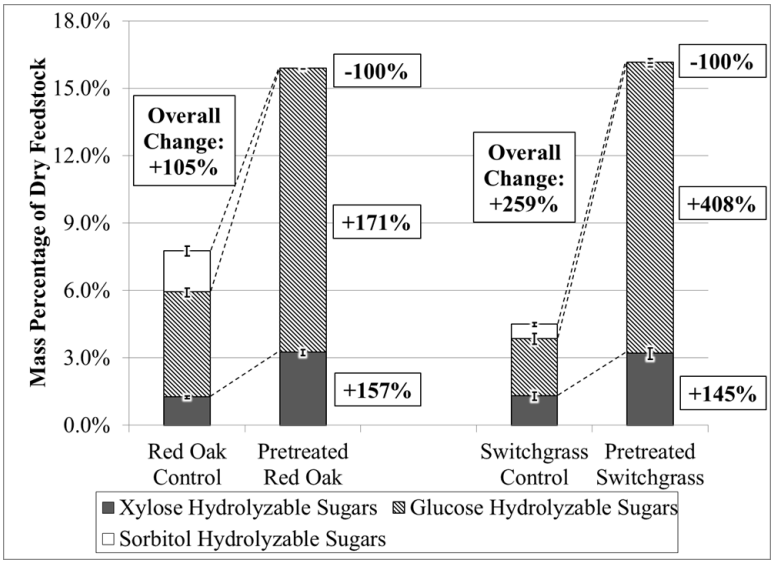

Figure 3: Total sugar yields from control and AAEM passivated feedstocks.

Looking at the yield of individual hydrolysis products, sorbitol was completely eliminated in both of the AAEM passivated feedstocks. Sorbitol, a sugar alcohol, is the most highly hydrated of the analyzed sugars. Dehydration by the acid used for AAEM passivation likely prevented formation of the more hydrated compounds, thus decreasing the yield of sorbitol hydrolysable sugars. Glucose hydrolysable sugars accounted for the largest difference with AAEM passivation, increasing by 171% in red oak and by 408% in switchgrass. The increase for switchgrass is similar to the increase in levoglucosan as would be expected. For red oak the yield of levoglucosan increased by 316%, whereas the glucose hydrolysable sugars increased by only 171%. The large discrepancy between increase in levoglucosan and increase in glucose hydrolysable sugars suggests that a significant portion of the glucose hydrolysable sugars from untreated red oak are derived from sugars other than levoglucosan, possibly oligosaccharides or some of the unknown anhydrosugar derivatives.

Xylose hydrolyzable sugars increased by nearly 150% from both red oak and switchgrass after AAEM passivation; however the yield of the anhydrosugar precursor xylosan decreased from each feedstock. The increase in xylose hydrolysable sugars suggests that the AAEM passivation is effective at increasing yield of pentoses and pentosans from hemicellulose; however, several of the individual pentosans have not yet been identified or quantified. The overall yield of sugars accounted for via HPLC and GC analysis was slightly higher than the yield of total sugars measured via hydrolysis. The difference in quantity of anhydrosugars and hydrolysable sugars suggests that several of the anhydrosugars might not be hydrolysable to glucose, xylose, or sorbitol.

For instance, previous experiments have shown that levoglucosenone, a double dehydration product of levoglucosan, is not capable of hydrolyzing to glucose with the hydrolysis method used here. It is expected that several of the other anhydrosugars exhibit similar behavior, especially certain isomers or glycosides that contain additional functionalities.

Non-Condensable Gases and Light Oxygenates

As shown in Figure 4, NCGs decreased by 46% for both AAEM passivated red oak and switchgrass. In red oak the result was not significant at the 90% confidence interval, whereas it was statistically significant for switchgrass. Patwardhan et al. [6] showed that light oxygenates, including NCGs, were major products of AAEM catalyzed pyranose ring fragmentation in cellulose. The decrease in NCGs is therefore an indication of less ring fragmentation during pyrolysis as a result of AAEM passivation [6].

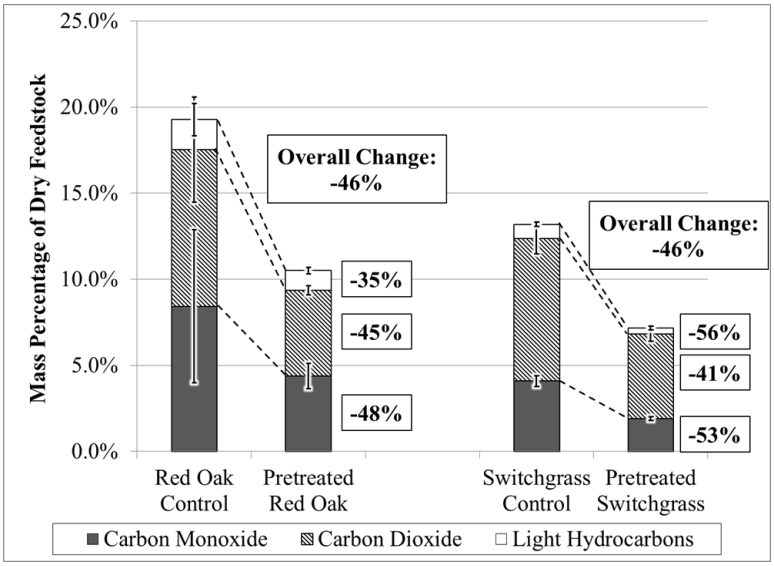

Figure 4: Non-condensable gas yields from control and AAEM passivated feedstocks.

As shown in Figure 5, light aldehydes decreased by 56% from red oak (1.06 wt. % to 0.47 wt. % of feedstock) and by 32% from switchgrass (0.74 wt. % to 0.50 wt. % of feedstock) after AAEM passivation. Acetaldehyde and glycolaldehyde are the only two aldehydes which were quantified in this work, although several other aldehydes including formaldehyde and larger aldehydes have been observed by other researchers to be major products of AAEM catalyzed fragmentation of glucose rings [4, 6, 8, 25]. The decrease in aldehydes is therefore indicative of less pyranose and furanose ring fragmentation from holocellulose pyrolysis after AAEM passivation.

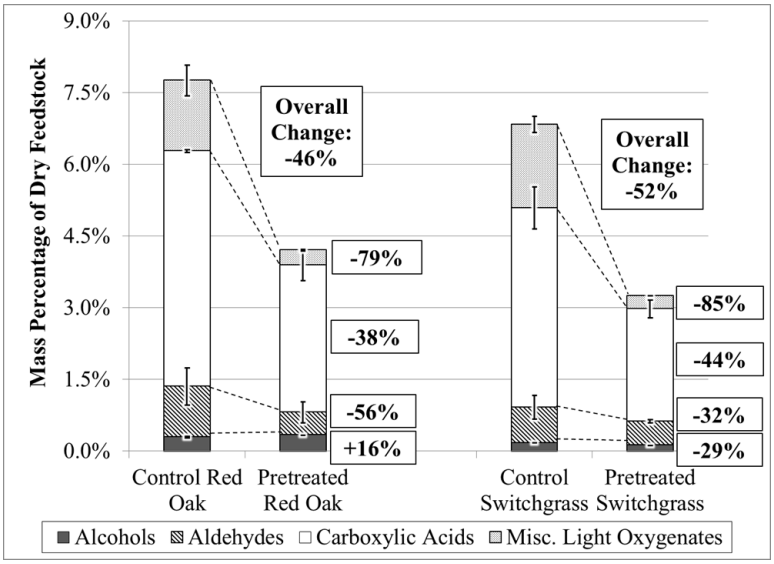

Figure 5: Light oxygenates yield from control and AAEM passivated feedstocks.

Aldehydes are known to undergo polymerization and condensation reactions such as aldol condensation and Diels-Alder cyclization reactions; both of which are catalyzed by acids. The mixture of aldehydes, alcohols, and carboxylic acids in bio-oil therefore lead it to be very unstable; quickly polymerizing to form resinous

material [26]. Glycolaldehyde itself is so reactive toward polymerization, even with itself, that the monomer is not available for purchase as a standard. Therefore glycolaldehyde could only be confirmed via mass spec and quantified via theoretical response factors. Glycolaldehyde nonetheless is commonly reported in bio-oils. Due to its reactivity toward polymerization it is doubtful that glycolaldehyde is a constituent of bio-oil and is more likely a degradation product of unstable bio-oil components during analysis. To our knowledge glycolaldehyde is always quantified via GC, meaning that the bio-oil is first subject to a high temperature injector where it can form from degradation of intermediates, such as those found by Smith et al. [23]. Regardless, the decrease in aldehydes will lead to a more stable bio-oil.

Carboxylic acids decreased by 29% from red oak (3.63 wt. % to 2.57 wt. % of feedstock) and by 44% from switchgrass (4.17 wt. % to 2.36 wt. % of feedstock) after AAEM passivation. Carboxylic acids, especially acetic acid, are known to form from the pyrolysis and fragmentation of all three biomass constituents, with the majority of fragmented acetyl groups coming from pentosans in the hemicellulose [27, 28]. The work by Kuzhiyil et al. [7] showed that AAEM passivation was effective on preventing ring fragmentation in cellulose; however AAEM passivation was not tested on hemicellulose. Since most of the acetic acid is derived from hemicellulose, the decrease in acetic acid likely indicates that AAEM passivation is effective on preventing ring fragmentation in hemicellulose.

The category labeled “miscellaneous light oxygenates” consists of primarily light ketones; hydroxyacetone making up the majority. Miscellaneous light oxygenates

decreased by79% from red oak (1.47 wt. % to 0.31 wt. % of feedstock) and by 85% from switchgrass (1.75 wt. % to 0.27 wt. % of feedstock) with AAEM passivation. Anything grouped under the category miscellaneous light oxygenates is expected to come from fragmentation of carbohydrates; similar to all of the other light oxygenates. Therefore, the decrease in miscellaneous light oxygenates likely reflects reduced fragmentation of biomass carbohydrates.

Overall light oxygenates decreased by 46% and 52% from red oak and switchgrass, respectively, with AAEM passivation. The decrease in light oxygenates corresponds with a decrease in NCGs, suggesting light oxygenates and NCGS form via similar mechanisms; likely the mechanisms described by Patwardhan et al. [6]. The sum of NCGs and light oxygenates decreased by 12.4 wt. % from red oak and 9.5 wt. % from switchgrass with AAEM passivation. The sugar yield increased by 8.1 wt. % from red oak and 11.7 wt. % from switchgrass. Therefore, the decrease in light oxygenates is inversely proportional to the increase in sugars, further supporting the hypothesis that AAEM passivation preferentially increases depolymerization of holocellulose and decreases sugar motif fragmentation. Hence, it would be expected that light oxygenates would decrease as sugars increase since they are formed from the same material.

Reaction Water

Reaction water was calculated by first determining the total mass of water in the bio-oil using Karl Fischer titration followed by subtracting the mass of water that was contributed from moisture in the feedstock. As shown in Figure 6, the reaction water increased with AAEM passivation and was greater for AAEM passivated red oak. The

increase in water correlates with an increase in char; each being a product of biomass carbonization [29]. The increase in water may also be due to increased dehydration due to the catalytic effects of the acid.

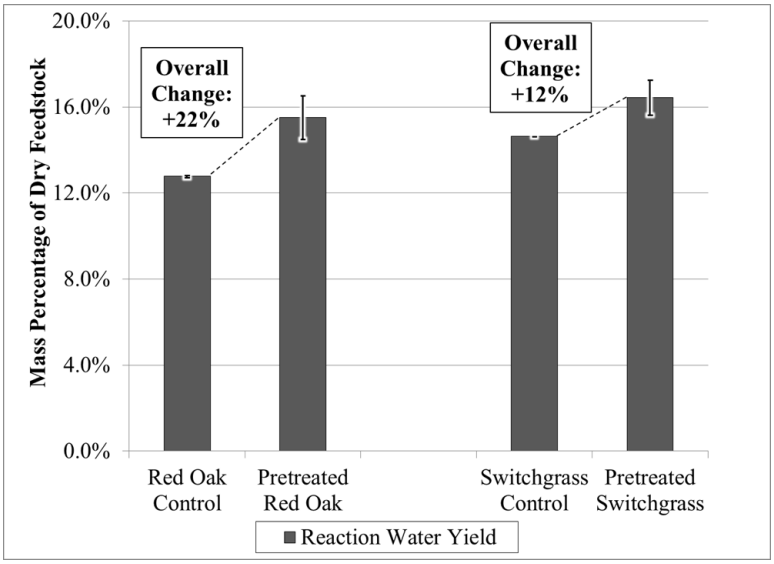

Figure 6: Reaction water yield from control and AAEM passivated feedstocks.

Carbohydrate Dehydration Products

Compounds initially expected to come from dehydration of carbohydrates include furans, tetrahydrofurans, lactones, cyclopentanes, pyrans, and miscellaneous furanoids. Each compound classification was categorized into the carbohydrate dehydration products (CDPs) group since each of them have a higher carbon-to-oxygen ratio than anhydrosugars, however do not contain benzene rings typical of lignin products. As shown in Figure 7, overall CDPs decreased with AAEM passivation, which was the case for all classifications except furans. Acid catalyzed dehydration of carbohydrates is expected to increase CDPs in AAEM passivated feedstocks due to the addition of acid. However, the AAEM passivated feedstocks produced less CDPs than

the control. Therefore, it is likely that several of the CDPs are formed from reactions other than carbohydrate dehydration.

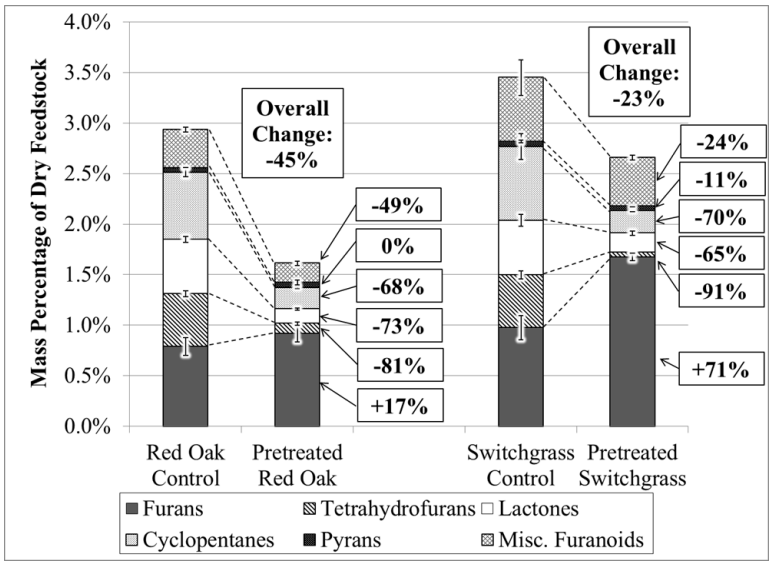

Figure 7: Carbohydrate dehydration product yields from control and AAEM passivated feedstocks.

Cyclopentanes decreased by nearly 70% from each AAEM passivated feedstock; decreasing from 0.66 wt. % to 0.19 wt. % of feedstock from red oak and 0.68 wt. % to 0.21 wt. % of feedstock from switchgrass. Cyclopentanes have been identified by many researchers; however, to our knowledge their formation has not been investigated in detail. Lack of research on cyclopentanes is most likely due to their low yield of typically less than 1 wt. % of the original biomass. Cyclopentanes have been investigated more extensively in the flavor and fragrance industry [30] and in the roasting of coffee [31]. Due to the limited vapor pressure [32] and absence of odor for anhydrosugars, cyclopentanes, lactones, and related compounds are likely major contributors to the typically sweet smell of bio-oil. Shaw et al. [33] found cyclopentanes

and lactones to be produced in the acid catalyzed degradation of carbohydrates in an aqueous phase, which may be a source of carbohydrate degradation commonly observed in bio-oil aging. Niemela et al. [34] found similar compounds to result from the condensation of light oxygenate precursors through aldol-condensation reactions that also occurred in the condensed phase. The AAEM passivated feedstocks would be expected to increase cyclopentanes due to acid catalyzed dehydration if in fact cyclopentanes were primary products resulting from dehydration during pyrolysis. Cyclopentanes however decreased in AAEM passivated feedstocks and the decrease directly correlated with a decrease in light oxygenates. Therefore it is likely that cyclopentanes are secondary products resulting from condensation of light oxygenates in the condensed bio-oil.

Similar to cyclopentanes, lactones decreased by nearly 70% from both AAEM passivated feedstocks; decreasing from 0.54 wt. % to 0.13 wt. % of feedstock from red oak and 0.51 wt. % to 0.19 wt. % of feedstock from switchgrass. It is likely that, similar to cyclopentanes, lactones are formed via condensation reactions of light oxygenates in the bio-oil as was found by Niemela et al. [34].

Tetrahydrofurans decreased with AAEM passivation by 81% from red oak (0.52 wt. % to 0.09 wt. % of feedstock) and 91% from switchgrass (0.49 wt. % to 0.04 wt. % of feedstock). To our knowledge, no mechanisms have been found to directly produce tetrahydrofurans from biomass pyrolysis. The saturated furan ring is unlikely to be formed from carbohydrates as the elimination of hydroxyl groups from furan moiety in carbohydrate dehydration would more likely produce unsaturated furan

moieties. Similar to cyclopentanes and lactones, the tetrahydrofurans are likely formed via secondary condensation of light oxygenates in the bio-oil.

Furans increased by 16% (from 0.79 wt. % to 0.92 wt. % of feedstock) from red oak and 70% (from 0.98 wt. % to 1.67 wt. % of feedstock) from switchgrass. Furans, especially furfural and 5-(hydroxymethyl)furfural, are known to be products of carbohydrate dehydration [4, 35-37]. The more significant increase with switchgrass is likely due to the increased acid used in AAEM passivation which likely aids in acid catalyzed dehydration of carbohydrates [35]. The increase in furans from AAEM passivated feedstock is consistent with observations of Kuzhiyil et al. [7] and with those of several others investigating different methods of using acid to increase sugar yields [14, 38].

The group labeled "miscellaneous furanoids" consists of compounds that were not structurally identified; however have molecular formulas and fragmentation patterns similar to furans, lactones, or cyclopentanes. The compound labeled in *Appendix A* and *Appendix B* as "Furan Derivative 16A" was the most dominant of the unknown furanoids, yielding as much as 0.5 wt. % from pyrolysis of the untreated switchgrass. Alkali and alkaline earth metal passivation reduced miscellaneous furanoids from 0.28 wt. % to 0.13 wt. % of feedstock from red oak and from 0.49 wt. % to 0.32 wt. % of feedstock from switchgrass. Like all CDPs except furans, miscellaneous furanoids decreased with AAEM passivation. Miscellaneous furanoids are therefore likely cyclopentanes, lactones, or tetrahydrofurans as opposed to simple furan derivatives.

Lignin Products

Alkali and alkaline earth metal passivated feedstock produced fewer water insoluble lignin oligomers, also known as pyrolytic lignin. As shown in Figure 8, lignin oligomers from AAEM passivated red oak decreased from 9.8 wt. % to 5.0 wt. % of feedstock, a reduction of 49%. Switchgrass showed a similar trend decreasing from 9.0 wt. % to 7.7 wt. % of feedstock, although the decrease was not significant at the 90% confidence interval. Mass yields of volatile lignin products are shown in Figure 9. Phenols, containing no methoxyl side chains, decreased by 54% from AAEM passivated red oak, from 0.51 wt. % to 0.23 wt. % of feedstock. Total phenols from switchgrass decreased by 63%, from 1.06 wt. % to 0.39 wt. % of feedstock.

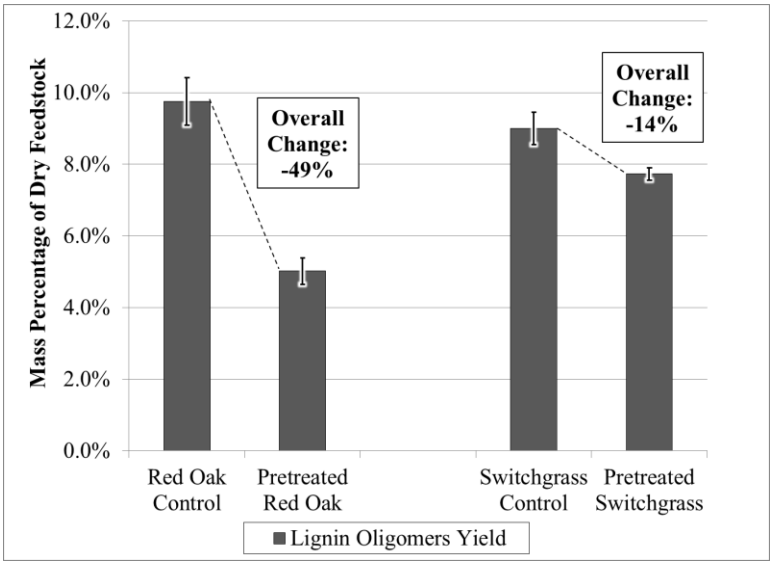

Figure 8: Lignin oligomer yields from control and AAEM passivated feedstocks.

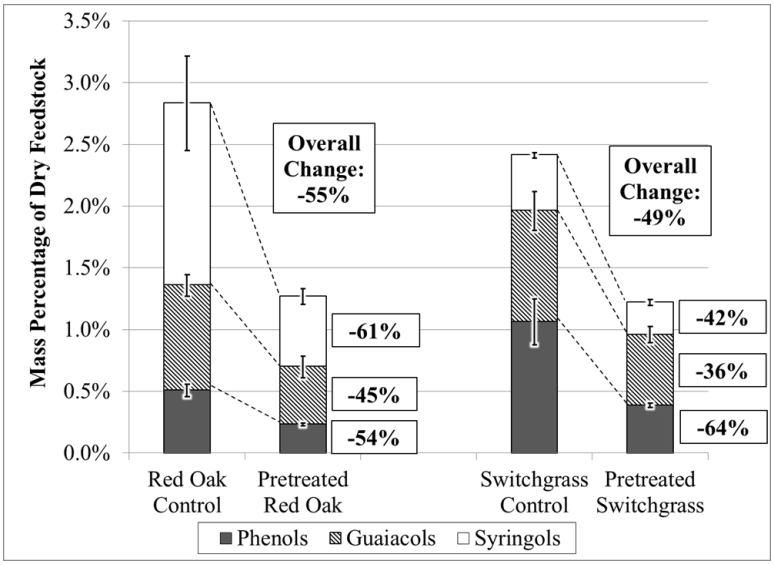

Figure 9: Volatile lignin product yields from control and AAEM passivated feedstocks.

Guaiacols, containing one methoxyl side chain, decreased by 45% from AAEM passivated red oak, from 0.85 wt. % to 0.47 wt. % of feedstock. Guaiacols from AAEM passivated switchgrass decreased by 36%, from 0.90 wt. % to 0.57 wt. % of feedstock. Guaiacols with unsaturated side chains such as eugenol, isoeugenol, and methyleugenol, decreased most dramatically to near undetectable levels in bio-oil from AAEM passivated feedstock. 1-(4-hydroxy-3-methoxyphenyl)ethanone is another compound that was significantly affected by AAEM passivation; decreasing by nearly 70% from both feedstocks.

Syringols, containing two methoxyl side chains, decreased by 67% from AAEM passivated red oak, from 1.47 wt. % to 0.49 wt. % of feedstock. Switchgrass showed a similar trend with a decrease of 42%, from 0.45 wt. % to 0.26 wt. % of feedstock from AAEM passivation. Similar to guaiacols, syringols with unsaturated side chains such as

2,6-dimethoxy-4-vinylphenol, 4-(2-propenyl)-2,6-dimethoxyphenol, and 4-(1-propenyl)-2,6-dimethoxyphenol, decreased the most significantly from AAEM passivation.

Total phenolic compounds decreased more significantly from red oak than switchgrass after AAEM passivation. Red oak, being a hardwood, is known to contain more S-lignin compared to switchgrass [39]. The decrease in red oak lignin products is therefore consistent with the observation of Asmadi et al. [40] who found S-lignin to be more reactive in secondary polymerization and coking reactions than G-lignin. Asmadi et al. [40] found the methoxyl side chains of guaiacol and syringol to undergo homolysis and rearrangement at temperatures as low as 400-450°C; well below the pyrolysis temperatures used in this work. Homolysis of ether bonds from both the guaiacol and syringol moieties at low temperatures produces highly reactive radicals that then likely polymerize to produce char and oligomers from lignin. In another study Asmadi et al. [41] found that the reactivity of phenolic monomers generally increased with increasing numbers of substituents groups. Compounds from S-lignin would therefore have the highest number of substituents per benzene moiety making them the most reactive.

In contrast, Mullen et al. [42] found S-lignin to be less reactive in recombination reactions from comparison of oak and barley hull pyrolysis. Scholze et al. [43] also found conflicting results and attributed the higher reactivity of G-lignin to the open C5 position on guaiacol moieties which is prone to condensation reactions. Conflicting results may indicate that several mechanisms are responsible for the formation of char and oligomers from lignin. Mechanisms involving the quinone methide intermediate, as suggested by Hosoya et al. [44, 45], would lead to bond formation on the methide side

chain. Mechanism involving the open C5 position on guaiacol moieties, as suggested by Scholze et al. [43], would more likely form bonds directly on the aromatic ring. Therefore, in addition to the methoxy groups on the lignin moieties, the linkage type and proximity to constituents capable of cross-linking likely plays a role in char formation. A more detailed analysis of char and lignin oligomer structure would need to be performed in order to determine the most important mechanisms in their formation.

Biochar

The biochar yield from red oak increased from 14.3 wt. % to 23.8 wt. % of dry feedstock for AAEM passivated feedstock, an increase of 65%. The biochar yield from switchgrass increased from 21.2 wt. % from the control to 27.6 wt. % of feedstock from AAEM passivated switchgrass, an increase of 30%. Char produced from the AAEM passivated feedstocks had different physical properties than char produced from untreated material. Figure 10 provides a visual comparison of each feedstock and the corresponding char after pyrolysis.

The control and AAEM passivated feedstocks look similar except for a minor change in color. Char produced from each of the control feedstocks is similar in size to the original biomass although black in color and more porous. Char produced from AAEM passivated red oak ranges in size from fine powder to large agglomerates that encapsulated some of the heat carrier. Char from AAEM passivated switchgrass also contained both fine powder and agglomerates; however large agglomerates were not as prevalent. Char from both AAEM passivated feedstocks took on a vitreous luster and appeared as if it was in a molten state before dehydrating to large clumps. The finer

material is likely the product of agglomerates being mechanically pulverized as they proceeded down the auger reactor.

Figure 10: Biomass and biochar comparisons. (Top Row: Red Oak Control, AAEM Passivated Red Oak, Switchgrass Control, AAEM Passivated Switchgrass; Bottom Row: Red Oak Control Char, AAEM Passivated Red Oak Char, Switchgrass Control Char, AAEM Passivated Switchgrass Char)

Agglomerated material was difficult to separate from the heat carrier. Feedstock had been sieved prior to pyrolysis to pass a 710 μm screen whereas heat carrier material was sieved to eliminate all particles below 710 μm. Thus, in the absence of agglomeration, char particles would be expected to be smaller than the heat carrier. As shown in Figure 11, over 95% of the char was separated from the heat carrier by sieving from each of the control feedstocks. Therefore, only 5% of the char had to be burned from the heat carrier using the char burn-off procedure. In contrast, from pyrolysis of AAEM passivated red oak only about 10% of the char was recovered by sieving and 90% of the char had to be removed via the char burn-off procedure. From switchgrass

the split was approximately half and half between biochar that could be removed by sieving and biochar agglomerated with heat carrier. The substantial differences in char from AAEM passivated feedstocks suggest that the origin and mechanism of char formation are likely different for each feedstock.

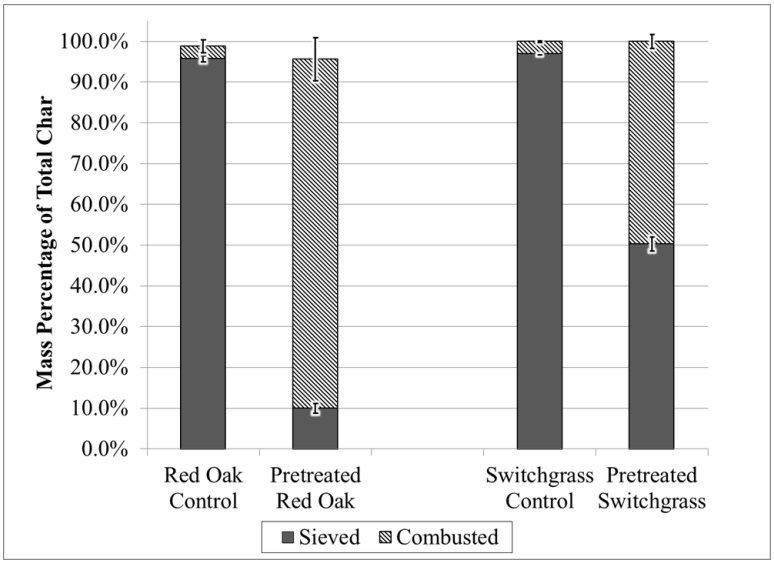

Figure 11: Char separation comparison for control and AAEM passivated feedstocks.

Biochar increased by 9.5 wt. % and 6.4 wt. % from AAEM passivated red oak and switchgrass, respectively. Simultaneously lignin-derived products decreased by 6.4 wt. % and 2.4 wt. % from red oak and switchgrass, respectively, as a result of AAEM passivation. Decrease in lignin-derived phenolic compounds can therefore respectively explain 67% and 38% of the char increase for AAEM passivated red oak and switchgrass. Bio-oil from the red oak control also had a higher level of methoxyl containing S- lignin volatile products. Therefore red oak lignin has more methoxyl groups and AAEM passivated red oak produces more lignin-derived char. Taken

together, the facts that red oak lignin contains more methoxyl groups and AAEM passivated red oak produces more lignin derived char suggests that methoxyl groups are likely precursors to char formation after AAEM passivation.

The number of methoxyl side chains in lignin has been observed to affect reactivity of the lignin toward secondary polymerization and coking reactions [40,46]. Hosoya et al. [44] postulated a mechanism for the formation of char from methoxyl side chains in lignin where electron donating properties of the methoxyl side chain contributed to its higher reactivity. The reaction is thought to be initiated by H-abstraction from the phenolic hydroxyl group followed by rearrangement and dehydration within the aromatic ring to form an o-quinone methide intermediate. Zhou et al. [46] found Douglas fir, containing a high level of G-lignin, to produce additional char after being treated with sulfuric acid and postulate that sulfuric acid catalyzes the dehydration step in the mechanism found by Hosoya et al. Red oak, being a hardwood, contains many more methoxyl side chains than the lignin in switchgrass. Therefore, the increased lignin-derived char from red oak can likely be explained by the additional methoxyl side chains of the S-lignin in red oak, compared to the H-lignin of switchgrass.

The remaining 33% char increase from AAEM passivated red oak (3.1 wt. % char) and 62% char increase from switchgrass (4.0 wt. % char) must be attributable to carbonization of carbohydrate. Kuzhiyil et al. [7] found that micropyrolysis trials of AAEM passivated red oak and switchgrass produced 23.4 wt. % and 15.4 wt. % levoglucosan, respectively. Although the red oak and switchgrass used in this work

were AAEM passivated in the same manner, the levoglucosan yield was just 11.0 wt. % for AAEM passivated red oak and 8.3 wt. % for AAEM passivated switchgrass. Comparing levoglucosan yields from this work to those found by Kuzhiyil et al. [7] results in a difference of 12.4 wt. % from AAEM passivated red oak and 7.1 wt. % from AAEM passivated switchgrass which could easily account for char not derived from lignin.

Micropyrolyzers use microgram scale batches of biomass and have a high sweep gas-to-biomass ratio. The continuous flow auger reactor, on the other hand, has gram scale amounts of biomass constantly added to the system and uses a much lower sweep gas-to-biomass ratio. Therefore mass transfer is much more limited in the continuous flow auger reactor. The initial product of cellulose depolymerization is liquid levoglucosan. The relatively low vapor pressure of levoglucosan, even at pyrolysis temperatures, leads it to be subject to competing processes of volatilization and oligomerization [47, 48, 49]. Carbohydrate oligomers formed from polymerization of levoglucosan are susceptible to dehydration and char formation. Mass transfer limitation in the auger reactor therefore likely decrease volatilization; enhancing the oligomerization reactions. Carbohydrate oligomers, being less likely to volatilize, would instead remain in the reactor and eventually dehydrate to char. Mass transfer of carbohydrate products may be further hindered by the increased polymerization and charring of lignin-derived products which essentially act to trap carbohydrate vapors within the biomass particle. Increased reaction water from AAEM passivated feedstocks is a likely indicator of increased dehydration reactions coming from char formation.

Another possible source of the increased carbohydrate-derived char is from the carmelization of sugars during pyrolysis. Carmelization reactions of sugars have been shown to proceed via Maillard type reactions leading to both light products such as furans, and heavy products referred to as caramelans, caramelens, and caramelins [50-52]. Hodge et al. [53] found the enolization and dehydration steps during carmelization to be catalyzed by acids and acid salts. Carbohydrate carmelization reactions in AAEM passivated feedstocks would therefore be expected to be catalyzed by acid salts formed during the passivation process. Caramelized products with higher molecular weights would be involatile and likely remain in the reactor eventually dehydrating to char.

Acid catalyzed carmelization of carbohydrates can also explain the different yields of carbohydrate-derived char from red oak and switchgrass. Assuming the entire decrease in lignin-derived products resulted in char, the remaining 3.1 wt. % and 4.0 wt. % char from red oak and switchgrass, respectively, would be carbohydrate derived. Switchgrass had a much higher level of AAEMs and therefore required more sulfuric acid for AAEM passivation (0.4 wt. % acid for red oak versus 2.0 wt. % acid for switchgrass). Acid salts produced from AAEM passivation would therefore be more prevalent in switchgrass than in red oak. More acid salts likely result in more acid catalyzed carmelization and dehydration of carbohydrates during pyrolysis. Furans, known to result from both carmelization and dehydration of carbohydrates, increased more significantly with switchgrass (a 71% increase from switchgrass versus a 16% increase from red oak). The increase in furans is another likely indicator of increased

carmelization and dehydration with additional acid salts. Along with furans, increased carmelization would also result in increased carbohydrate oligomers. More carbohydrate oligomers that are unable to volatilize would lead to more carbohydrate-derived char. Therefore the increased carbohydrate-derived char from AAEM passivated switchgrass is likely due to the higher abundance of acid salts.

Conclusions

Alkali and alkaline earth metal passivation of red oak and switchgrass prior to pyrolysis was shown to substantially increase total sugar yield on a continuous, lab-scale, auger pyrolyzer. Light oxygenates and non-condensable gases decreased in direct proportion to the increase in sugars. The combined increase in anhydrosugar yield and decrease in light oxygenates yield supports the hypothesis that AAEM passivation enhances glycosidic bond cleavage as opposed to pyranose and furanose ring scission within plant polysaccharides. Biochar increased with AAEM passivation of both feedstocks compared to their control. Alkali and alkaline earth metal passivated red oak resulted in more lignin-derived char, whereas AAEM passivated switchgrass resulted in more carbohydrate-derived char. The higher S-lignin content of red oak is expected to produce the additional lignin-derived char. Acid catalyzed carmelization of carbohydrates is hypothesized to be responsible for the increase in carbohydrate-derived char. The demonstration of increased sugar production from AAEM passivated feedstocks on a continuous auger pyrolyzer at the kilogram scale is an important step for developing fast pyrolysis of lignocellulosic biomass into a commercial process.

Acknowledgements

We gratefully acknowledge generous funding from the Phillips 66 Company and the U.S. Department of Energy. The authors appreciate the assistance of Nate Hamlett, Emily Hansen, Nick Miller, Jordan Donner, William Paisley, and Nicholas Jaegers in running pyrolysis experiments and preparing samples for analysis. We would like to thank Ryan Smith and Marjorie Rover for their help in many aspects of this project. We also thank Dr. Max Morris for discussions on statistical analysis of the results. We appreciate the assistance of Dr. Steve Vessey at the Chemical Instrumentation Facility at Iowa State University for training and assistance pertaining to the Waters GC-TOF results included in this publication.

References

1. Regalbuto, J.R., *Cellulosic Biofuels-"Got Gasoline?* Science, 2009. **325**(5942): p. 822-824.

2. Huber, G.W., S. Iborra, and A. Corma, *Synthesis of Transportation Fuels from Biomass: Chemistry, Catalysts, and Engineering.* Chemical Reviews, 2006. **106**(9): p. 4044-4098.

3. Shafizadeh, F., R.H. Furneaux, T.G. Cochran, J.P. Scholl, and Y. Sakai, *Production of levoglucosan and glucose from pyrolysis of cellulosic materials.* Journal of Applied Polymer Science, 1979. **23**(12): p. 3525-3539.

4. Patwardhan, P.R., J.A. Satrio, R.C. Brown, and B.H. Shanks, *Product distribution from fast pyrolysis of glucose-based carbohydrates.* Journal of Analytical and Applied Pyrolysis, 2009. **86**(2): p. 323-330.

5. Piskorz, J., D.S.A.G. Radlein, D.S. Scott, and S. Czernik, *Pretreatment of wood and cellulose for production of sugars by fast pyrolysis.* Journal of Analytical and Applied Pyrolysis, 1989. **16**(2): p. 127-142.

6. Patwardhan, P.R., J.A. Satrio, R.C. Brown, and B.H. Shanks, *Influence of inorganic salts on the primary pyrolysis products of cellulose.* Bioresource Technology, 2009. **101**(12): p. 4646-4655.

7. Kuzhiyil, N., D. Dalluge, X. Bai, K.H. Kim, and R.C. Brown, *Pyrolytic Sugars from Cellulosic Biomass.* ChemSusChem, 2012. **5**(11): p. 2228-2236.

8. Yang, C.-y., X.-s. Lu, W.-g. Lin, X.-m. Yang, and J.-z. Yao, *TG-FTIR study on corn straw pyrolysis-influence of minerals.* Chemical Research in Chinese Universities, 2006. **22**(4): p. 524-532.

9. Zhou, S., D. Mourant, C. Lievens, Y. Wang, C.-Z. Li, and M. Garcia-Perez, *Effect of sulfuric acid concentration on the yield and properties of the bio-oils obtained from the auger and fast pyrolysis of Douglas Fir.* Fuel, 2013. **104**: p. 536-546.

10. Brown, R.C., D. Radlein, and J. Piskorz, *Pretreatment Processes to Increase Pyrolytic Yield of Levoglucosan from Herbaceous Feedstocks*, in *Chemicals and Materials from Renewable Resources*2001, American Chemical Society. p. 123-132.

11. Hassan, E.B., H. Abou-Yousef, and P. Steele, *Increasing the efficiency of fast pyrolysis process through sugar yield maximization and separation from aqueous fraction bio-oil.* Fuel Processing Technology, 2013. **110**: p. 65-72.

12. Scott, D.S., L. Paterson, J. Piskorz, and D. Radlein, *Pretreatment of poplar wood for fast pyrolysis: rate of cation removal.* Journal of Analytical and Applied Pyrolysis, 2001. **57**(2): p. 169-176.

13. Oudenhoven, S., R. Westerhof, N. Aldenkamp, D. Brilman, and S. Kersten, *Demineralization of wood using wood-derived acid: Towards a selective pyrolysis process for fuel and chemicals production.* Journal of Analytical and Applied Pyrolysis, 2012.

14. Di Blasi, C., C. Branca, and A. Galgano, *Thermal and catalytic decomposition of wood impregnated with sulfur-and phosphorus-containing ammonium salts.* Polymer Degradation and Stability, 2008. **93**(2): p. 335-346.

15. Brown, J.N., *Development of a lab-scale auger reactor for biomass fast pyrolysis and process optimization usingresponse surface methodology*, 2009, Iowa State University: Ames, Iowa.

16. Dalluge, D.L., Y.S. Choi, B.H. Shanks, and R.C. Brown, *Comparison of Direct Contact and Indirect Contact Heat Exchange in Levoglucosan Recovery from*

Cellulose Fast Pyrolysis. Manuscript submitted for publication (copy on file with author), 2013.

17. Johnston, P.A. and R.C. Brown, *Sugar Quantification withou Neutralization in Fast Pyrolysis Oils: Using High Performance Liquid Chromatography (HPLC) after Acid Hydrolysis.* Analytical Chemistry, 2013.

18. Kováts, E., *Gas-chromatographische Charakterisierung organischer Verbindungen. Teil 1: Retentionsindices aliphatischer Halogenide, Alkohole, Aldehyde und Ketone.* Helvetica Chimica Acta, 1958. **41**(7): p. 1915-1932.

19. Faix, O., I. Fortmann, J. Bremer, and D. Meier, *Thermal degradation products of wood.* Holz als Roh- und Werkstoff, 1991. **49**(7-8): p. 299-304.

20. Faix, O., D. Meier, and I. Fortmann, *Thermal degradation products of wood.* Holz als Roh- und Werkstoff, 1990. **48**(9): p. 351-354.

21. de Saint Laumer, J.-Y., E. Cicchetti, P. Merle, J. Egger, and A. Chaintreau, *Quantification in Gas Chromatography: Prediction of Flame Ionization Detector Response Factors from Combustion Enthalpies and Molecular Structures.* Analytical Chemistry, 2010. **82**(15): p. 6457-6462.

22. Nimlos, M.R. and R.J. Evans, *Levoglucosan Pyrolysis.* Fuel Chem Div Prepr, 2002. **47**(1): p. 393-394.

23. Smith, E.A., C.P. Hutchinson, D.P. Cole, and Y.-J. Lee. *A High Resolution Mass Spectrometry Platform for Studying Kinetics of Biomass Pyrolysis: Single Particle Pyrolysis Utilizing μPy-APCI-TOF*. In *Proceedings of the 61st ASMS Conference on Mass Spectrometry and Allied Topics*. 2013. Minneapolis, MN.

24. Chaiwat, W., I. Hasegawa, T. Tani, K. Sunagawa, and K. Mae, *Analysis of cross-linking behavior during pyrolysis of cellulose for elucidating reaction pathway.* Energy & Fuels, 2009. **23**(12): p. 5765-5772.

25. Nowakowski, D.J., J.M. Jones, R. Brydson, and A.B. Ross, *Potassium catalysis in the pyrolysis behaviour of short rotation willow coppice.* Fuel, 2007. **86**(15): p. 2389-2402.

26. Diebold, J.P., I. Thermalchemie, and L. National Renewable Energy, *A review of the chemical and physical mechanisms of the storage stability of fast pyrolysis bio-oils*2000, Golden, CO: National Renewable Energy Laboratory.

27. Demirbaş, A., *Mechanisms of liquefaction and pyrolysis reactions of biomass.* Energy Conversion and Management, 2000. **41**(6): p. 633-646.

28. Mohan, D., C.U. Pittman, and P.H. Steele, *Pyrolysis of Wood/Biomass for Bio-oil: A Critical Review.* Energy & Fuels, 2006. **20**(3): p. 848-889.

29. Antal, M.J. and M. Grønli, *The Art, Science, and Technology of Charcoal Production†.* Industrial & Engineering Chemistry Research, 2003. **42**(8): p. 1619-1640.

30. Leffingwell & Associates. *Burnt Sugar, Caramel & Maple Notes*. 2010 [cited 2013; Available from: http://www.leffingwell.com/burnt.htm.

31. Nishimura, O. and S. Mihara, *Investigation of 2-hydroxy-2-cyclopenten-1-ones in roasted coffee.* Journal of Agricultural and Food Chemistry, 1990. **38**(4): p. 1038-1041.

32. Suuberg, E.M. and V. Oja, *Vapor pressures and heats of vaporization of primary coal tars*, 1997, Federal Energy Technology Center, Morgantown, WV (US); Federal Energy Technology Center, Pittsburgh, PA (US).

33. Shaw, P.E., J.H. Tatum, and R.E. Berry, *Acid-catalyzed degradation of D-fructose.* Carbohydrate Research, 1967. **5**(3): p. 266-273.

34. Niemela, K., *The formation of 2-hydroxy-2-cyclopenten-1-ones from polysaccharides during kraft pulping of pine wood.* Carbohydrate Research, 1988. **184**: p. 131-137.

35. Mettler, M.S., S.H. Mushrif, A.D. Paulsen, A.D. Javadekar, D.G. Vlachos, and P.J. Dauenhauer, *Revealing pyrolysis chemistry for biofuels production: Conversion of cellulose to furans and small oxygenates.* Energy & Environmental Science, 2012. **5**(1): p. 5414-5424.

36. Patwardhan, P.R., D.L. Dalluge, B.H. Shanks, and R.C. Brown, *Distinguishing primary and secondary reactions of cellulose pyrolysis.* Bioresource Technology, 2011. **102**(8): p. 5265-5269.

37. Alonso, D.M., J.Q. Bond, and J.A. Dumesic, *Catalytic conversion of biomass to biofuels.* Green Chemistry, 2010. **12**(9): p. 1493-1513.

38. Branca, C., A. Galgano, C. Blasi, M. Esposito, and C. Di Blasi, *H2SO4-catalyzed pyrolysis of corncobs.* Energy & Fuels, 2010. **25**(1): p. 359-369.

39. Simoneit, B.R., W. Rogge, M. Mazurek, L. Standley, L. Hildemann, and G. Cass, *Lignin pyrolysis products, lignans, and resin acids as specific tracers of plant classes in emissions from biomass combustion.* Environmental Science & Technology, 1993. **27**(12): p. 2533-2541.

40. Asmadi, M., H. Kawamoto, and S. Saka, *Gas- and solid/liquid-phase reactions during pyrolysis of softwood and hardwood lignins.* Journal of Analytical and Applied Pyrolysis, 2011. **92**(2): p. 417-425.

41. Asmadi, M., H. Kawamoto, and S. Saka, *Thermal reactivities of catechols/pyrogallols and cresols/xylenols as lignin pyrolysis intermediates.* Journal of Analytical and Applied Pyrolysis, 2011. **92**(1): p. 76-87.

42. Mullen, C.A. and A.A. Boateng, *Characterization of water insoluble solids isolated from various biomass fast pyrolysis oils.* Journal of Analytical and Applied Pyrolysis, 2011. **90**(2): p. 197-203.

43. Scholze, B., C. Hanser, and D. Meier, *Characterization of the water-insoluble fraction from fast pyrolysis liquids (pyrolytic lignin): Part II. GPC, carbonyl goups, and 13C-NMR.* Journal of Analytical and Applied Pyrolysis, 2001. **58**: p. 387-400.

44. Hosoya, T., H. Kawamoto, and S. Saka, *Role of methoxyl group in char formation from lignin-related compounds.* Journal of Analytical and Applied Pyrolysis, 2009. **84**(1): p. 79-83.

45. Hosoya, T., H. Kawamoto, and S. Saka, *Solid/liquid-and vapor-phase interactions between cellulose-and lignin-derived pyrolysis products.* Journal of Analytical and Applied Pyrolysis, 2009. **85**(1): p. 237-246.

46. Zhou, S., N.B. Osman, H. Li, A.G. McDonald, D. Mourant, C.-Z. Li, and M. Garcia-Perez, *Effect of sulfuric acid addition on the yield and composition of lignin derived oligomers obtained by the auger and fast pyrolysis of Douglas-fir wood.* Fuel, 2013. **103**: p. 512-523.

47. Bai, X., P. Johnston, and R.C. Brown, *An experimental study of the competing processes of evaporation and polymerization of levoglucosan in cellulose pyrolysis.* Journal of Analytical and Applied Pyrolysis, 2013. **99**: p. 130-136.

48. Bai, X., P. Johnston, S. Sadula, and R.C. Brown, *Role of levoglucosan physiochemistry in cellulose pyrolysis.* Journal of Analytical and Applied Pyrolysis, 2013. **99**: p. 58-65.

49. Oja, V. and E. Suuberg, *Vapor pressures and enthalpies of sublimation of D-glucose, D-xylose, cellobiose, and levoglucosan.* Journal of Chemical & Engineering Data, 1999. **44**(1): p. 26-29.

50. Wageningen University. *Caramelization*. 2013 August 2013]; Available from: http://www.food-info.net/uk/colour/caramel.htm.

51. Villamiel, M., M.D. del Castillo, and N. Corzo, *Browning Reactions,* in *Food Biochemistry and Food Processing*2007, Blackwell Publishing. p. 71-100.

52. Kroh, L.W., *Caramelisation in food and beverages.* Food Chemistry, 1994. **51**(4): p. 373-379.

53. Hodge, J.E., *Dehydrated Foods, Chemistry of Browning Reactions in Model Systems.* Journal of Agricultural and Food Chemistry, 1953. **1**(15): p. 928-943.

CHAPTER 3

THE INFLUENCE OF ALKALI AND ALKALINE EARTH METALS ON CHAR AND VOLATILE AROMATICS FROM LIGNIN FAST PYROLYSIS

A paper prepared for submission to the *Journal of Analytical and Applied Pyrolysis*

Dustin L. Dalluge, Kwang Ho Kim, and Robert C. Brown

Abstract

The effect of alkali and alkaline earth metals (AAEMs) on biomass carbohydrate pyrolysis has been well documented, however the effects of AAEMs on lignin pyrolysis has provided mixed results. To test the effect of AAEMs on lignin pyrolysis, AAEM acetates were infused into organosolv cornstover lignin at approximately 1.0 mmol AAEM cation per gram lignin and pyrolyzed in the temperature range from 300-800°C at 100°C increments. Both alkali and alkaline earth metals increased char yield with alkali metals having a more dramatic effect. Reactivity of the alkali metals was observed to be a function of atomic mass and corresponding electropositivity of the metal. Alkali metals increased the overall yield of volatile aromatic compounds while alkaline earth metals decreased overall yield.

Changes to side chains of volatile aromatics with addition of AAEMs were also observed. Alkali metals were most active in reducing alkenyl side chains on volatile aromatics. Alkali metals also significantly increased methanol yield. The simultaneous reduction in alkenyl side chains and increase in methanol, which are hypothesized to come from the β and γ carbons of the 3-hydroxyprop-1-enyl side chain respectively, likely indicate that alkali metals act to catalyze cleavage of linkages connecting benzene moieties within the lignin structure.

Introduction

Lignocellulosic biomass consists of three major components: cellulose, hemicellulose, and lignin. Lignin represents up to 30% of lignocellulosic biomass [1] and has a much higher carbon-to-oxygen ratio than carbohydrates, giving it an energy content similar to certain bituminous coals [2]. The fact that lignin has the highest energy density of any of the biopolymers and makes up such a significant portion of the lignocellulose makes its efficient utilization essential to the economic feasibility of biofuels.

The plant cell wall consists of a matrix of lignin and hemicellulose surrounding cellulose fibrils. Lignin is essential to protect the holocellulose from microbial attack while the plant is living and growing [3]; however, the recalcitrance of lignin presents several challenges to conversion of the biomass to fuels and chemicals. Saccharification for biochemical conversion involves the action of enzymes or acids to hydrolyze holocellulose into monosaccharides suitable for fermentation. High yields of fermentable monosaccharides require extensive pretreatments such as mechanical comminution, steam explosion, or ammonia fiber explosion to increase the porosity of the biomass particle and make the holocellulose accessible to enzymes or acids [4]. The pretreatment required to efficiently convert cellulosic biomass into ethanol leads to production costs nearly twice that of grain ethanol [5]. Biochemical conversion of cellulosic feedstocks leaves lignin unconverted [6]. As a result, it is mainly used for low value applications such as combustion for process heat.

Several thermochemical processes have been developed that use the entirety of the lignocellulosic biomass for production of fuels which gives them an advantage over purely biochemical pathways; one such thermochemical pathway is fast pyrolysis. Fast pyrolysis is the depolymerization of biomass by rapidly heating over 0.5-2.0 s at moderate temperatures (400-600°C) in the absence of oxygen to produce solids, liquids and gases. The liquids, known as bio-oil, can account for up to 78% of the total feedstock mass [7].

Fast pyrolysis of pure holocellulose produces predominately anhydrosugars, furans, and light oxygenates while lignin depolymerizes to a wide range of phenolic compounds exhibiting various side chains. Separating the products of biomass pyrolysis has been investigated by several researchers [8] as a potential approach to optimizing the intermediates to fuels and chemicals.

Although the major components of lignocellulosic biomass are cellulose, hemicellulose, and lignin, biomass also contains lesser amounts of proteins, lipids, non-structural sugars, nitrogenous compounds, chlorophyll, waxes, and mineral matter [9]. Mineral matter includes alkali and alkaline earth metals (AAEMs), which are known to catalyze pyranose and furanose ring fragmentation in holocellulose rather than the preferred pathway of cleaving glycosidic bonds [10-13]. Work by Kuzhiyil et al. [28] showed that passivating AAEMs in biomass can be accomplished by titrating with sulfuric or phosphoric acids to produce thermally stable sulfate or phosphate salts. Passivating the AAEMs in biomass prior to pyrolysis can lead to a substantial increase in sugar yield [14]. An increase in char and decrease in lignin-derived compounds was

observed for AAEM passivated biomass which suggests that AAEMs also influence lignin depolymerization. The goal of this work is to gain a better understanding of the effect of thermally active AAEM salts on the depolymerization of lignin.

Experimental

Lignin Washing Method

Lignin obtained from the Archer Daniels Midland (ADM) company was isolated from cornstover using the organosolv process. Organosolv lignin may be expected to have a slightly different structure than native lignin; however, El Hage et al. [15] found organosolv lignin to have a similar core structure to that of native lignin. Therefore the organosolv lignin was deemed an adequate surrogate for native lignin. Common impurities from the organosolv process include residual hemicellulose, acetic acid, and minerals. The lignin was therefore washed using the procedure outlined below prior to experiments in order to minimize contaminants.

Approximately 30 grams of the fine brown lignin powder were ball milled in a Retsch PM 100® planetary ball mill using a 250 mL stainless steel milling jar and fifty 10 mm stainless steel balls. The mill was programed to rotate at 400 rpm for 30 minutes and alternate rotation direction at 5 minute intervals. The milled lignin was washed with 300 mL of 0.1 N hydrochloric acid by stirring in a beaker with a magnetic stirrer at 600 rpm for 30 minutes. Next the mixture of dilute acid and lignin was separated using a 70 mm Whatman® GF/F glass microfiber filter with 0.7 μm particle size retention. The filter was placed in a Buchner funnel and a mild vacuum was applied to assist in pulling

the wash solution through the filter paper. The nearly dry lignin was recovered from the filter paper and the washing process repeated using deionized water for three repetitions. The lignin was next spread out on a watch glass and dried in an oven at 40°C overnight. The washing method reduced the lignin ash content to 0.14 wt. %.

Alkali and Alkaline Earth Metal Salt Infusion

Alkali and alkaline earth metal acetates were used since they significantly altered lignin pyrolysis products in preliminary trials. Investigations by Judd et al. [16] confirmed that AAEM acetates decompose at temperatures within the pyrolysis regime. Decomposition of the acetate salts leads to an active form of the metal that interacts with the lignin during pyrolysis and changes the pyrolysis products.

Washed lignin was infused with approximately 1.0 mmol AAEM cation per gram of lignin. The ratio of AAEM to lignin used is likely higher than the ratio found in native biomass, however was chosen to amplify any catalytic effects for improving analysis of the data. The metals lithium, cesium, barium, and copper are not found in any appreciable quantity in biomass; however were tested to discern any trends within the periodic table. For example, the copper (II) cation shares the same valence charge (+2) and similar effective ionic radius as magnesium (72pm for Mg vs. 73pm for Cu (II)) but has a much different electronegativity (1.31 for Mg vs. 1.90 for Cu (II)).

Many of the salts were available as hygroscopic anhydrous salts or hydrated salts. The hygroscopic salts were extremely difficult to accurately weigh since they would readily absorb moisture from the air leading to a constantly increasing mass on the laboratory balance. To prevent inaccuracies in weighing hygroscopic salts the salts

were first dissolved in 18.2 MΩ-cm deionized (DI) water to achieve a solution of approximately 5 wt. % AAEM cation. Approximately 300 mg of the washed lignin was weighed out in a small plastic weigh boat and a calculated weight of salt solution was added to achieve the desired ratio of salt to lignin. Slightly more DI water was then added to bring the total mass up to 700 mg of combined water and salt solution, which was enough water to homogeneously saturate the entirety of the lignin. The lignin and water mixture were thoroughly mixed until a uniform slurry was obtained. The slurry was spread out in the plastic weigh boat and placed in an oven at 40°C to dry for approximately 24 hours. Table 1 shows the final mmol concentration of AAEM per gram of lignin and its equivalent weight percentage.

Proximate Analysis

A Mettler-Toledo TGA/DSC 1® integrated with STARe® software was used to perform proximate analysis of the AAEM infused lignin samples. Approximately 10 mg lignin was loaded into a 150 uL alumina pan which was subject to a temperature program developed from ASTM method D7582. The temperature program started at 25°C and was then ramped at 10°C/min to 105°C where it was held for 40 minutes with a nitrogen gas flow rate of 100 mL/min. Any mass loss from this stage is considered to be moisture. Next the oven was ramped at 10°C/min to 900°C where it was held for 20 minutes; still with a constant flow of 100 mL/min of nitrogen. Any mass loss from this stage was considered volatiles. The oven then continued to hold 900°C; however the gas flow was switched over to air at a rate of 100 mL/min. Any mass loss from this stage

due to combustion was considered fixed carbon. The remaining residue after holding at 900°C with air flow for 30 minutes was considered ash.

Table 1: AAEM content of lignin samples.

Treatment	mmol AAEM cation/gram lignin	Weight % AAEM Cation
Control (Pure Lignin)	0.00	0.000
Lithium	0.95	0.66%
Sodium	0.92	2.1%
Potassium	0.98	3.8%
Cesium	0.93	12.4%
Magnesium	0.93	2.3%
Calcium	0.95	3.8%
Barium	1.00	13.7%
Copper (II)	0.94	6.0%

Each of the pure salts was subject to proximate analysis to determine the amount of ash produced from the salts that would remain with the char. The mass of ash contributed by involatile AAEM salts could then easily be subtracted from the char yield knowing the mass of salt in the original sample and the mass percentage of ash it would produce. Subtracting the mass of ash added due to AAEM acetate infusion allows all of the samples to be normalized back to a pure lignin basis. Therefore, any differences in char yield are solely attributed to char formation from the organic content of lignin.

Micropyrolysis-Gas Chromatography of Lignin

A Frontier single-shot 2020iS® micropyrolyzer with an AS-1020E® autosampler was used for pyrolysis. For all samples, other than those performed at 300°C, the interface temperature was held constant at 320°C and the furnace temperature was varied from 400-800°C at 100°C increments. For the 300°C tests both the interface and furnace were held at a constant 300°C. A Bruker 430-Gas Chromatograph ® (GC) with a flame ionization detector (FID) was used for analysis. A 60 m by 0.25 mm Agilent VF-1701ms® capillary column with 14% cyanopropylphenyl, 86% polydimethylsiloxane stationary phase was used for separation of volatile compounds. The GC method operated with an injector temperature of 300°C at a split ratio of 100. The oven program started at 35°C, held for 3 minutes, ramped at 5°C/min to 300°C and held for 4 minutes resulting in a total runtime of 60 minutes per experiment. The column pneumatics was set for constant flow at 1 mL/min helium carrier gas. The FID was operated at 300°C with 25 mL/min helium makeup flow, 30 mL/min hydrogen flow, and 300 mL/min air flow.

The instrument was calibrated using liquid standards. Compounds used for calibration were found from literature as well as from preliminary trials in a Micropyrolyzer-GC-Mass Spectrometer (Py-GC-MS). Pure standards purchased from Sigma Aldrich® were dissolved in methanol within the range expected for pyrolysis of approximately 500 μg of pure lignin. Each compound was calibrated at 3-5 levels with 2-8 injections per level depending on reproducibility of the results. Each compound produced a linear calibration with an R^2 of at least 0.99 with the exception of

1,2-benzenedimethanol, xylenes, methanol, m-tolualdehyde, coniferyl aldehyde, and sinapylaldehyde which each achieve an R^2 of at least 0.96 for the linear range used for quantification. Compounds calibrated for are listed in Table 2.

Table 2: GC-FID calibrated compounds.

Light Oxygenates	Acetaldehyde; Methanol; Acetone; Acetic Acid
Aromatic Hydrocarbons	Benzene; Toluene; Ethylbenzene; m-xylene; o-xylene; p-xylene; Styrene
Anisoles	Anisole; 2-methylanisole; 3-methylanisole; 4-methylanisole; 4-vinylanisole
Phenols	Phenol; m-tolualdehyde; o-cresol; m-cresol; p-cresol; 2,6-dimethylphenol; 2-ethylphenol;2,4-dimethylphenol; 2,5-dimethylphenol; 3,5-dimethylphenol; 4-ethylphenol, 3-ethylphenol; 3,4-dimethylphenol; 3-ethyl-5-methylphenol; 4-vinylphenol; 4-(1-propenyl)phenol*; p-coumaryl alcohol
Guaiacols	2-methoxyphenol; 2-methoxy-4-methylphenol; 4-ethyl-2-methoxyphenol; 2-methoxy-4-vinylphenol; Eugenol; 2-methoxy-4-propylphenol; Isoeugenol (cis and trans); Vanillin, 4'-hydroxy-3'-methoxyacetophenone; 1-(4-hydroxy-3-methoxyphenyl)propan-2-one (Guaiacyl Acetone); Coniferyl Alcohol; Coniferaldehyde

Table 2: GC-FID calibrated compounds (continued).

Syringols	2,6-dimethoxyphenol; 4-methyl-2,6-dimethoxyphenol; 4-ethyl-2,6-dimethoxyphenol*; 2,6-dimethoxy-4-vinylphenol*; 4-allyl-2,6-dimethoxyphenol; 2,6-dimethoxy-4-(1-propenyl)phenol (trans)*; 3,5-dimethoxy-4-hydroxybenzaldehyde; 3',5'-dimethoxy-4'-hydroxyacetophenone; 1-(4-hydroxy-3,5-dimethoxyphenyl)-2-propanone*; Sinapyl Alcohol; Sinapyl Aldehyde
Misc. Aromatics	2,3-dimethoxytoluene; 3,4-dimethoxytoluene; 1,2,3-trimethoxybenzene; 1,2,4-trimethoxybenzene; 3-methoxy-5-methylphenol; 1,4-benzenediol; 1,3-benzenediol; 1,2-benzenedimethanol; 2,5-dimethoxybenzylalcohol; 3',4'-dimethoxyacetophenone; 2',4'-dimethoxyacetophenone; 2,6-dihydroxy-4'-methoxyacetophenone
Compounds with an "*"note that a standard was not available; however the compound was identified via Micropyrolyzer-GC-MS running an identical program as the FID system. The mass yield of each of these compounds was found using the calibration for the compound that was most similar in both structure and empirical formula. (4-(1-propenyl)phenol used 4-vinylanisole; 4-ethyl-2,6-dimethoxyphenol used 4-methyl-2,6-dimethoxyphenol; 2,6-dimethoxy-4-vinylphenol used coniferyl alcohol; 2,6-dimethoxy-4-(1-propenyl)phenol used 4-allyl-2,6-dimethoxyphenol; and 1-(4-hydroxy-3,5-dimethoxy)-2-propanone used 3',5'-dimethoxy-4'-hydroxyacetophenone).	

Char yields were measured from separate experiments using a manual cup drop rather than the autosampler, which prevented char loss from the cups as they were automatically discarded from the furnace. Quartz wool is typically used in GC experiments to prevent char from elutriating and contaminating the GC column. The quartz wool has been found to lose mass due to evaporation of moisture and therefore was not used in experiments for which char was measured. In experiments used to measure char the volatiles were caught in a solvent bath rather than directly injected into

a GC in which entrained char could clog the injector or column. At least five replicates were performed to collect sufficient char to perform mass balances. Samples were repeated until a coefficient of variation of less than 10% was achieved or a maximum of 15 replicates were completed. Error bars reported in the figures are based off the 95% confidence interval taking into consideration all of the replicates.

Results and Discussion

Proximate Analysis of AAEM Infused Lignin

Proximate analysis was performed on both lignin and the pure AAEM salts. Pure lignin, being composed of only carbon, hydrogen and oxygen, is not expected to produce ash upon pyrolysis. Therefore, both the moisture and ash content were subtracted from the sample mass in order to normalize to a pure lignin basis. Results of the proximate analysis are summarized in Table 3 where both volatiles and fixed carbon are summed in the column labeled "lignin."

Mass Balances from Micropyrolysis

Char Yield

The term char is used to describe any remaining residue after pyrolysis, less the mass of the ash content contributed by the infusion of AAEM salts. Much of the residue remaining at low temperature is likely the result of incomplete pyrolysis; however, was labeled as char for consistency between samples. Char yield for the control decreased monotonically with increasing temperature as shown in the first row of Figure 1. From the control a maximum char yield of near 80 wt. % occurred at 300°C, which decreased to a minimum of 25 wt. % at 700-800°C. Alkali and alkaline earth metals both increased

Table 3: Proximate analysis of lignin samples.

Infused Acetate Salt	Moisture	Ash	Lignin
Control	3.71% ± 0.02%	0.14% ± 0.08%	95.05% ± 0.08%
Lithium	5.55% ± 0.03%	1.32% ± 0.08%	92.33% ± 0.08%
Sodium	5.53% ± 0.05%	2.66% ± 0.18%	90.33% ± 0.19%
Potassium	5.54% ± 0.02%	5.54% ± 0.24%	88.68% ± 0.24%
Cesium	6.53% ± 0.64%	5.76% ± 0.76%	87.71% ± 0.99%
Magnesium	7.15% ± 0.81%	2.49% ± 1.29%	89.92% ± 1.52%
Calcium	4.36% ± 0.03%	4.98% ± 0.36%	90.35% ± 0.36%
Barium	3.73% ± 0.30%	13.83% ± 0.36%	80.41% ± 0.47%
Copper (II)	4.13% ± 0.06%	6.13% ± 0.12%	87.47% ± 0.14%

char yield; however, alkali metals had the most dramatic effect. Each of the alkali metals had an approximate uniform increase in char yield up to 400°C, increasing from near 50 wt. % for the control to near 60 wt. % for lignin infused with alkali metal acetates. In the range of 500-800°C alkali metals increased char yield compared to the control. Within the range of 500-800°C alkali metals with a higher atomic mass increased char yield more significantly, i.e., lithium increased char yield the least and

cesium increased it the most. The largest increase in char yield occurred with cesium at 800°C, where the control produced near 25 wt. % char and the cesium infused sample produced near 45 wt. % char. Therefore higher atomic mass elements with higher electropositivity have a higher catalytic activity toward production of char.

Alkali and alkaline earth metal cations are known to catalyze carbonization of aromatic hydrocarbons in coal, asphalt, and phenol-formaldehyde resins [17-22]. Mochida et al. [18, 19] found alkali metal catalyzed carbonization of aromatic hydrocarbons to start with an anion radical that is formed from a charge transfer. The charge transfer proceeds by a valence electron of the alkali metal transferring to a carbon in the aromatic structure. Both an aromatic anion and an alkali metal cation are formed as a result of the charge transfer; each being a radical since only one electron is transferred. The alkali metal cation then substitutes for a hydrogen atom in the aromatic structure which results in dehydrogenation of the carbon compound and coupling of ionic radicals. Mochida et al. [18,19] found AAEMs to catalyze carbonization of aromatic hydrocarbons at a temperature range similar to that used for pyrolysis. Therefore the aromatic structure of lignin is expected to behave similarly during pyrolysis which results in char.

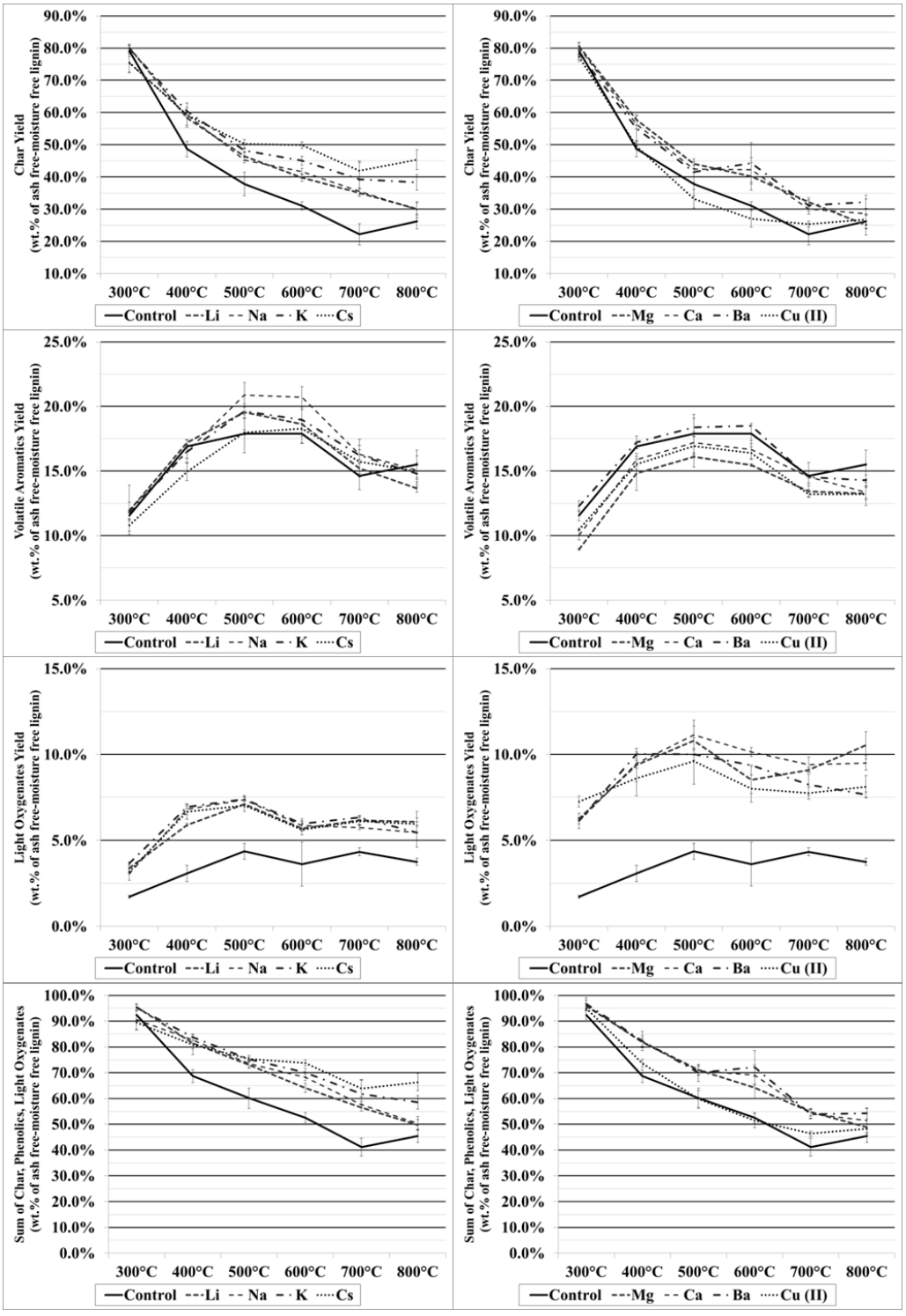

Figure 1: Char mass yield (Row 1), Volatile aromatics mass yield (Row 2), Light oxygenates mass yield (Row 3), Total mass balance (Row 4)

Mochida et al. [18, 19] found the yield of carbonization product to increase at 500°C in the order of K>Na>Li>control which is identical to the order of reactivity for char production found in this work. The difference in char yield from different alkali metals might be explained by higher electropositive elements having a much lower electron affinity. A lower electron affinity means that less energy is required for the metal to lose an electron during the charge transfer process. Since less energy is required the process can occur at lower temperatures and proceed faster at higher temperatures.

Yamashita and Ouchi [20-22] found a similar reaction pathway for alkali metal catalyzed carbonization of coal, asphalt, and 3,5-dimethylphenol-formaledehyde resin. Alkali metals substituted for hydrogen in the carbonaceous structure which released much of the hydrogen as gas. The order of reactivity, determined by the amount of char produced, was found to be Na>K>Li>control. The reaction pathway is thought to proceed via NaO- groups (from NaOH) replacing HO- groups on the aromatic structure. The Na is recycled by carbon reduction of Na_2O to metallic Na and CO. Metallic Na can then directly react with additional aromatic rings or with water formed during reaction to again form NaOH which starts the process over. Carbonates produced a similar effect, however at higher temperature. Alkali carbonates are reduced with carbon at high temperature to metallic alkali and CO which again starts the catalytic process over.

Alkali metal acetates are known to decompose to carbonates and/or oxides at pyrolysis temperatures. Once in the carbonate or oxide form the alkali metals can react

with the aromatic lignin structure via the same mechanisms found by Mochida et al. [18,19] and Yamashita and Ouchi [20-22]. Therefore the mechanism of alkali metal catalyzed char formation from lignin pyrolysis is likely to proceed in the same manner as alkali metal catalyzed carbonization of aromatic hydrocarbons.

It should also be noted that Yamashita and Ouchi [21] found younger coals, which have a structure more similar to lignin, to be more reactive toward carbonization due to activation of polar oxygen containing groups. The highly oxygenated phenolic and methoxyl groups in lignin are likely to produce a similar effect.

A more detailed investigation of non-condensable gases and char would be necessary to provide further evidence that char is formed via mechanisms similar to those found by Mochida et al. [18, 19] and Yamashita and Ouchi [20-22]. The char structure should exhibit more aromatic character than the char from the control if it is formed via alkali metal catalyzed carbonization. Evidence of alkali metal substitution on the aromatic rings would be indicated by release of additional hydrogen. Carbon monoxide would likely increase as the alkali oxides and carbonates are reduced to metallic alkali during the reaction. Analysis of non-condensable gases and the char structure may help to determine if in fact the alkali metals are catalyzing carbonization of lignin via the mechanisms found by Mochida et al. [18,19] and Yamashita and Ouchi [20-22].

Alkaline earth metals showed a similar trend for char formation over the entire temperature range, increasing char by 5-10 wt. %, compared to 10-20 wt. % for alkali metals. Although significantly different from the control, the difference between each

alkaline earth metal was insignificant over the entire temperature range. The lower reactivity of alkaline earth metals suggests different catalytic activity and possibly mechanisms for alkali metal and alkaline earth metal catalyzed char formation. Alkali metals with a single valence charge produced a higher char yield with increasing atomic mass and electropositivity; however there was no discernible trend in char yield from electropositivity of alkaline earth metals. Yamashita and Ouchi [22] performed similar tests and found the order of reactivity to be Ba>Sr>Mg≈Ca>control; also observing the reaction with Mg and Ca was marginal compared to alkali metals.

Lignin infused with copper (II) acetate produced no significant change in char yield compared to the control across the entire temperature range. The copper (II) cation is similar in physical size to the magnesium cation but has a much different electropositivity. Therefore, the hypothesis that electropositivity of the cation is a dominant factor for increasing char yield, like it was in the case of alkali metals; is not supported due to the absence of any significant differences among the alkaline earth metals. Judd et al. [16] however observed that the first step in thermal decomposition of copper (II) acetate was the formation of copper (I) acetate and acetic acid. The copper (I) would then likely exhibit reactivity more akin to alkali metals. The formation of copper (I) from the copper (II) can likely explain why copper (II) had a much different effect than other metals with the same valence charge. Therefore, the hypothesis that the electropositivity of single valence charge metals affects the reactivity of the metal toward char formation is still plausible.

Volatile Aromatics

The group labeled "volatile aromatics" consists of all volatile compounds containing an aromatic ring that were quantified via GC/FID. As shown in the second row of Figure 1, all of the alkali metals except cesium increased the mass yield of volatile aromatics from the temperature range of 500-700°C. Lignin infused with sodium produced the most significant increase overall. At their peaks, the control produced 17.9 wt. % volatile aromatics, whereas sodium infused lignin produced 20.9 wt. %, a small but statistically significant difference.

Volatile aromatics produced from pyrolysis of AAEM infused lignin were structurally different than those coming from the control due to the presence of different side chains. The structural differences likely led to a different average molecular mass across all of the volatile aromatics. Therefore both average molecular mass and the number of molecules released from the lignin could affect the total mass yield. Comparing volatile aromatics on a mass basis provides no evidence as to if the average molecular mass of the volatile aromatic is simply changing or if an increased number of volatile aromatic molecules are actually released from the lignin structure. Therefore volatile aromatics were also compared on a molar basis. Molar yield of benzene moieties from each treatment is summarized in the first row of Figure 2.

The peak in mass yield of volatile aromatics occurred at 500°C with the infusion of sodium. The control produced 17.9 wt. % volatile aromatics and the sodium infused sample produced 20.9 wt. %, an increase of 16.8%. Comparing the molar yields at the same temperature, the control produced 1.37 mmol benzene moieties per gram lignin

and the sodium infused sample produced 1.59 mmol benzene moieties per gram lignin, a 16.0% increase. Trends in both mass and molar yield were therefore nearly identical across the entire temperature range with each of the alkali metals. Similar increases in both mass and molar yield suggest that the volatile aromatics have a similar average molecular mass regardless of treatment. Therefore alkali cations either help to release more benzene moieties from the lignin structure or produce more stable aromatic compounds that do not repolymerize in secondary reactions.

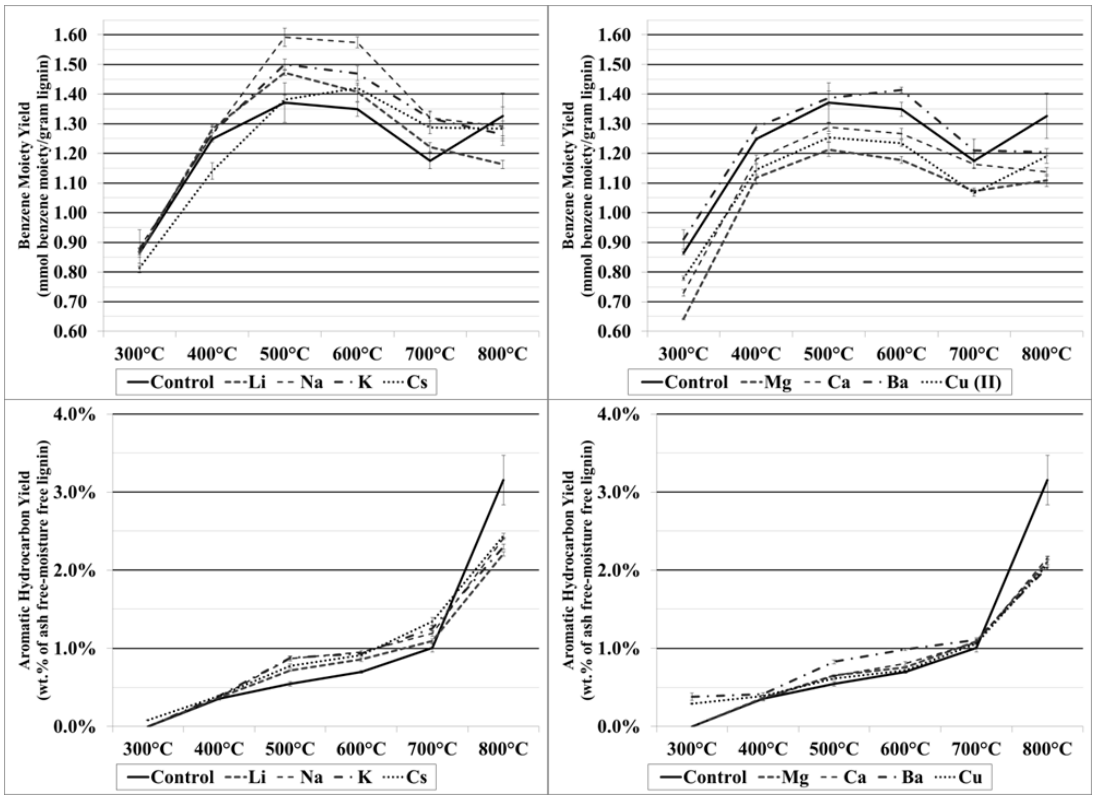

Figure 2: Benzene moiety molar yield (Row 1), Aromatic hydrocarbon mass yield (Row 2)

Conversely, the infusion of alkaline earth metals reduced the yield of volatile aromatics over the entire temperature range. The yield of volatile aromatics was in the order of control≈Ba>Ca>Mg. Similar to alkali metals, the differences in yield were small but statistically significant. The most significant decrease in volatile aromatics occurred at 600°C with the infusion of magnesium acetate, with the control producing 17.9 wt. % volatile aromatics and the magnesium infused sample producing just 15.5 wt. % volatile aromatics, a decrease of 13.4%. Comparing the volatile aromatics on a molar basis, the control lignin produced 1.35 mmol benzene moieties per gram lignin at 600°C; whereas the magnesium infused lignin produced just 1.18 benzene moieties per gram lignin, a decrease of 12.6%. Similar to alkali metals, yields on mass and molar bases were nearly identical. Therefore, changes in mass yield are not simply due to functionality changes on the benzene moieties and the differences in yield must then depend upon the number of benzene moieties that are released from the lignin structure.

Side chains attached to volatile aromatics were also investigated in greater detail. Each volatile aromatic compound was broken down into its individual side chains and parent benzene moiety. The moles of a specific side chain divided by the moles of benzene moieties produced at that point were calculated and termed MMB (**m**ole of side chain per **m**ole **b**enzene moiety) for the remainder of this manuscript. For example, the compound methylbenzene contains one methyl side chain and one C_6H_5 benzene moiety. The compound dimethylbenzene contains two methyl side chains and one C_6H_4 benzene moiety. Each C_6 ring, containing anywhere from zero to six hydrogens is termed a benzene moiety. Therefore, methylbenzene would have a methyl MMB of 1.0 and

dimethylbenzene would have a methyl MMB of 2.0. Another example, 2,6-dimethoxyphenol contains one hydroxyl side chain, two methoxyl side chains, and one C_6H_3 benzene moiety. Therefore, 2,6-dimethoxyphenol would have a hydroxyl MMB of 1.0 and a methoxyl MMB of 2.0.

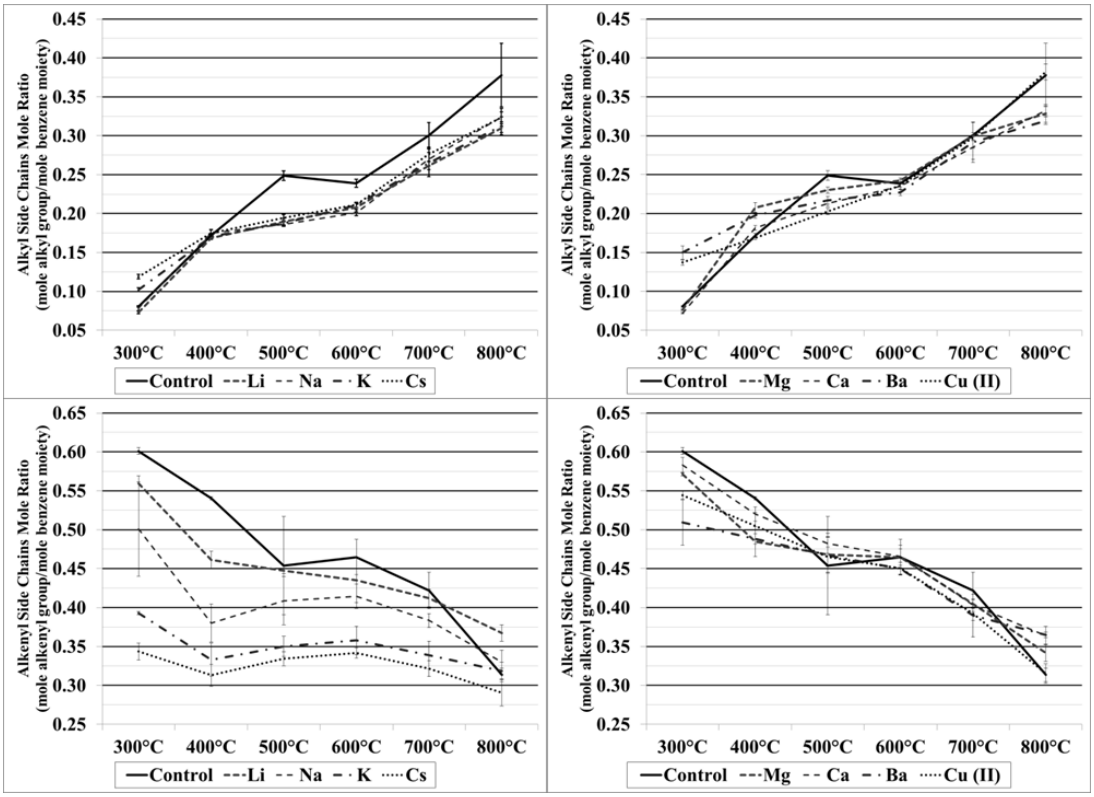

Figure 3: Aliphatic MMB for both alkali and alkaline earth metals; Alkyl MMB (Row 1), Alkenyl MMB (Row 2).

As shown in the first row of Figure 3, the alkyl (methyl, ethyl, and propyl) MMB from the control increased with increasing temperature. Lignin infused with alkali metals produced a monotonic increase in alkyl MMB throughout the temperature range; however, the yield was significantly less than the control. Infusion of alkaline earth

metals and copper (II) produced a monotonic increase in alkyl MMB with a slight increase over the control at 300-400°C and a slight decrease from 500-800°C. The decrease was not as significant as that from alkali metals.

The major difference in aliphatic side chains occurred in the alkenyl MMB. Vinyl (ethenyl) side chains made up from 87-98% of the alkenyl side chains; with the remainder consisting of 1-propenyl and 2-propenyl side chains. As shown in the second row of Figure 3, alkali metals had a dramatic effect on alkenyl MMB with higher atomic mass and higher electropositive alkali metals having a more significant effect. Alkenyl MMB from the control decreased nearly monotonically over the entire temperature range from a maximum of 0.60 at 300°C to a minimum of 0.31 at 800°C. Lignin infused with alkali metals produced a similar trend; however catalytic effects of the alkali metals decreased the alkenyl MMB more significantly than the temperature alone. Cesium, being the highest atomic mass and most electropositive alkali metal, produced a nearly uniform alkenyl MMB over the entire temperature range. The effect of alkali metals is in stark contrast to lignin infused with alkaline earth metals and copper (II), which produced slightly lower alkenyl MMB than the control at 300-400°C and a similar MMB to the control at higher temperatures.

From the limited analysis used in this work, the mechanisms responsible for decreasing alkenyl side chains among volatile aromatics after infusion of alkali metals is not evident; however, the authors hypothesize two possible mechanisms.

First, similar to the action of alkali metals on carbohydrates; alkali metals may coordinate to the oxygen atom of the monolignol β-O-4 linkages making them cleave

differently during pyrolysis. The vinyl functionalities are known to be released from the cleavage of β-O-4 bonds in the lignin structure [23-26], which make up the majority of lignin linkages. Therefore any changes to the cleavage of β-O-4 linkages would likely affect the resulting number of vinyl side chains. Patwardhan et al. [27] found AAEM chlorides not to be active in altering lignin pyrolysis products and attributed this to AAEM cations being incapable of coordinating to aromatic rings due to size restrictions. Instead it is likely that Patwardhan observed no changes with the addition of chlorides because alkali chlorides are thermally stable and therefore not catalytically active at pyrolysis temperatures [28]. Regardless, the aromatic rings would lead to size restrictions for coordination with cations; however the bonds of various linkages between aromatic substituents would be much more open and susceptible to catalytic action by AAEM cations.

Second, it is possible that alkali metals actually act to polymerize vinyl side chains forming carbon-carbon bonds in oligomers at lower temperatures. The newly formed carbon-carbon bonds may then be cleaved at higher temperatures to produce depolymerization products without vinyl side chains. The highest alkenyl MMB occurred with the control at 300°C, which is the lowest temperature tested. Once released, the alkenyl side chains, especially the vinyl side chain, are known to be highly reactive toward repolymerization reactions [29]. Gas phase polymerization of volatile aromatics with vinyl side chains could proceed similarly to gas phase thermal polymerization of styrene; however polyvinylphenols would be produced rather than polystyrene [30]. There were no clear indicators of other volatile products formed with

the decreasing vinyl functionality that would account for the loss. Analysis of gases and non-volatile oligomers, which was not performed in this work, would help to discern the fate of the alkenyl side chains. Interestingly, the alkenyl MMB converged to a minimum between 0.31 and 0.37 from the control and AAEM infused lignin. The convergence of alkenyl MMB to a similar number for all alkali metals likely suggests that the alkali metals are catalytically active in depolymerizing certain linkages within the lignin structure, however are not active on others.

Alkoxy side chains (hydroxyl, methoxyl, and carbonyl) were also investigated in further detail. As shown in the first row of Figure 4, hydroxyl MMB was marginally affected by both alkali and alkaline earth metals. The hydroxyl MMB was near 1.0 at 300°C for all samples as might be expected since almost all volatile aromatics from lignin pyrolysis are phenols. For both alkali and alkaline earth metals hydroxyl MMB was nearly constant up to 600°C, at which it started to decrease to a minimum of around 0.71 at 800°C. The cleavage of hydroxyl groups at temperatures above 600°C suggests that the hydroxyl groups begin to cleave from the benzene rings at 600-700°C producing a higher yield of aromatic hydrocarbons which is indicated in the second row of Figure 2. Neither alkali nor alkaline earth metals had a significant effect on the hydroxyl MMB.

Methoxyl MMB resulting from all of the treatments is shown in the second row of Figure 4. Methoxyl side chains arise from guaiacol and syringol moieties in lignin. The lignin used in this work was from corn stover, an herbaceous crop, therefore contains predominately hydroxyphenyl type lignin and is already low in methoxyl side

chains [31]. Methoxyl MMB from the control peaked at around 0.66 in the temperature range of 300-500°C. The methoxyl MMB quickly decreased at temperatures above 500°C to a minimum of 0.28 at 800°C. Alkali metals slightly increased the methoxyl MMB for sodium infused lignin, producing a peak near 0.70 at 300-500°C. Increasing

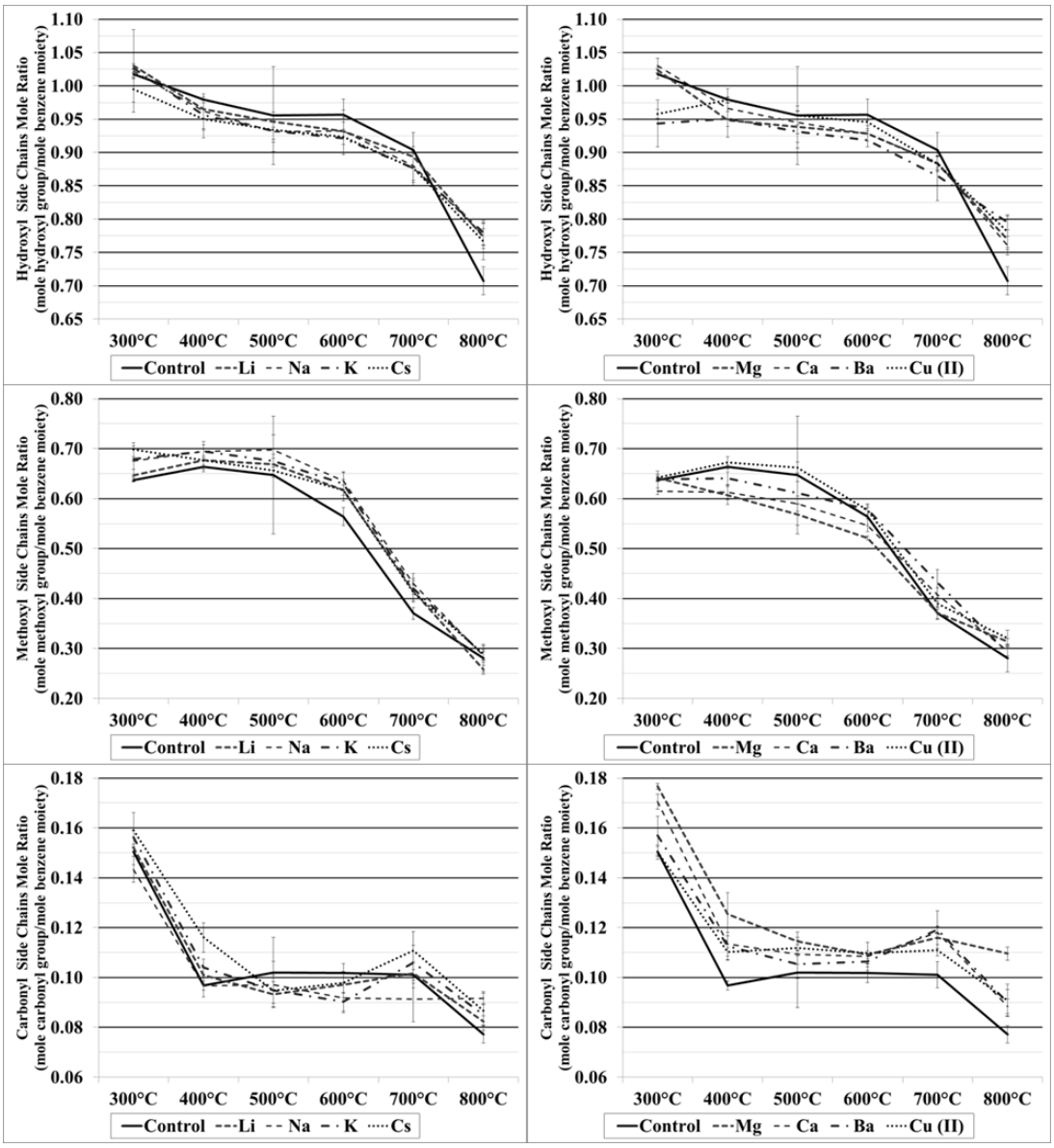

Figure 4: Alkoxy MMB for both alkali and alkaline earth metals; Hydroxyl MMB (Row 1), Methoxyl MMB (Row 2), Carbonyl MMB (Row 3)

methoxyl MMB with lignin infused with alkali metals is consistent with an increase in volatile aromatics mass yield and benzene moiety molar yield. Alkali metals therefore likely act to either release more methoxy substituted phenols from the lignin structure or prevent the cleaving of methoxyl side chains.

Alkaline earth metals slightly decrease the methoxyl MMB from 300-600°C, and slightly increase thereafter; although the changes were not statistically significant. The slight decrease at lower temperatures is consistent with lower volatile aromatic mass yields and benzene moiety molar yields.

Infusion of copper (II) produced a similar methoxyl MMB as the control, which is more consistent with alkali metals. Judd et al. [16] found that thermal decomposition of copper (II) acetate first results in copper (I) acetate, which then, with a valence charge of one, likely reacts similar to alkali metals.

Carbonyl side chains were a dominant group among several of the volatile aromatics and included aldehydes from compounds such as vanillin and sinapyl aldehyde, and ketones from acetophenones and phenylacetones. The changes in carbonyl MMB are shown in the third row of Figure 4. Carbonyl MMB peaked near 0.15 at 300°C and then quickly leveled off in the temperature range of 400-800°C to near 0.10. Alkali metals had no significant effect on the carbonyl MMB at any temperature.

Alkaline earth metals and copper (II) both slightly increase carbonyl MMB over the control. Less electropositive alkaline earth metals produced a more dominant effect; i.e. carbonyl MMB decreased in the order of Mg>Ca>Ba>control. The maximum

carbonyl MMB of 0.18 occurred with magnesium infused lignin at 300°C, which was an increase of 17% compared to the control. The increase in carbonyl MMB is inversely proportional to the decrease in volatile aromatics mass yield and benzene moiety molar yield, decreasing by 22.6% and 25.7%, respectively. The effect of alkaline earth metals on carbonyl MMB was therefore directly opposite that of the volatile aromatics mass yield, i.e. magnesium infused lignin produced the lowest volatile aromatics yield, but the highest carbonyl MMB of all of the alkaline earth metals. Therefore the decrease in volatile aromatics yield by infusion of alkaline earth metals is likely coming from compounds without carbonyl side chains. As the carbonyl side chains likely result from cleavage of linkages within the lignin structure, it is likely that alkaline earth metals act to catalyze cleavage of monolignols linkages. A different fragmentation of the lignin structure then leads to a different product distribution from alkaline earth metal infused lignin.

Light Oxygenates

As shown in the third row of Figure 1, the mass yield of light oxygenates increased drastically with the addition of both alkali and alkaline earth metal acetates. The first row of Figure 5 shows that much of the total increase in light oxygenates is the result of an increase in acetic acid. An ion exchange of AAEM acetates with the lignin structure is likely to account for a majority of the increase in acetic acid. Both Jakab et al. [32] and Gray et al. [33] have observed lignin to ion exchange with AAEM salts using sodium hydroxide and calcium acetate, respectively. The ion exchange is therefore likely to occur with the AAEM acetates used in this study. A cation exchange

results in binding of AAEM cations to the lignin structure and formation of a hydrogen exchanged salt; e.g. both of the acetate anions from calcium acetate would produce acetic acid and the calcium cation would be bound to the lignin structure. As shown in the first row of Figure 5, acetic acid nearly doubled with infusion of alkaline earth metals compared to alkali metals. The difference in acetic acid yield between alkali metals and alkaline earth metals is therefore directly correlated with the valence charge of the respective metal. Alkaline earth metals, with a valence charge of two, would contribute two acetate groups per mole of cation, whereas alkali metals, with a valence charge of one, would contribute only one mole of acetate per mole of cation. The facts that acetic acid yield correlated with valence charge of the AAEM cation and ion exchange has been previously observed from AAEM salts with lignin suggest that ion exchange is a likely mechanism for increased acetic acid yield with infusion of AAEM acetates.

A relatively low acetone yield provides further evidence that acetate salts ion exchanged with the lignin structure. Judd et al. [16] found that both calcium and sodium acetate thermally decompose to produce acetone and the carbonate salt of the respective cation. A similar decomposition pathway can be assumed to occur with the remainder of the alkali and alkaline earth metals, however the decomposition temperatures are likely different. Therefore a significant increase in acetone yield from AAEM acetate infused lignin would suggest a similar decomposition pathway of the acetates after they are infused into the lignin. As shown in the third row of Figure 5, the yield of acetone was less than 0.40 wt. % at all temperatures tested and with infusion of all AAEM acetates.

The low yield of acetone cannot account for the amount of acetone that would be released from thermal decomposition of the acetates infused into the lignin samples under the normal thermal decomposition pathway. Therefore the low acetone yield from infusion of AAEM acetates indicates that the decomposition pathway of the acetate salts is significantly altered after infusion into lignin. The altered decomposition pathway suggests the acetate is in a different form, which is likely acetic acid that is formed from the ion exchange process.

Thermal decomposition of acetic acid and other light oxygenates is one possible explanation as to why light oxygenates yield peaks near 500°C and decreases slightly at higher temperatures. Acetic acid is known to decompose to methane, carbon dioxide, ethenone, and water at elevated temperatures within the pyrolysis temperature regime [34]. All of the acetic acid decomposition products are therefore gases at the operating conditions of the GC used in this study and therefore could not be separated and accounted. A detailed analysis of gases coming from lignin pyrolysis would need to be performed in order to determine if acetic acid decomposition products are prevalent at higher pyrolysis temperatures. However, with the available data, thermal decomposition of light oxygenates at higher temperature is the most likely explanation for the slight decrease in light oxygenates at temperatures above 500°C.

The second row of Figure 5 shows that methanol yield significantly increased with infusion of alkali acetates, the increase correlating with atomic mass and electropositivity of the metal cation. Similar to acetic acid, the yield of methanol peaked at 500°C for all lignin infused with AAEM cations. At temperatures above 500°C the

methanol yield quickly decreased, which is a likely indicator of methanol thermal decomposition. Cleavage of methoxyl groups from syringol and guaiacol derivatives seems like a likely sources of methanol; however, there was no decrease in methoxyl MMB among volatile aromatics with addition of alkali salts, as shown in Figure 4. Therefore, methanol must result from mechanisms other than conversion of methoxyl groups of syringol and guaiacol derivatives.

Another possible explanation of increased methanol with infusion of AAEM acetates is cleavage of methoxyl groups within the aromatic structure of the char, which was not accounted in this study. The alkali metals all increased char yield over the control, however the char structure was not analyzed. Many of the volatile aromatics from lignin pyrolysis exhibited methoxyl side chains, indicating that many of the char precursors would also have methoxyl side chains. The formation of more char from lignin infused with alkali metals would therefore lead to more methoxyl groups within the char. Alkali metals could then catalyze cleavage of methoxyl groups from the char to produce methanol.

Hosoya et al. [35] proposed the formation of char from lignin via Diels-Alder reactions through an o-quinone methide intermediate. Methoxyl side chains of guaiacol moieties were observed to be a key precursor in formation of the intermediate. Alkali and alkaline earth metal cations can act as Lewis acids, which are known to catalyze Diels-Alder cycloadditions [36]. Alkali and alkaline earth metal catalyzed cycloadditions likely produce char that is more polyaromatic in structure compared to the control. A more detailed analysis of char structure would need to be performed in

order to investigate alkali catalyzed char formation from lignin. However, with the given data, formation of char via alkali catalyzed Diels-Alder reactions with the production of methanol appears as a possible explanation for the increased methanol yield from alkali infused lignin.

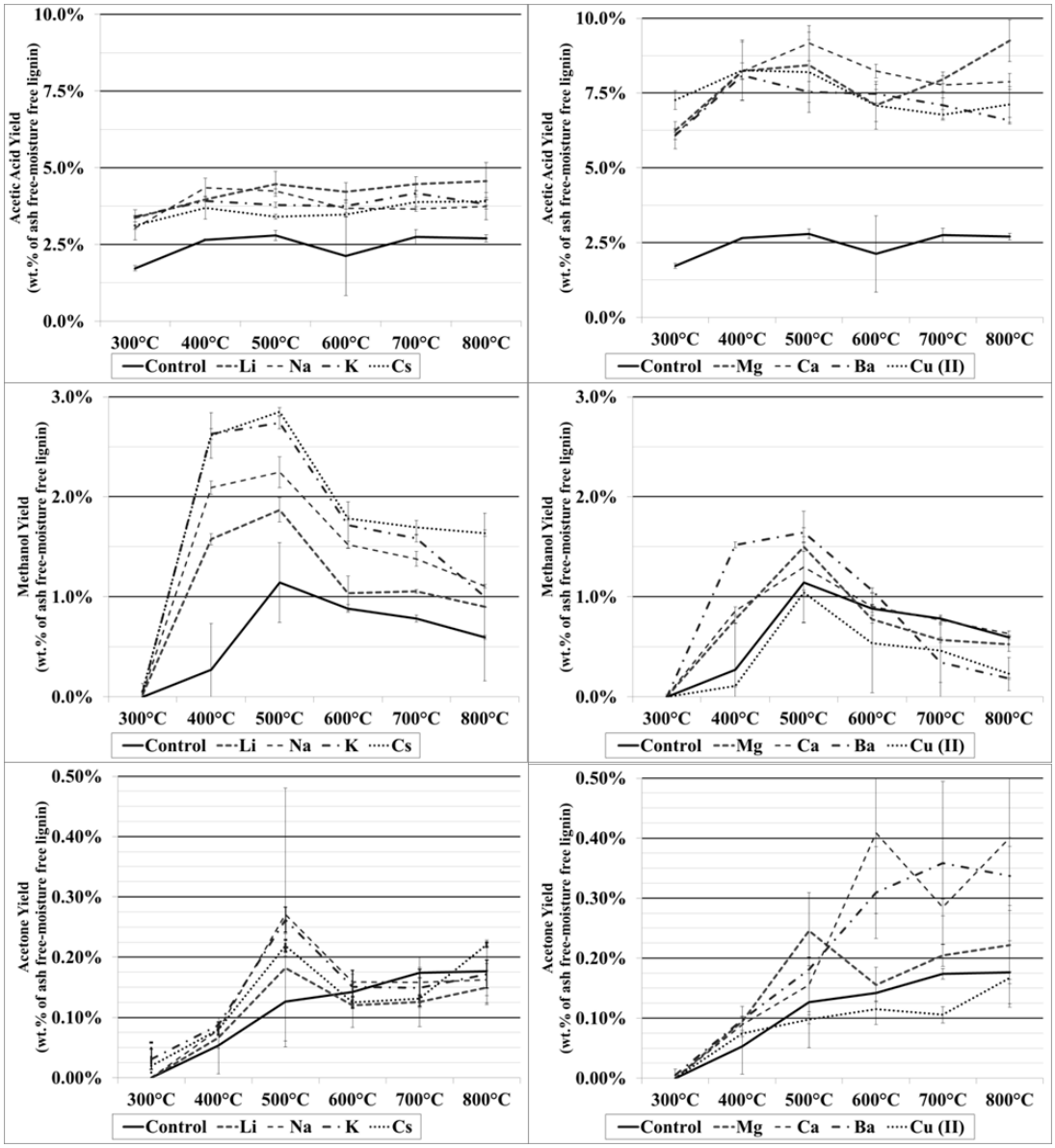

Figure 5: Light oxygenates mass yield; Acetic acid mass yield (Row 1), Methanol mass yield (Row 2), Acetone mass yield (Row 3)

One other likely source of methanol is from cleavage of the γ-carbon of the 3-hydroxyprop-1-enyl side chain, which is present in several of the α- and β-linked monolignols. Methanol increased substantially with the infusion of alkali metals; however there was no decrease in methoxyl MMB. Therefore the increase in methanol can be ruled out from coming from methoxyl side chains on volatile aromatics. Alkenyl side chains, many of which are known to form from cleavage of the β-O-4 linkage, decreased with addition of alkali metals. Taking into consideration that both the increase in methanol and the decrease in alkenyl side chains come from cleavage of linkages between monolignols provides further evidence that alkali metals alter the cleavage of linkages within the lignin structure.

Conclusions

Thermally active AAEM acetate salts had a significant effect on lignin fast pyrolysis. Lignin infused with alkali metals produced an increased yield of char, light oxygenates, and volatile aromatics compared to the control. Quantity of alkenyl side chains among volatile aromatics decreased for lignin infused with alkali metal acetates. In general the atomic mass and electropositivity of the alkali metal correlated with the metals effect on pyrolysis products; i.e. the more electropositive the metal, the more significant its effect. The increase in volatile aromatics, decrease in alkenyl side chains, and increase in light oxygenates from lignin infused with alkali metals suggests that alkali metals alter cleavage of bonds linking monolignols in the lignin structure.

Volatile aromatics yield was one major outlier from the correlation of metal electropositivity and its effect on pyrolysis products. The yield of volatile aromatics was influenced most significantly by sodium; increasing by 17% compared to the control at 500°C. The higher reactivity of sodium compared to other alkali metals has been observed by other researchers as well, however the mechanism is still not clear.

Lignin infused with alkaline earth metals produced increased char and light oxygenates compared to the control. The increase in char from alkaline earth metals was not as drastic as that for alkali metals; however the yield of light oxygenates nearly doubled. In contrast to alkali metals, volatile aromatics decreased from lignin infused with alkaline earth metals. Similar to alkali metals, the alkaline earth metals showed trends due to atomic mass and electropositivity of the metal although the correlations were not as strong.

Acknowledgements

The authors would like to thank the Phillips 66 Company for their generous funding of this project. We would also like to thank staff scientists, Patrick Johnston and Marjorie Rover of the Center for Sustainable Environmental Technologies for assistance in running instrumentation and developing methods used on analytical equipment. We would like to thank Ryan Smith, Deputy Director of the Center for Sustainable Environmental Technologies, for providing administrative support to this project. We are also thankful to Jordan Donner for assistance in running the experiments.

References

1. U.S. Department of Energy, *Biomass Feedstock Composition and Property Database*, 2006, Energy Efficiency and Renewable Energy - Biomass Program.

2. Boateng, A.A., P.J. Weimer, H.G. Jung, and J.F.S. Lamb, *Response of Thermochemical and Biochemical Conversion Processes to Lignin Concentration in Alfalfa Stems †.* Energy & Fuels, 2008. **22**(4): p. 2810-2815.

3. Vance, C.P., T.K. Kirk, and R.T. Sherwood, *Lignification as a Mechanism of Disease Resistance.* Annual Review of Phytopathology, 1980. **18**(1): p. 259-288.

4. Carroll, A. and C. Somerville, *Cellulosic Biofuels*, in *Annual Review of Plant Biology*2009, Annual Reviews: Palo Alto. p. 165-182.

5. Regalbuto, J.R., *Cellulosic Biofuels—Got Gasoline?* Science, 2009. **325**(5942): p. 822-824.

6. Wyman, C.E., *What is (and is not) vital to advancing cellulosic ethanol.* Trends in Biotechnology, 2007. **25**(4): p. 153-157.

7. Brown, R.C., *Biorenewable resources : engineering new products from agriculture*. 1st ed2003, Ames, Iowa: Iowa State Press. xii, 286 p.

8. Pollard, A.S., M.R. Rover, and R.C. Brown, *Characterization of bio-oil recovered as stage fractions with unique chemical and physical properties.* Journal of Analytical and Applied Pyrolysis, 2012. **93**: p. 129-138.

9. A. Sluiter, R.R., C. Scarlata, J. Sluiter, and D. Templeton, *Determination of Extractives in Biomass*, 2008, National Renewable Energy Laboratory: Golden, Colorado.

10. Ponder, G.R. and G.N. Richards, *A review of some recent studies on mechanisms of pyrolysis of polysaccharides.* Biomass and Bioenergy, 1994. **7**(1–6): p. 1-24.

11. Ponder, G.R. and G.N. Richards, *Pyrolysis of inulin, glucose and fructose.* Carbohydrate Research, 1983. **244**(2): p. 341-359.

12. Richards, G.N. and F. Shafizadeh, *Formation of "Glucometasaccharinolactones" in the pyrolysis of curdlan, A (1→3)-β-d-glucan.* Carbohydrate Research, 1982. **106**(1): p. 83-91.

13. Patwardhan, P.R., J.A. Satrio, R.C. Brown, and B.H. Shanks, *Influence of inorganic salts on the primary pyrolysis products of cellulose.* Bioresource Technology, 2010. **101**(12): p. 4646-4655.

14. Dalluge, D., T. Daugaard, P. Johnston, N. Kuzhiyil, M. Wright, and R. Brown, *Passivation of Alkali and Alkaline Earth Metals with Sulfuric Acid to Produce High Yields of Sugars from Fast Pyrolysis of a Wood y and Herbaceous Feedstock using an Auger Reactor.* Manuscript submitted for publication (copy on file with author), 2013.

15. El Hage, R., N. Brosse, L. Chrusciel, C. Sanchez, P. Sannigrahi, and A. Ragauskas, *Characterization of milled wood lignin and ethanol organosolv lignin from miscanthus.* Polymer Degradation and Stability, 2009. **94**(10): p. 1632-1638.

16. Judd, M., B. Plunkett, and M. Pope, *The thermal decomposition of calcium, sodium, silver and copper (II) acetates.* Journal of thermal analysis, 1974. **6**(5): p. 555-563.

17. Beguin, F. and R. Setton, *Activation par les metaux alcalins du processus de carbonisation des hydrocarbures aromatiques polycondensés.* Carbon, 1972. **10**(5): p. 539-551.

18. Mochida, I., E.-I. Nakamura, K. Maeda, and K. Takeshita, *Carbonization of aromatic hydrocarbons—IV: Reaction path of carbonization catalyzed by alkali metals.* Carbon, 1976. **14**(2): p. 123-129.

19. Mochida, I., E.-i. Nakamura, K. Maeda, and K. Takeshita, *Carbonization of aromatic hydrocarbons—III: Carbonization catalyzed by alkali metals.* Carbon, 1975. **13**(6): p. 489-493.

20. Yamashita, Y. and K. Ouchi, *Influence of alkali on the carbonization process—I: Carbonization of 3, 5-dimethylphenol-formaldehyde resin with NaOH.* Carbon, 1982. **20**(1): p. 41-45.

21. Yamashita, Y. and K. Ouchi, *Influence of alkali on the carbonization process—II: Carbonization of various coals and asphalt with NaOH.* Carbon, 1982. **20**(1): p. 47-53.

22. Yamashita, Y. and K. Ouchi, *Influence of alkali on the carbonization process—III: Dependence on type of alkali and of alkali earth compounds.* Carbon, 1982. **20**(1): p. 55-58.

23. Jarvis, M.W., J.W. Daily, H.-H. Carstensen, A.M. Dean, S. Sharma, D.C. Dayton, D.J. Robichaud, and M.R. Nimlos, *Direct detection of products from the pyrolysis of 2-phenethyl phenyl ether.* The Journal of Physical Chemistry A, 2011. **115**(4): p. 428-438.

24. Klein, M., *Lignin thermolysis pathways*, 1981, Ph. D. Dissertation, Department of Chemical Engineering, Massachussetts Institute of Technology, 1981.(27) Karagöz, S.

25. Evans, R.J., T.A. Milne, and M.N. Soltys, *Direct mass-spectrometric studies of the pyrolysis of carbonaceous fuels: III. Primary pyrolysis of lignin.* Journal of Analytical and Applied Pyrolysis, 1986. **9**(3): p. 207-236.

26. Amen-Chen, C., H. Pakdel, and C. Roy, *Production of monomeric phenols by thermochemical conversion of biomass: a review.* Bioresource Technology, 2001. **79**(3): p. 277-299.

27. Patwardhan, P.R., R.C. Brown, and B.H. Shanks, *Understanding the Fast Pyrolysis of Lignin.* ChemSusChem, 2011. **4**(11): p. 1629-1636.

28. Kuzhiyil, N., D. Dalluge, X. Bai, K.H. Kim, and R.C. Brown, *Pyrolytic Sugars from Cellulosic Biomass.* ChemSusChem, 2012. **5**(11): p. 2228-2236.

29. Dalluge, D.L. and R.C. Brown. *Pyrolytic Pathways to Increasing the Lignin-Derived Monomer/Oligomer Ratio in Bio-oil*. in *The International Conference on Thermochemical Conversion Science (TCBiomass 2011)*. 2011. Chicago, Illinios.

30. Alsharaeh, E.H., Y.M. Ibrahim, and M.S. El-Shall, *Direct evidence for the gas phase thermal polymerization of styrene. Determination of the initiation mechanism and structures of the early oligomers by ion mobility.* Journal of the American Chemical Society, 2005. **127**(17): p. 6164-6165.

31. Simoneit, B.R., W. Rogge, M. Mazurek, L. Standley, L. Hildemann, and G. Cass, *Lignin pyrolysis products, lignans, and resin acids as specific tracers of plant classes in emissions from biomass combustion.* Environmental Science & Technology, 1993. **27**(12): p. 2533-2541.

32. Jakab, E., O. Faix, F. Till, and T. Székely, *The effect of cations on the thermal decomposition of lignins.* Journal of Analytical and Applied Pyrolysis, 1993. **25**: p. 185-194.

33. Gray, M.R., W.H. Corcoran, and G.R. Gavalas, *Pyrolysis of a wood-derived material. Effects of moisture and ash content.* Industrial & Engineering Chemistry Process Design and Development, 1985. **24**(3): p. 646-651.

34. Nguyen, M.T., D. Sengupta, G. Raspoet, and L.G. Vanquickenborne, *Theoretical Study of the Thermal Decomposition of Acetic Acid: Decarboxylation Versus Dehydration.* The Journal of Physical Chemistry, 1995. **99**(31): p. 11883-11888.

35. Hosoya, T., H. Kawamoto, and S. Saka, *Role of methoxyl group in char formation from lignin-related compounds.* Journal of Analytical and Applied Pyrolysis, 2009. **84**(1): p. 79-83.

36. Houk, K. and R. Strozier, *Lewis acid catalysis of Diels-Alder reactions.* Journal of the American Chemical Society, 1973. **95**(12): p. 4094-4096.

CHAPTER 4

COMPARISON OF DIRECT CONTACT AND INDIRECT CONTACT HEAT EXCHANGE IN LEVOGLUCOSAN RECOVERY FROM CELLULOSE FAST PYROLYSIS

A paper prepared for submission to *Bioresources Technology*

Dustin L. Dalluge, Yong S. Choi, Brent H. Shanks, Robert C. Brown

Abstract

This study investigates the effect of bio-oil collection conditions on overall bio-oil composition. Pure cellulose was pyrolyzed in a fluidized bed pyrolyzer at 500^{o}C with bio-oil collected in either a conventional water cooled condenser system or a novel cold-gas quench system. The quench system was estimated to achieve an approximate seven fold increase in cooling rate over the conventional system. Direct contact cooling utilized in the quench system also eliminates temperature gradients commonly encountered within the bio-oil film while it accumulates along the walls of water cooled condensers. Both a faster bio-oil cooling rate and the elimination of temperature gradients helped to reduce thermal polymerization and secondary decomposition of primary pyrolysis products, especially anhydrosugars such as levoglucosan. The quench system increased levoglucosan yield in the bio-oil by 23% while minimally effecting yield of other volatile compounds.

Introduction and background

Renewable energy and sustainable energy production are top priorities for the nation to help provide national, economic, and environmental security. Among the renewable

energy sources, biomass is most promising for production of liquid fuels that can be utilized in the existing infrastructure, so called "drop-in fuels." Biomass, like many other renewable energy sources, utilizes solar energy; however, in contrast to many other forms of renewable energy, it also offers the advantage of being a storable form of energy. Biomass offers advantages since it can be regrown annually almost anywhere sunlight, water, soil, and nutrients are available. Biomass also extracts carbon dioxide from the atmosphere as it grows, which gives it the potential to produce carbon-neutral or even carbon-negative fuels. Biomass derived fuels therefore essentially close the carbon-cycle and can be useful for mitigating concern of atmospheric carbon dioxide concentration [1].

Two main pathways exist for conversion of biomass to liquid fuels and chemicals: the biochemical pathway, which is commonly used in ethanol manufacturing plants using microorganisms to ferment starches to ethanol, and the thermochemical pathway, which uses heat and/or catalysts for the main conversion step. Fast pyrolysis is an example of one of the many thermochemical pathways being considered for commercial production of biorenewable fuels and chemicals. Fast pyrolysis, i.e. the rapid thermal decomposition of organic compounds in the absence of oxygen, is a capable of producing a variety of compounds from biomass including phenolics and sugars suitable for upgrading to transportation fuels. Monosaccharides resulting from the depolymerization of cellulose and hemicellulose offer advantages in that they can be directly upgraded to liquid fuels by processes such as aqueous phase carbohydrate upgrading [2, 3], or fermented to produce alcohols via micro-organisms using so-called

hybrid processing [4]. In either case, cellulose must first be depolymerized to monosaccharides before it can be utilized by microorganisms in hybrid processing or upgraded to hydrocarbons via aqueous phase carbohydrate upgrading. Fast pyrolysis is quickly gaining interest as a cost-effective approach to converting biomass into sugar rich bio-oil due to its relatively simple and fast conversion step [5].

Achieving high yields of sugar-rich bio-oil is dependent on feedstock, operating conditions, and bio-oil collection systems. Previous research by Kuzhiyil et al. [6] showed that biomass feedstocks can be optimized for sugar production by preventing alkali and alkaline earth metals (AAEMs) from fragmenting biomass carbohydrates to light oxygenates during pyrolysis. The process involves pretreating the biomass with a specific quantity of mineral acid that acts to passivate AAEMs. Reactor operating conditions, such as temperature and sweep gas flow rate, also contribute significantly to the overall sugar yield from biomass. Bio-oil collection has been explored by several other researchers [7-9]; however the process has not been optimized for sugar production. The goal of this research is to determine the effects of bio-oil collection parameters on sugar yield from cellulose fast pyrolysis.

Materials and Methods

Materials

Pure cellulose was used as the feedstock for the present work. The cellulose was purchased from Sigma-Aldrich under the trade name Sigmacell®, a microcrystalline

cellulose powder with an approximate particle diameter of 50 μm (Sigma Aldrich SKU: S5504). Ash content of the cellulose was analyzed to be less than 0.01 wt. %.

Fluidized Bed Reactor

A 100 g/hr. bubbling fluidized bed reactor was used to pyrolyze the cellulose powder. A diagram of the reactor system is shown in Figure 1. The reactor consists of a volumetric feed system, an injection auger, the bubbling fluidized bed reactor, dual cyclones for solids separation and the bio-oil collection system.

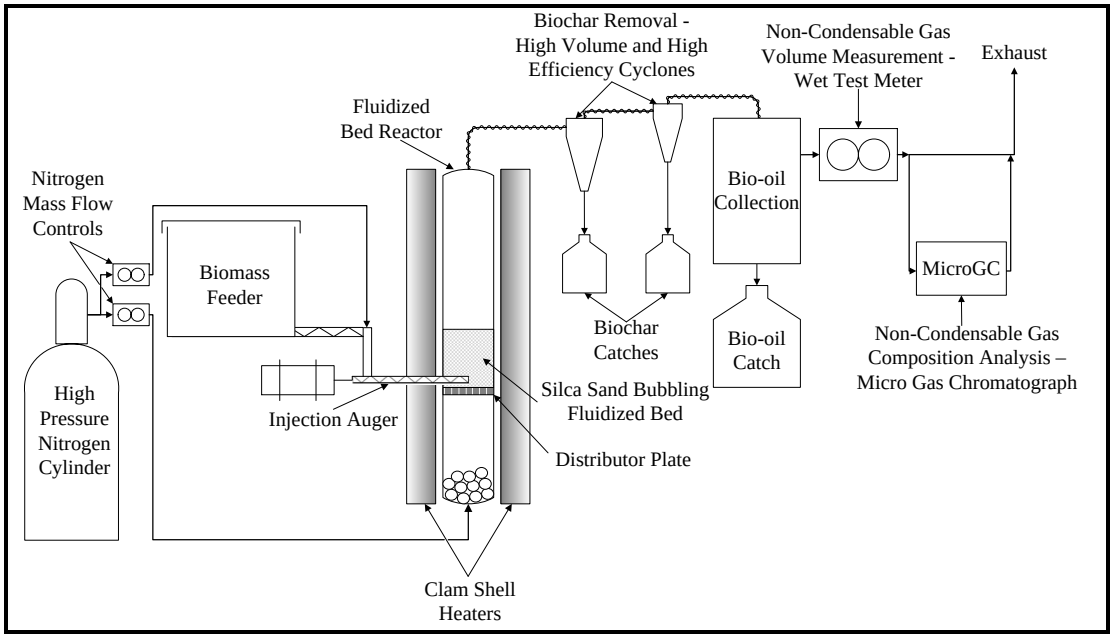

Figure 1: Fluidized bed reactor diagram.

The volumetric feeder was calibrated to feed cellulose to the fluidized bed reactor at a rate of 100 g/hr. The volumetric feeder delivered the cellulose into an injection auger which operated at a constant 60 rpm. The injection auger introduced the cellulose directly into the silica sand bed of the bubbling fluidized bed reactor.

The bubbling fluidized bed reactor consisted of a 316 stainless steel pipe 0.34 m in height with an inner diameter of 38.1 mm. The plenum, which was designed to both preheat the nitrogen sweep gas and provide a uniform supply of nitrogen through the porous distributor plate, was 0.17 m in height with an inner diameter of 38.1 mm. Watlow® ceramic clamshell heaters were used to maintain the plenum and reactor temperatures at 500°C.

The fluidization media consisted of 100 g of silica sand with a mean sieve size of 520 μm which corresponded to a packed bed height of approximately 55 mm. Nitrogen sweep gas was introduced into the plenum at 8 standard liters per minute (SLPM) and purged through the feed system at 2 SLPM leading to a total flow rate of 10 SLPM. The flow rates corresponded to a superficial velocity of 36 cm/s and a ratio of superficial gas velocity to minimum fluidization velocity (U/Umf) of approximately 2.6.

Solids separation consisted of a series of two cyclonic separators, the first being used to remove the majority of the char (high volume) and the second used to remove any remaining char down to very fine particle size (high efficiency). The cyclones and all required piping up to the bio-oil collection system were heat traced with BriskHeat® heating tapes to maintain 475°C.

After solids separation the pyrolysis vapor stream entered the bio-oil collection system. Figure 1 shows the fluidized bed system where the component labeled "Bio-oil collection" was alternated between a conventional water cooled condensation system and a novel cold-gas quench system. Each of the bio-oil collection systems has distinct operating parameters including cooling rates, residence times, temperature gradients, and

separation between stage fractions. Vapor residence time in the reactor and piping prior to the bio-oil collection system was approximately 1.3 s.

Conventional Condenser System

The conventional condenser system consisted of two water cooled condensers, an electrostatic precipitator, and a final condenser as shown in Figure 2. Each component collects a separate fraction of bio-oil where each is labeled sequentially as a separate stage fraction (SF1, SF2, etc.). The first two condensers were stepped down in surface temperature to selectively condense higher molecular weight products in the first condenser (SF1) and lower molecular weight products in the second condenser (SF2). The condensers had enough cooling capacity to condense the bio-oil compounds; however, they were not capable of removing a majority of the aerosols formed during the cooling process. Any entrained aerosols were removed in an electrostatic precipitator to produce bio-oil stage fraction 3 (SF3). The final condenser (SF4), operated with a surface temperature of -10°C and collected any remaining moisture or light oxygenates.

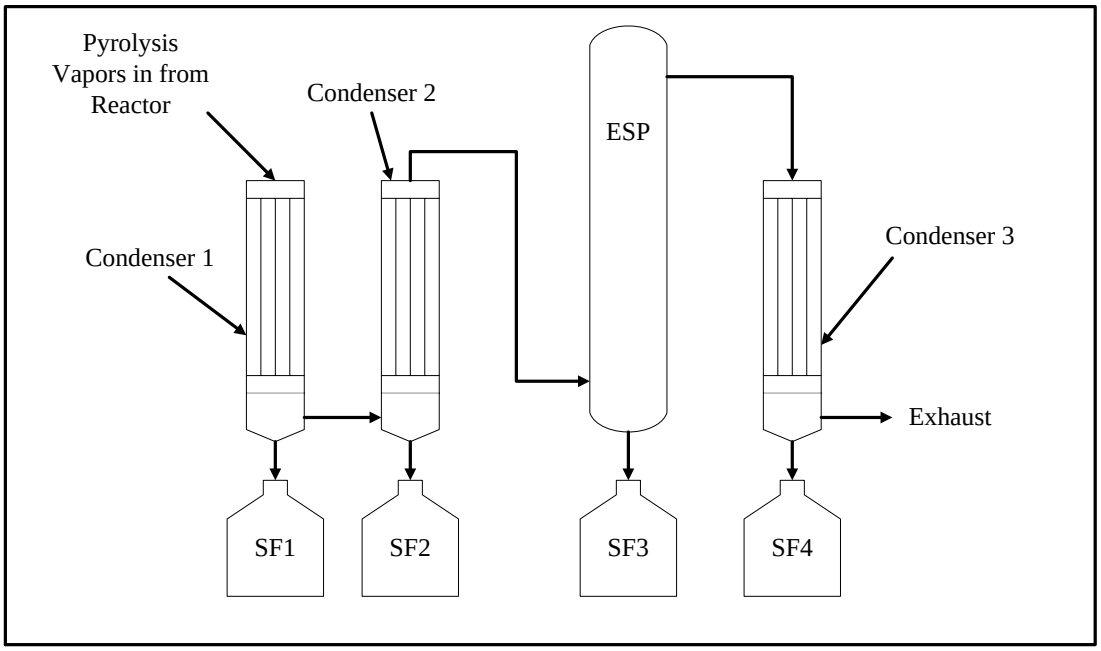

Figure 2: Conventional bio-oil recovery system diagram.

Cold Gas Quench System

A novel cold-gas quench bio-oil collection system was developed by Iowa State University and the Phillips 66 Company [10] to both quickly quench the pyrolysis vapors and separate compounds based on their dew point. As shown in Figure 3, the quench system consisted of a quench chamber, a liquid nitrogen injection line, an electrostatic precipitator, and a final condenser. Bio-oil was collected in two stage fractions. The first stage fraction collected in the electrostatic precipitator and contained higher boiling point organic compounds. The second stage fraction collected in a final shell and tube condenser and contained lower boiling point organic compounds and water.

Liquid nitrogen was injected into the quench chamber by passing gaseous nitrogen into a heat transfer coil that was submerged in a dewar of liquid nitrogen. A heavily

insulated stainless steel tube connected the heat transfer coil to a nozzle in the quench chamber. As the liquid nitrogen emerged from the spray nozzle it immediately contacted the hot pyrolysis vapor stream. Mass flow rate of the liquid nitrogen was controlled to cool the pyrolysis vapor stream to a specified temperature. Aerosol droplets quickly formed from bio-oil vapors as they cooled below their dew points due to contact with liquid nitrogen. An electrostatic precipitator was used to separate the aerosols from the pyrolysis vapor stream, collecting them into a distinct bio-oil fraction (SF1).

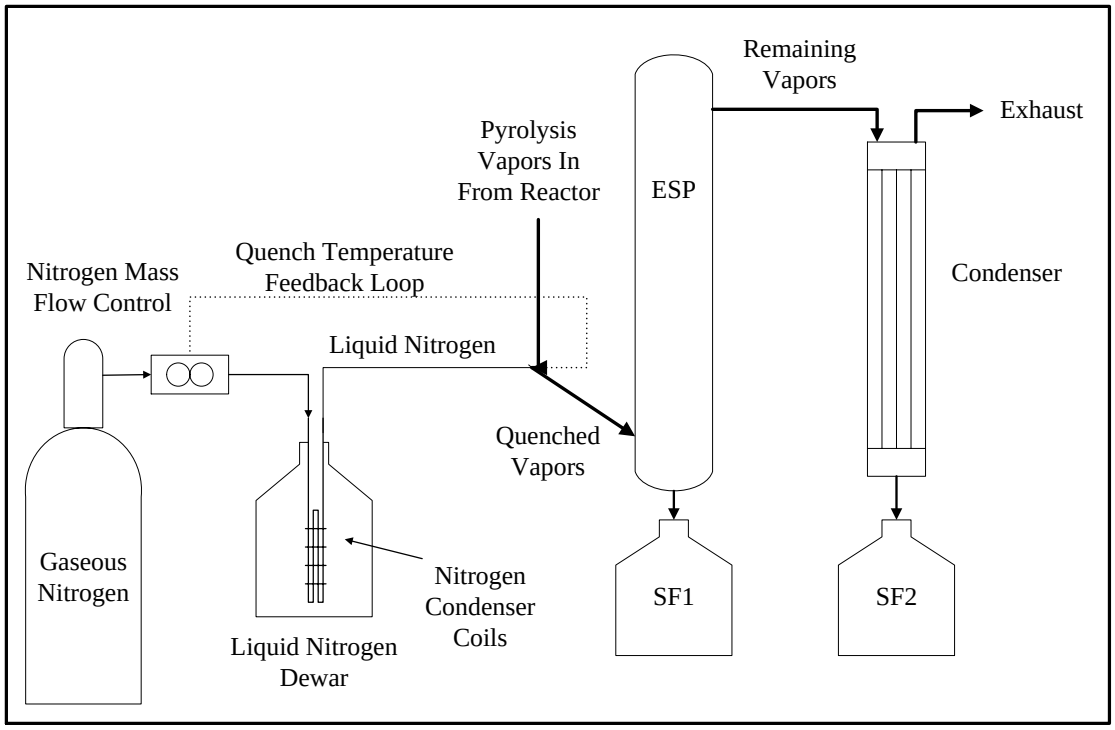

Figure 3: Cold-gas quench bio-oil recovery system diagram.

The liquid nitrogen flow rate was set up in a cooling control loop to provide precise temperature control. The temperature of the quenched vapors was fed back into a control loop which regulated the mass flow of nitrogen to maintain the quench

temperature at 90°C. A quench temperature of 90°C was chosen as it was calculated to be just above the dew point of water and well below the dew point of levoglucosan, therefore providing an SF1 rich in levoglucosan and low in moisture. The surface of the ESP was heated to 100°C both to reduce the viscosity of the collected bio-oil to keep it flowing downward into the collection bottle and to evaporate any condensed moisture.

Any remaining pyrolysis vapors discharged the ESP at around 90°C and passed into a shell and tube heat exchanger, also known as the condenser, operating with a wall temperature of -10°C. The condenser collected the bio-oil aqueous phase consisting of water and light oxygenates, such as carboxylic acids, in a second bio-oil fraction (SF2).

In order to determine cooling rate effects on the yield of sugar compounds, the temperature change across specific bio-oil collection components was divided by the residence time of the vapors within the system up to that point and termed "cumulative effective cooling rate." The quench system collected all of the sugars in SF1; therefore the cumulative effective cooling rate was calculated starting from the outlet of the reactor and ending at the entrance to the isothermal ESP that collected SF1. The conventional system collected sugars in SF1, SF2, and SF3; therefore the cumulative effective cooling rate was calculated starting from the outlet of the reactor and ending at the entrance to the isothermal ESP that collects SF3. As shown in Table 1 and Table 2, the conventional system provided a cooling rate of approximately 450°C/s whereas the quench system resulted in a cooling rate of approximately 3360°C/s.

The quench system increased cumulative effective cooling rate via two mechanisms; 1) increased heat transfer rate and 2) decreased residence time. The pyrolysis vapor

stream encountered less thermal resistance when directly contacted with liquid in comparison to indirect cooling with water cooled condensers, which leads to the increased heat transfer rate. Liquid nitrogen, which entered the quench system at -196°C, quickly flashed to gaseous nitrogen at temperatures encountered in the quench system. The quantity of liquid nitrogen utilized to cool the pyrolysis vapor stream, once expanded to the gas phase, approximately doubled the gas flow rate through the system, thus decreasing overall residence time. Additionally the pyrolysis vapor stream encountered less system volume in the quench system, which decreased residence time. Cooling rate in the quench system increased by almost seven fold over the conventional system as a result of the increased heat transfer rate and decreased residence time.

Table 1: Conventional bio-oil recovery system operating parameters.

Component	Average Flow Rate (SLPM)	Vapor Temperature In (°C)	Vapor Temperature Out (°C)	Wall Temperature (°C)	Component Residence Time (s)	Cumulative Residence Time (s)	Cumulative Effective Cooling Rate (°C/s)
Condenser 1	9.7	460	135	68	0.36	0.36	900
Condenser 2		135	45	26	0.57	0.93	***450***
ESP		45	45	54	12.23	13.16	30
Condenser 3		45	10	-10	4.31	17.47	30

Table 2: Cold-gas quench bio-oil recovery system operating parameters.

Component	Average Flow Rate (SLPM)	Vapor Temperature In (°C)	Vapor Temperature Out (°C)	Wall Temperature (°C)	Component Residence Time (s)	Cumulative Residence Time (s)	Cumulative Effective Cooling Rate (°C/s)
Quench	20.3	460	90	475	0.11	0.11	***3360***
ESP		90	90	100	5.25	5.36	70
Condenser		90	10	-10	1.91	7.27	60

Mass Balances

Mass balances for bio-oil and char were measured gravimetrically by weighing the char catches and bio-oil collection system components before and after each test. The difference in mass from before the experiment to after the experiment was used for calculating the mass balance.

Non-Condensable Gas Measurement

Concentrations of non-condensable gases in the exhaust stream were measured using a Varian® CP-4900 micro-Gas Chromatograph (microGC) interfaced with Galaxy® Chromatography software. A split-line off of the main exhaust line and a sampling pump were used to supply the GC with a constant flow of approximately 0.5 L/min. The microGC was programmed to sample for 30 s followed by 140 s run time for analysis. The sample line and injectors one and two were set to operate isothermally at 110°C with a 40 ms injection time. Injector three operated isothermally at 80°C with an 80 ms injection time. A thermal conductivity detector was used for gas detection on each channel. Channel one was setup with a Varian® Molesieve 5 Å column operating at 100°C with argon carrier gas at 151.7 kPa. Channel one was calibrated to measure helium, hydrogen, oxygen, nitrogen, methane and carbon monoxide. A Varian® PoraPLOT Q column was setup on channel two operating at 58°C with helium carrier gas at 117.2 kPa. Channel two was calibrated to measure carbon dioxide, ethylene, acetylene, and ethane. A Varian® Al2O3 column was setup on channel three operating at 60°C with helium carrier gas at 55.2 kPa. Channel three was calibrated to measure propane.

Total gas volume leaving the reactor was measured using a Ritter® TG5/4-ER-1 bar wet test meter. The mass of non-condensable gases produced during the reaction was calculated using the overall gas volume and the steady-state concentrations of gases exiting the system.

Water Soluble Sugar Analysis via High Performance Liquid Chromatography

Water soluble anhydrosugars cellobiosan (1,6-anhydro-β-D-cellobiose) and levoglucosan (1,6-anhydro-β-D-glucopyranose) were quantified via a water wash method followed by analysis with High Performance Liquid Chromatography (HPLC). Approximately 500 mg bio-oil was dissolved in 3 mL of water, thoroughly mixed with a vortex mixer, and then centrifuged at 3500 rpm for 15 min. The supernatant was poured off and the precipitate was washed three additional times with 3 mL of deionized water to ensure the water soluble sugars were fully dissolved. An additional 9 mL of water was added to the accumulated supernatant to bring the total up to 18 mL. The resulting solution was filtered through a Whatman® 0.45 μm glass microfiber filter prior to analysis.

A Dionex UltiMate® 3000 high performance liquid chromatography system interfaced with Chromeleon® software and a Refractive Index (RI) detector was used to quantify water soluble sugars. Two Bio-Rad® Aminex HPX-87P columns were used in series for separation with a guard column and Micro-guard cartridge. The column compartment was held at 75°C for analysis. Ultrapure deionized water of 18.2 MΩ-cm purity was used as eluent at a flow rate of 0.6 mL/min. Water soluble sugars

levoglucosan and cellobiosan were calibrated in the range from 0-10 mg/mL using a linear five point calibration.

Total Sugar Analysis via Acid Hydrolysis and HPLC

Monomeric and dimeric sugars resulting from cellulose pyrolysis are largely soluble in water; however, monomeric and dimeric sugars can also polymerize to form water-insoluble polysaccharides [11]. In order to jointly quantify water soluble and water insoluble sugars, all sugars were first hydrolyzed to glucose and xylose via acid hydrolysis. The total sugar yield was calculated based on the quantity of bio-oil that was capable of hydrolysis.

Approximately 60 mg of bio-oil was first placed in a hydrolysis reactor vessel (HRV) and then dissolved in 6 mL of 400 mM sulfuric acid. A Teflon gasket and a cap were placed on the HRV which was then placed in a 125°C oil bath. After 45 minutes in the oil bath the HRV was quickly chilled to room temperature in a freezer followed by centrifuging at 3500 rpm for 15 min. The supernatant was filtered with a Whatman® 0.45 μm glass microfiber filter and injected into a 2 mL glass vial.

A Dionex UltiMate® 3000 high performance liquid chromatography system interfaced with Chromeleon® software was used for HPLC analysis. A 300 mm X 7.7 mm, 8 μm particle size HyperRez XP® Carbohydrate analytical column was used for separation of the carbohydrates. A Carbohydrate H+® cartridge was used as the guard column prior to the HyperRez XP® column. The mobile phase was 18.2 MΩ-cm deionized water at a flow rate of 0.2 mL/min. The column compartment was held

isothermally at 55°C. Further details of the hydrolysis method are available from Johnston and Brown [12].

Moisture Analysis

Moisture analysis was performed using a Karl Fischer MKS-500® moisture titrator. Hydranal Working Medium K® was used as the solvent and Hydranal Composite 5 K® was used as the titrant. The instrument was calibrated using deionized water prior to sample analysis.

Carboxylic Acids Analysis

Approximately 100 mg of bio-oil was dissolved in 1.5 mL methanol and 6 mL deionized water for organic acids analysis of fractions with relatively low organic acid content. To remain within the calibrated range, samples with high organic acid content were diluted with an additional 34 mL of deionized water i.e. 1.5 mL of methanol and 40 mL of water. The sample was filtered through a Whatman® 0.45 μm glass microfiber filter prior to analysis.

A Dionex® ICS3000 ion chromatography system with a conductivity detector and an Anion Micromembrane Suppressor (AMMS-ICE 300) was used for analysis of the bio-oil samples. The Dionex system was interfaced with Chromeleon® software version 6.8.

Tetrabutylammonium hydroxide in water at a concentration of 5 mM was used to regenerate the suppressor at a flow rate of 4-5 mL/min. Heptaflourobutyric acid diluted in water to 1.0 mM was used as the eluent at a flow rate of 0.120 mL/min at 19°C. An IonPac® ICE-AS1 4x50 mm guard column in series with an IonPac® ICE-AS1 4x250

mm analytical column were used for separation. Standards of acetate, propionate, formate and glycolate were purchased from Inorganic Ventures (Christiansburg, Virginia) to calibrate the instrument. The concentrated standard was certified at 200.0 ± 1.3 mg/L for all acids and was diluted down with ultrapure deionized water to concentrations of 10, 25, 67, 100, and 200 mg/L to achieve a 5 point linear calibration.

Gas Chromatography/Flame Ionization Detector (GC/FID) Analysis of Volatile Organic Compounds

Phenanthrene was mixed in a methanol stock solution to provide an internal standard for comparison between chromatograms. Approximately 500 mg of bio-oil was mixed in 1.0 g of methanol stock solution for an approximate 33% bio-oil solution. The mixture was mixed on a vortex mixer for several minutes to ensure all of the bio-oil was dissolved. The resulting bio-oil solutions were filtered through a Whatman 0.45 μm glass microfiber filter prior to analysis.

A Bruker® 430-GC Gas Chromatograph with a Varian® CP-8400 liquid injection autosampler interfaced with Galaxy® software was used for GC/FID analysis. A 60 m Zebron® ZB-1701 column with a 0.25 mm inner diameter was used for separation of volatile species. The GC method operated with an injector temperature of 300°C and a split ratio of 30. The oven program started at 35°C, held for 3 min, ramped at 5°C/min to 300°C and held for 4 min for a total run time of 60 min. The column pneumatics was set for constant flow at 1 mL/min helium carrier gas. The FID operated at 300°C with 25 mL/min helium makeup flow, 30 mL/min hydrogen, and 300 mL/min air flow. A four point linear calibration was developed from known standards. Standard were not

available for xylosan (1,4-anhydro-α-D-xylopyranose) or levoglucosan-furanose (1,6-anhydro-β-D-glucofuranose) at the time of analysis and therefore were quantified using the response factor of levoglucosan. Retention time of both xylosan and levoglucosan-furanose were found by comparing chromatograms from the FID with chromatograms from a mass spectrometer operating with identical GC conditions. Glycolaldehyde couldn't be purchased as a pure compound and was therefore calibrated via pyrolysis of the dimer at 500°C with different mass loadings. One major peak was observed with a few minor peaks and the major peak was identified to be the glycolaldehyde monomer via GC/MS. Although this method may not fully account for all of the glycolaldehyde produced it should serve well for comparison purposes.

Water Insolubles Analysis

Bio-oil resulting from cellulose contained a small amount of water insoluble content, which is likely to be carbohydrate oligomers. Water insoluble content was quantified by a method developed in-house. Water was heated to 80°C prior to mixing with bio-oil at a ratio of 80:1 water-to-bio-oil on a mass basis. The mixture contained in a 50 mL centrifuge tube was thoroughly mixed using a vortex mixer for one minute. Following vortex mixing each centrifuge tube was sonicated for 30 min. The mixture was then centrifuged at 2500 rpm for 20 minutes. The supernatant was next filtered through a Whatman® 2 µm filter. The centrifuge tube and filter paper containing the water insolubles were then dried at 50°C for 24 hours. Accumulated mass on both the filter paper and centrifuge tube were considered water insoluble content.

Results and Discussion

Overall Mass Balance

Mass balances and bio-oil composition were compared for each system using a Student t-Test. The t-statistic for the comparison of each mean is indicated in the column labeled "Prob. > t." A t-statistic of 0.05 indicates a 95% probability that the mean for the quench system is significantly greater than the mean for the conventional system. Similarly, a t-statistic of 0.95 indicates a 95% probability that the mean for the conventional system is significantly greater than the mean for the quench system. As shown in Table 3, mass balances from each system were similar as might be expected since the reactor operating conditions were identical. Bio-oil yield from the conventional recovery system averaged 87.4 wt. % whereas yield from the quench system averaged 83.3 wt. %. The t-statistic from comparing the average bio-oil yield was 0.97 indicating that the conventional system resulted in a statistically significant increase in bio-oil yield. Three factors are expected to contribute to the higher bio-oil yield in the conventional system: 1) lower dew points of bio-oil compounds in the quench system, 2) higher gas velocities in the quench system, and 3) contribution of char to the bio-oil mass in the conventional system.

The rapid cooling of pyrolysis vapors by the addition of cold nitrogen to the pyrolysis vapor stream discouraged secondary reactions; however, the diluting effect of the nitrogen reduced the dew points of bio-oil compounds, making them more difficult to separate from the pyrolysis vapor stream. Since the same temperatures were used for the final condenser on each system, but the partial pressures were lower in the quench

system which lead to lower dew points; some of the bio-oil that would normally be collected in the conventional system likely remained as a vapor in the quench system. The uncollected bio-oil would therefore contribute to the difference in bio-oil yields between the two systems.

Higher gas velocity through the quench system due to the injected nitrogen may have prevented some aerosols from condensing with the cooled vapor. Later tests using the quench system with an additional electrostatic precipitator placed in series after the SF2 condenser collected an additional 1-3 wt. % bio-oil that was rich in levoglucosan. Therefore, it can be expected that some of the bio-oil remains entrained through the final condenser when using the quench system. Uncollected bio-oil from aerosol entrainment would therefore contribute to the lower bio-oil yield from the quench system.

Table 3: Mass balance comparisons.

Product	Quench Average (wt.% of cellulose feedstock)	Conventional Average (wt.% of cellulose feedstock)	Prob > t
Bio-oil	83.3%	87.4%	0.97
Char	3.4%	2.5%	0.25
Non-Condensable Gases	4.2%	5.4%	0.79
Mass Closure	90.8%	95.3%	0.94

Increased char formation from secondary reactions is likely another contributing factor to higher bio-oil yields from the conventional bio-oil collection system. Both the conventional system and the quench system produced some secondary char at the inlets to the bio-oil collection system which is thought to form when vapors condense or aerosols impinge on the high temperature inlets. The hot bio-oil polymerizes and dehydrates to char at the inlet and some of it ends up being collected with the bio-oil. The secondary char couldn't be separated from the bio-oil due to the intrinsic mixing of

the two at the inlet. Mass balances were determined by simply weighing the bio-oil collection system components and therefore secondary char would contribute to the bio-oil mass. As will be discussed in more detail later, the slower cooling rate of the conventional system leads to longer residence times of the bio-oil at high temperature which encourages char formation from secondary reactions. Therefore bio-oil yield from the conventional bio-oil collection system is more likely to be inflated due to including the mass of secondary char.

The reported char yield considered only char collected in the gas cyclones ahead of the bio-oil collection system. Thus, the char yield does not include any secondary char produced in the bio-oil collection system. Char yield for the two systems were similar at 3.4 wt. % for the quench system and 2.5 wt. % for the conventional system. The t-statistic of 0.25 suggests there is no statistical significance between the char yields as might be expected since the pyrolysis conditions were identical for the two systems.

Non-condensable gas yield was similar for each system. The quench system averaged 4.2 wt. % and the conventional system averaged 5.4 wt. % non-condensable gases. The t-statistic from comparison of the means was 0.79 suggesting no statistical significance between non-condensable gases from each system.

Overall mass closures were approximately 91 wt. % for the quench system and 95 wt. % for the conventional system. The lower mass closure for the quench system correlates directly with lower bio-oil yield. As discussed earlier, there are several factors contributing to the higher bio-oil yield in the conventional system, also leading to the higher mass closure.

Figure 4: Char formation at high temperature condenser inlet.

Bio-oil Composition

In order to determine the effect of the cooling rate on bio-oil composition, the concentrations of compounds from each stage fraction were combined to provide a "whole bio-oil" composition. Table 4 summarizes the bio-oil composition resulting from the two bio-oil recovery systems. Approximately 90% of the collected bio-oil was accounted for from each system.

Table 4: Bio-oil composition comparison.

Compound/ Compound Group	Quench System Average (wt.% bio-oil)	Conventional System Average (wt.% bio-oil)	Prob > t
Carboxylic Acids	**1.27%**	**1.92%**	**0.77**
Acetic Acid	0.39%	0.63%	0.78
Formic Acid	0.55%	0.78%	0.77
Glycolic Acid	0.33%	0.51%	0.75
Furans	**0.87%**	**1.18%**	**0.48**
2(5H)-Furanone	0.14%	0.17%	0.59
2-Furanmethanol	0.03%	0.04%	0.58
5-(Hydroxymethyl)furfural	0.23%	0.55%	0.71
5-Methylfurfural	0.09%	0.08%	0.46
Furfural	0.30%	0.24%	0.26
Methylcyclopentenolone	0.08%	0.10%	0.63
Light Oxygenates	**13.0%**	**12.1%**	**0.43**
Acetol	0.6%	0.1%	0.07
Formaldehyde	4.4%	3.9%	0.45
Glycolaldehyde	8.0%	7.7%	0.44
Total Sugars	**63.2%**	**57.8%**	**0.15**
1,4:3,6-dianhydro-D-glucose	0.3%	0.2%	0.25
Cellobiosan	5.6%	8.0%	0.89
Levoglucosan	45.5%	37.1%	0.04
Levoglucosan-Furanose	1.5%	1.0%	0.09
Xylosan	2.8%	2.6%	0.31
Water	**11.8%**	**11.9%**	**0.54**
Water Insolubles	**2.5%**	**2.4%**	**0.79**
Total Accounted	**92.6%**	**87.3%**	

Carboxylic acids including acetic acid, formic acid, and glycolic acid, were quantified via ion chromatography. The quench system produced an average carboxylic acid concentration of 1.3 wt. % and the conventional system produced an average of 1.9 wt. %. Variability between runs however led to a t-statistic of 0.77 which indicates the difference was not statistically significant.

Furans were quantified via GC/FID and included 2(5H)-furanone, 2-furanmethanol, 5-(hydroxymethyl)furfural, 5-methylfurfural, furfural, and methylcyclopentenolone.

The quench system produced an average 0.87 wt. % furans and the conventional system produced an average 1.18 wt. % furans. Comparing the two means resulted in a t-statistic of 0.48 indicating that there is no statistical significance in furan yield between the two systems.

Light oxygenates including glycolaldehyde, formaldehyde, and acetol were quantified via GC/FID. Bio-oil from the quench system contained 13.0 wt. % light oxygenates while the conventional system averaged 12.1 wt. %. The t-statistic resulting from comparison of the means was 0.43 indicating no statistically significant difference in bio-oil light oxygenates from the two systems. Acetol concentration averaged 0.6 wt. % from the quench system and 0.1 wt. % from the conventional system. The t-statistic from comparing the average acetol yield from each system was 0.07 indicating there may be some statistical significance. Glycolaldehyde made up the majority of bio-oil light oxygenates at a concentration of 8 wt. % bio-oil from both systems. Formaldehyde averaged 4.4 wt. % from the quench and 3.9 wt. % from the conventional system; however, the difference was not statistically significant.

Total glucose hydrolysable sugars were measured via acid hydrolysis. Total glucose hydrolysable sugars made up 57.8 wt. % of bio-oil from the conventional recovery system and 63.2 wt. % of bio-oil from the quench system. The t-statistic from comparing glucose hydrolysable sugars was 0.15 which indicates some statistical significance. It is important to note that analysis of total sugars includes water added to anhydrosugar from the hydrolysis process. Therefore the mass sum of all anhydrosugars will actually be slightly less than the mass of glucose hydrolysable sugars. Water could

not be subtracted from the total sugar yield because not all sugars could be explicitly analyzed and accounted for before hydrolysis; therefore it is not known how much water was added. Water added to the sugars shouldn't however make a difference in comparing glucose hydrolysable sugars from each system since they were analyzed identically.

Levoglucosan was measured via HPLC. Bio-oil from the conventional recovery system contained 37.1 wt. % levoglucosan and bio-oil from the quench system contained 45.5 wt. % levoglucosan; a 23% increase. The t-statistic from comparing levoglucosan yields was 0.04 indicating more than 95% confidence that the difference is statistically significant.

Cellobiosan yield was measured via HPLC. The conventional and quench systems produced bio-oil containing 8.0 wt. % and 5.6 wt. % cellobiosan, respectively. The t-statistic from comparing the average cellobiosan concentration was 0.89 which indicates some statistical significance.

Levoglucosan is known to thermally polymerize when subjected to elevated temperatures especially above 280°C [11, 13-17]. Kawamoto et al. [16] found that the oligosaccharides formed from levoglucosan polymerization can be reversibly pyrolyzed to again produce levoglucosan; however once they begin to dehydrate and fragment they tend to carbonize and release decomposition products such as furans and light oxygenates. Therefore, levoglucosan exposed to temperatures of 250°C or higher will either volatilize or polymerize depending upon reaction conditions.

A major difference between the two bio-oil recovery systems is the more gradual temperature gradient that exists in conventional shell and tube condensers. The formation of char is commonly observed at the high temperature inlet to water-cooled condensers in conventional condenser system. Bio-oil is likely to condense on the heat transfer walls via film wise condensation where the film establishes a large temperature gradient between the wall and the hot gas stream. The wall temperature was close to 68°C while the gas stream ranged anywhere from 460°C at the condenser inlet to 135°C at the outlet. The difference in velocity between the downward flowing bio-oil film and the hot pyrolysis vapor stream led the surface of the bio-oil film to reach temperatures exceeding 250°C under certain circumstances. Anywhere the levoglucosan in the bio-oil is subject to temperatures above 250°C it is expected to undergo competing polymerization and evaporation. The higher molecular weight oligosaccharides and polysaccharides resulting from the thermal polymerization of levoglucosan have higher glass transition temperatures and viscosity [18]. The higher viscosity of the polysaccharides impedes their downward flow through condenser, which provides time for them to dehydrate and form char.

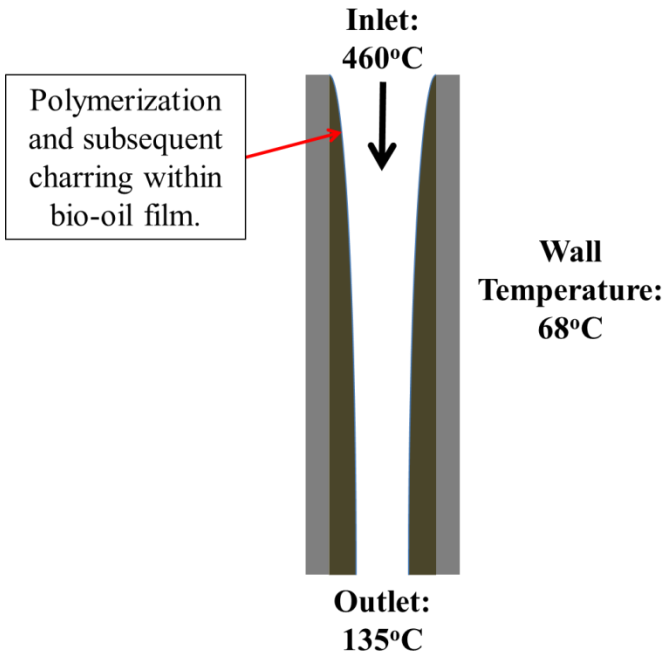

Figure 5: Illustration of the temperature gradient encountered in water cooled condensers.

Another possibility is that the levoglucosan vapors condense to liquid aerosols in which polymerization can occur. Levoglucosan and other anhydrosugars are known to have a small but appreciable vapor pressure [19], which allows them to escape the pyrolysis reactor as vapor. The low vapor pressure of levoglucosan results in liquid levoglucosan forming from cellulose faster than it can evaporate [11, 20]. At the high temperatures existing in a pyrolyzer the levoglucosan liquid would be subject to the competitive processes of volatilization and thermal polymerization [11, 20]. Under some circumstances, the pyrolysis product stream might become saturated with levoglucosan due to its relatively low saturation vapor pressure. Since the vapor stream cools in transport lines, nucleation of vapor to aerosols is a distinct possibility. If the

temperature remains higher than 250°C, the liquid levoglucosan might polymerize within the aerosol droplets to form cellobiosan and other polysaccharides.

Minor sugar components, including 1,4:3,6-dianhydro-D-glucose, levoglucosan-furanose, and xylosan, were measured via GC/FID and collectively made up around 5 wt. % of the bio-oil for each collection system. There was no statistically significant difference in the amount of 1,4:3,6-dianhydro-D-glucose or xylosan found in the bio-oil from either of the recovery systems, with t-statistics of 0.25 and 0.31, respectively. The furanose isomer of levoglucosan accounted for 1.5 wt. % and 1.0 wt. %, respectively, of bio-oil from the quench and conventional systems; a statistically significant difference at the 90% confidence level (t-statistic of 0.09). The increase in levoglucosan-furanose is directly correlated with the increase the pyranose isomer of levoglucosan.

Moisture in the bio-oil was measured via Karl Fischer titration. Moisture yield was nearly identical between the two systems 11.9 wt. % of bio-oil from the conventional system and 11.8 wt. % of bio-oil from the quench system.

Water insoluble content was almost identical between systems at 2.5 wt. % of bio-oil from the quench system and 2.4 wt. % of bio-oil from the conventional system. Water insoluble content from pyrolysis of cellulose is expected to be mostly carbohydrate oligomers but may contain some secondary char. It should be noted that only bio-oil from the collection bottles was tested with the water insolubles analysis. A significant portion of bio-oil, water insoluble content, and secondary char is also present along the walls of bio-oil collection system components, which would have been included in the mass balance, but was not analyzed separately. Any additional water insoluble content

derived from thermal polymerization near the inlet of the condensers therefore would not be quantified. Therefore water insoluble content, especially from the conventional collection system, may be underestimated with the method used here.

Conclusions

Rate at which bio-oil is cooled and condensed from the pyrolysis vapor stream has proven to play a significant role on levoglucosan yield. The quench system increased levoglucosan in the bio-oil by 23% compared to the conventional system. Quenching the pyrolysis vapor stream with liquid nitrogen acted to both decrease residence time at high temperature and dilute the vapor stream, both of which appear to contribute to levoglucosan yield. Elimination of temperature gradients in the quench system also helped to reduce thermal polymerization of levoglucosan and formation of secondary char.

Acknowledgements

The authors would like to thank the Phillips 66 company and the National Advanced Biofuels Consortium for their generous financial support of this project. We would also like to thank Marjorie Rover, Patrick Johnston, and Ryan Smith of the Center for Sustainable Environmental Technologies for assistance with many aspects of the work involved in this project. The authors would also like to thank undergraduate research assistants Jordan Donner, Sean Smith, Chris Quinett, and Nick Miller for helping run the experiments and analyze samples.

References

1. Lehmann, J. and S. Joseph, *Biochar for environmental management: science and technology*2009: Earthscan.

2. Elliott, D.C., T.R. Hart, G.G. Neuenschwander, L.J. Rotness, and A.H. Zacher, *Catalytic hydroprocessing of biomass fast pyrolysis bio-oil to produce hydrocarbon products.* Environmental Progress & Sustainable Energy, 2009. **28**(3): p. 441-449.

3. Regalbuto, J.R., *The sea change in US biofuels' funding: from cellulosic ethanol to green gasoline.* Biofuels, Bioproducts and Biorefining, 2011. **5**(5): p. 495-504.

4. Jarboe, L.R., W. Zhiyou, C. DongWon, and R.C. Brown, *Hybrid thermochemical processing: fermentation of pyrolysis-derived bio-oil.* Applied Microbiology & Biotechnology, 2011. **91**(6): p. 1519-1523.

5. Zhang, Y., T.R. Brown, G. Hu, and R.C. Brown, *Techno-economic analysis of monosaccharide production via fast pyrolysis of lignocellulose.* Bioresource Technology, 2013. **127**: p. 358-365.

6. Kuzhiyil, N., D. Dalluge, X. Bai, K.H. Kim, and R.C. Brown, *Pyrolytic Sugars from Cellulosic Biomass.* ChemSusChem, 2012. **5**(11): p. 2228-2236.

7. Li, Q., P.H. Steele, F. Yu, B. Mitchell, and E.-B.M. Hassan, *Pyrolytic spray increases levoglucosan production during fast pyrolysis.* Journal of Analytical and Applied Pyrolysis, 2013. **100**: p. 33-40.

8. Pollard, A.S., M.R. Rover, and R.C. Brown, *Characterization of bio-oil recovered as stage fractions with unique chemical and physical properties.* Journal of Analytical and Applied Pyrolysis, 2012. **93**: p. 129-138.

9. Westerhof, R.J.M., N.J.M. Kuipers, S.R.A. Kersten, and W.P.M. van Swaaij, *Controlling the Water Content of Biomass Fast Pyrolysis Oil.* Industrial & Engineering Chemistry Research, 2007. **46**(26): p. 9238-9247.

10. Daugaard, D.E., S.T. Jones, D.L. Dalluge, and R.C. Brown, *Selective Temperature Quench and Electrostatic Recovery of Bio-oil Fractions. U.S. Patent Application 13/114,846*, in *http://www.freepatentsonline.com/y2011/0315537.html*2011.

11. Bai, X., P. Johnston, S. Sadula, and R.C. Brown, *Role of levoglucosan physiochemistry in cellulose pyrolysis.* Journal of Analytical and Applied Pyrolysis, 2013. **99**: p. 58-65.

12. Johnston, P.A. and R.C. Brown, *Sugar Quantification withou Neutralization in Fast Pyrolysis Oils: Using High Performance Liquid Chromatography (HPLC) after Acid Hydrolysis.* Submitted to the Journal of Chromatography A, 2013.

13. Shafizadeh, F., *Saccharification of Lignocellulosic Materials.* Pure & Appl. Chem., 1983. **55**(4): p. 705-720.

14. Shafizadeh, F., C.W. Philpot, and N. Ostojic, *Thermal analysis of 1,6-anhydro-β-D-glucopyranose.* Carbohydrate Research, 1971. **16**(2): p. 279-287.

15. Wolfrom, M., A. Thompson, R. Ward, D. Horton, and R. Moore, *The Composition of Pyrodextrins. III. Thermal Polymerization of Levoglucosan1*. The Journal of Organic Chemistry, 1961. **26**(11): p. 4617-4620.

16. Kawamoto, H., M. Murayama, and S. Saka, *Pyrolysis behavior of levoglucosan as an intermediate in cellulose pyrolysis: polymerization into polysaccharide as a key reaction to carbonized product formation.* Journal of Wood Science, 2003. **49**(5): p. 469-473.

17. Houminer, Y. and S. Patai, *Thermal polymerization of levoglucosan.* Journal of Polymer Science Part A-1: Polymer Chemistry, 1969. **7**(10): p. 3005-3014.

18. Jiang, B., Y. Liu, B. Bhandari, and W. Zhou, *Impact of Caramelization on the Glass Transition Temperature of Several Caramelized Sugars. Part I: Chemical Analyses.* Journal of Agricultural and Food Chemistry, 2008. **56**(13): p. 5138-5147.

19. Suuberg, E.M. and V. Oja, *Vapor pressures and heats of vaporization of primary coal tars*, 1997, Federal Energy Technology Center, Morgantown, WV (US); Federal Energy Technology Center, Pittsburgh, PA (US).

20. Bai, X., P. Johnston, and R.C. Brown, *An experimental study of the competing processes of evaporation and polymerization of levoglucosan in cellulose pyrolysis.* Journal of Analytical and Applied Pyrolysis, 2013. **99**: p. 130-136.

CHAPTER 5

CONCLUSIONS AND FUTURE WORK

Conclusions

Biomass derived fuels and chemicals have the potential to displace up to 30% of current U.S. petroleum consumption while providing vast opportunities for rural development and improvement to national, economic, and environmental securities. The majority of biofuels consumed today are produced from grain ethanol which sparks several controversies in itself, including the so called "food versus fuel" and "indirect land use" debates. Advanced biofuels technologies that utilize non-edible lignocellulosic biomass are in their infancy and generally require government subsidies and/or outside financing in order to survive. Therefore, achieving technoeconomic feasibility of advanced biofuels is essential to their success which can be achieved by a combination of increasing product value and decreasing production costs.

Fast pyrolysis offers advantages over several other advanced biofuels technologies including: conversion of the entire biomass feedstock into higher-value products and production of an energy dense bio-oil that can more economically be transported. Like any other new technology, fast pyrolysis requires further optimization in order to produce higher yields of the most valuable products which is necessary to compete with conventional petroleum derived fuels and chemicals. Work in this dissertation has investigated optimization of both pre- and post-processes of fast pyrolysis to improve the yield of high value products.

Chapter 2 focused on passivation of alkali and alkaline earth metals (AAEMs) to produce substantially increased yields of anhydrosugars from fast pyrolysis of biomass. Alkali and alkaline earth metals promote fragmentation of sugar moieties in the holocellulose structure to produce light oxygenates as opposed to depolymerization of the holocellulose to produce anhydrosugars. Catalytic activity of the inherit AAEM cations can however be suppressed by treating the feedstock with sulfuric acid at a rate correlated to the amount of AAEMs in the feedstock; a process known as passivation. The AAEMs form thermally stable sulfate salts as a result which exhibit much lower activity toward holocellulose fragmentation. Passivation of red oak and switchgrass prior to fast pyrolysis increased sugar yield by 105% and 259%, respectively. The increase in sugar directly correlated with a decrease in undesirable light oxygenates and non-condensable gases; which further supports the hypothesis that the passivation of AAEMs to produce thermally stable salts results in less sugar moiety fragmentation within the carbohydrate structure. Demonstrating fast pyrolysis of passivated feedstocks on a continuous basis provides important evidence for the feasibility of process scaling.

The simultaneous increase in biochar and decrease in lignin derived products from AAEM passivated feedstocks suggests that AAEM cations affect lignin pyrolysis which was the focus of *Chapter 3*. To test the effects AAEM cations on lignin pyrolysis, thermally unstable acetates of several AAEM cations were infused into pure organosolv cornstover lignin which was then pyrolyzed at temperatures ranging from 300-800°C. Infusion of AAEM acetates significantly affected the char and volatile product yields. Infusion of sodium acetate (the most influential AAEM cation) increased both the mass

and molar yields of volatile aromatics by almost 20% compared to the control. Volatile aromatics from fast pyrolysis of AAEM acetate infused lignin exhibited different side chains than volatile aromatics from the control. The most drastic change came from infusion of alkali acetates which reduced the alkenyl side chains on volatile aromatics by as much as 50%. All AAEMs increased the char yield during lignin fast pyrolysis with alkali metals having the more dramatic effect. Nearly all changes in product distribution from alkali metal infused lignin correlated with increasing atomic mass and electropositivity of the infused cation. Taking into account all of the observed differences in products from lignin pyrolysis in the presence AAEM acetates, it appears that AAEM cations act to catalytically cleave linkages between monolignols in the lignin structure.

Chapter 2 and *Chapter 3* focused largely on pre-processing methods of optimizing biomass fast pyrolysis; however post-processing methods have also proven to play a crucial role. *Chapter 4* focused on increasing the yield of valuable anhydrosugars from fast pyrolysis of pure cellulose by modifying the post-processing method of bio-oil collection. For the work in *Chapter 4*, pure cellulose was pyrolyzed under identical conditions in a bubbling fluidized bed reactor and either a conventional shell and tube condenser system or a novel cold-gas quench system was used to collect bio-oil. Bio-oil from the conventional condenser system contained higher concentrations of carbohydrate oligomers and char that formed at the high temperature inlets. Large radial temperature gradients encountered by the bio-oil film while collecting on the walls of conventional condensers are blamed for polymerization reactions leading the formation

of oligomers and char. Faster cooling rates and the elimination of radial temperature gradients accomplished with the cold-gas quench system led to a remarkable 23% increase in levoglucosan yield.

Overall both pre- and post-processing approaches have proven to increase the yield of valuable compounds in bio-oil from the fast pyrolysis of lignocellulosic biomass. Utilized together, both pre- and post-processing improvements can be used to dramatically increase the value of the bio-oil while decreasing the costs associated with processing. Improvements discussed in this dissertation will help to make fast pyrolysis of biomass a more technoeconomically feasible pathway to producing advanced biofuels and biochemicals.

Future Work

Work in this dissertation has helped to both discover new approaches and improve prior methods of producing higher value products from fast pyrolysis of lignocellulosic biomass. Further research will however be required to realize the full potential of the approaches discussed here.

One major area to focus on will be optimization of reactor design and operating conditions to achieve the highest possible yield of sugars from AAEM passivated feedstocks. Work in this dissertation has proven to increase the yield of total sugars to over 16 wt. % from red oak in a continuous 2 kg per hour auger pyrolyzer. However, previous trials on the micropyrolyzer have proven to produce over 24 wt. % levoglucosan from the same feedstock, equating to over 90% of the potential

levoglucosan yield. Different mass and heat transfer characteristics between the micropyrolyzer and bench-scale reactor contribute to the discrepancies. As discussed in *Chapter 2*, the AAEM passivated feedstock required a much lower biomass to heat carrier ratio compared to the control feedstock which is likely due to mass transfer limitations. A higher biomass to heat carrier ratio increases the concentration of pyrolysis products in the reactor at one time, likely preventing many of the products from volatilizing and escaping the reactor. Instead, the pyrolysis products remain in the reactor for extended time periods and eventually produce char. Experimental conditions used for the work in *Chapter 2* were determined by a limited number of preliminary trials. Further optimization of reactor conditions could likely increase the sugar yield from fast pyrolysis of AAEM passivated feedstocks more significantly.

Other areas on which to focus are the heat carrier material and its heat transfer characteristics. Stainless steel shot was used in this work and was assumed to be inert to the pyrolysis reaction. However, it is unknown as to whether or not the heat carrier itself exhibits catalytic effects that could result in increased char yield. Physical properties such as heat carrier size and surface area also affect transport phenomena. A larger particle size heat carrier would provide additional void space to aid mass transfer; however additional void space would likely decrease heat transfer in chorus. Investigating heat carriers with different physical and chemical properties may lead the discovery of a more suitable heat carrier material for an optimized process.

As described in *Chapter 3* the inherit AAEMs in biomass act as catalysts for lignin depolymerization. Infusion of sodium acetate at around 1.0 mmol per gram lignin

increased the yield of volatile aromatics from lignin pyrolysis by 17%. Even with the 17% increase in volatile aromatics, lignin still produced up to 50 wt. % char at typical fast pyrolysis temperatures. Further research will be required to discover methods of increasing volatile aromatics at the expense of char. The lignin is aromatic in nature and therefore very hydrogen deficient. A harsher pyrolysis method with addition of hydrogen and/or catalysts will likely be necessary to achieve higher yields of volatile aromatics. Currently it would appear as though several of the bonds between individual aromatic rings within the structure are easily cleaved during fast pyrolysis. Hydrogen deficiency and production of radicals, however, simply lead to radical coupling within the structure and produce char. Utilizing something such as hydrogen to cap radical reactions would likely prevent much of the cross linking and subsequent char formation, however would require the addition of catalysts or harsher conditions to activate the hydrogen.

The cold-gas quench bio-oil collection system has already proven to substantially increase the yield of levoglucosan from cellulose. Work on the quench system was however performed with the just the initial iteration of the system. Further concept development and optimization may additionally increase the yield, along with increasing separation between bio-oil compounds. It is possible to expand the fundamental concept of quenching to a desired set point temperature and subsequently removing the aerosols formed at that temperature with an electrostatic precipitator (ESP) in several subsequent stages. For instance, this author could imagine five distinct fractions of bio-oil that could beneficial to separate: high molecular mass lignin oligomers, anhydrosugars,

phenolics, furans, and light oxygenates (including water). Process optimization may be performed by developing a more extensive model to determine set point temperatures of the individual quench-ESP sub-assemblies to achieve the desired separation.

The quench nozzle and geometry still require further optimization. A simple quench nozzle consisting of a 1/16" outer diameter stainless steel tube was used to provide the liquid nitrogen for the quench process for the initial quench system iteration. The quench nozzle was prone to produce a pulsating stream that alternated between liquid nitrogen spray and cold gaseous nitrogen spray. Ensuring the nitrogen remains liquid before entering the quench system has the added benefit of providing cooling due to both latent heat and sensible heat absorption. Optimizing the nozzle to provide a more consistent flow and proper atomization of the liquid nitrogen would likely help to reduce the quantity of required quench gas and smooth the flow in the system.

All the work reported here utilized liquid nitrogen as the quench medium, however many other quench liquids or gases may be envisioned. Water seems like an obvious quench medium that is readily available and much cheaper than liquid nitrogen. Preliminary trials had been conducted using water with success, however were not reported in this manuscript. Very little water had to be injected relative to the gas stream due to the high specific and latent heat capacities of water, which gives it excellent quench medium properties. Washing heavy bio-oil fractions with water has proven to remove sugars from high molecular mass lignin oligomers. If properly setup, quenching the hot pyrolysis vapor stream with water could provide the added benefit of separating sugars and high molecular mass lignin oligomers online.

Other liquids or gases could also be used as a quench medium, such as hydrocarbons. The difference in polarity between the polar bio-oil compounds and non-polar hydrocarbons would allow them to be easily separated. The separated hydrocarbon quench medium could then be cooled and recycled. Recycling would reduce process inputs and therefore reduce overall operating expenses.

Another alternative would be to use a medium polar solvent, such as acetone or diethyl ether. Laboratory experiments by this author revealed that acetone readily dissolves phenolic compounds and sparingly dissolves sugars, such as levoglucosan. Quenching with acetone may provide washing of the toxic phenolic species from the heavy fraction while leaving behind a sugar rich substrate that could be diluted with water to make a better substrate for hybrid processing. Relatively low boiling point temperatures of solvents such as acetone or diethyl ether would improve the ability to separate the solvent from the bio-oil for recycling. Liquid nitrogen, water, hydrocarbons, acetone, and diethyl ether are just a few possibilities for alternative quench mediums. The possibilities are virtually endless and specific quench mediums may be better suited for different applications.

Modeling individual components using computational fluid dynamics may be beneficial in determining optimum geometry and wall temperature set points for collecting specific fractions of bio-oil. In preliminary trials, wall temperatures above 150°C led to char formation along the walls of bio-oil collection equipment. An optimum wall temperature likely exists that would prevent char formation, yet be

sufficiently high to decrease viscosity of the bio-oil for easier collection, while volatilizing any undesirable components from the bio-oil film as is falls.

Mixing effects may also be modeled and optimized. As mentioned previously, the nozzle used in the quench resulted in pulsating operation and poor atomization of the liquid nitrogen. The simple tube interface design may produce a cold jet of nitrogen that may not sufficiently mix with the hot pyrolysis vapor stream. Optimizing the geometry of the nozzle and quench chamber may therefore help to reduce residence time, increase cooling rate, and decrease quantity of quench medium; all of which would help to increase yields of higher value products and decrease input costs.

APPENDIX A

INDIVIDUAL COMPOUND SUMMARY FOR CONTROL AND AAEM PASSIVATED RED OAK

The data in the *Appendix A* is a summary of all the compounds investigated for red oak experiments in *Chapter 2*. Please note that all yields are given in mass percentage of dry feedstock.

		Red Oak Control	AAEM Passivated Red Oak	Change	P-value (2-tail)
		(wt. % of feedstock)	(wt. % of feedstock)	(Passivated-Control) / Control	
Mass Balance					
Bio-oil		57.89%	53.02%	-8.4%	0.128
Biochar		14.35%	23.79%	65.8%	***0.031***
	Sieved	95.72%	10.01%	-89.5%	***0.007***
	Combusted	3.11%	85.64%	2654.1%	***0.030***
Non-Condensable Gas		19.29%	10.52%	-45.5%	0.128
	Carbon Dioxide	9.10%	4.98%	-45.3%	0.231
	Carbon Monoxide	8.44%	4.40%	-47.9%	0.329
	Light Hydrocarbons (CH4, C2H6, C2H4)	1.75%	1.15%	-34.6%	0.433
Bio-oil Composition					
Lignin Products		12.60%	6.22%	-50.6%	*0.053*
Water Insoluble Content[d]		9.76%	5.03%	-48.5%	*0.072*
Phenols		0.51%	0.23%	-54.1%	***0.001***
	Anisole (C7H8O)[e]	0.01%	0.00%	-51.7%	***0.004***
	Phenol (C6H6O)[e]	0.03%	0.03%	-12.7%	***0.012***
	2-methylphenol (C7H8O)[e]	0.04%	0.01%	-59.3%	***0.003***
	2,6-dimethylphenol (C8H10O)[e]	0.05%	0.02%	-60.5%	***0.001***
	4-methylphenol (C7H8O)[e]	0.09%	0.02%	-76.9%	***0.004***

		Red Oak Control	AAEM Passivated Red Oak	Change	P-value (2-tail)
		(wt. % of feedstock)	(wt. % of feedstock)	(Passivated-Control) / Control	
	2,5-dimethylphenol (C8H10O)[e]	0.03%	0.01%	-73.0%	***0.002***
	2,3-dimethylphenol (C8H10O)[e]	0.03%	0.01%	-79.6%	***0.002***
	3,5-dimethylphenol (C8H10O)[e]	0.01%	0.00%	-74.1%	***0.001***
	3-ethylphenol (C8H10O)[e]	0.00%	0.00%	-15.5%	***0.042***
	4-ethylphenol (C8H10O)[e]	0.02%	0.00%	-72.3%	***0.001***
	3,4-dimethylphenol (C8H10O)[e]	0.05%	0.04%	-17.7%	***0.005***
	Phenolic Derivative 1 (C9H8O)**[e]	0.02%	0.01%	-66.3%	***0.001***
	4-vinylphenol (C8H8O)[e]	0.01%	0.01%	58.9%	***0.002***
	1,2-dihydroxybenzene (C6H6O2)[e]	0.06%	0.02%	-67.4%	***0.000***
	1,4-dihydroxybenzene (C6H6O2)[e]	0.06%	0.03%	-41.8%	***0.001***
	1,3-dihydroxybenzene (C6H6O2)[e]	0.01%	0.01%	-11.1%	***0.005***
Guaiacols		0.85%	0.47%	-45.3%	***0.001***
	2-methoxyphenol (C7H8O2)[e]	0.11%	0.05%	-53.3%	***0.001***
	2-methoxy-4-methylphenol (C8H10O2)[e]	0.10%	0.03%	-72.6%	***0.001***
	4-ethyl-2-methoxyphenol (C9H12O2)[e]	0.03%	0.01%	-77.6%	***0.001***
	2-methoxy-4-vinylphenol (C9H10O2)[e]	0.11%	0.15%	40.4%	***0.007***
	4-(2-propenyl)-2-methoxyphenol (C10H12O2)[e]	0.03%	0.00%	-88.0%	***0.001***
	2-methoxy-4-propylphenol (C10H14O2)[e]	0.02%	0.01%	-61.2%	***0.001***

		Red Oak Control	AAEM Passivated Red Oak	Change	P-value (2-tail)
		(wt. % of feedstock)	(wt. % of feedstock)	(Passivated-Control) / Control	
	4-(1-propenyl)-2-methoxyphenol (isomer) (C10H12O2)[e]	0.03%	0.01%	-76.7%	***0.001***
	3-methoxy-5-methylphenol (C8H10O2)[e]	0.01%	0.01%	-23.7%	***0.003***
	4-(1-propenyl)-2-methoxyphenol (isomer)(C10H12O2)[e]	0.11%	0.01%	-91.1%	***0.001***
	4-hydroxy-3-methoxybenzaldehyde (C8H8O3)[e]	0.07%	0.05%	-25.9%	***0.004***
	2-methoxy-4-methyl-6-propenylphenol (C11H14O2)*[e]	0.02%	0.00%	-79.8%	***0.000***
	2-(4-hydroxy-3-methoxyphenyl)acetaldehyde (C9H10O3)*[e]	0.04%	0.07%	77.6%	***0.007***
	1-(4-hydroxy-3-methoxyphenyl)ethanone (C9H10O3)*[e]	0.08%	0.02%	-76.4%	***0.001***
	4-hydroxy-3-methoxyphenylacetone (C10H12O3)[e]	0.04%	0.02%	-44.8%	***0.004***
	4-(3-hydroxy-1-propenyl)-2-methoxyphenol (C10H12O3)[e]	0.01%	0.01%	0.7%	0.530
	4-hydroxy-3-methoxycinnamaldehyde (C10H10O3)[e]	0.05%	0.03%	-37.1%	***0.008***
	3-(4-hydroxy-3-methoxyphenyl)-2-propenal (isomer) (C10H10O3)*[e]	0.01%	0.00%	-94.6%	***0.001***
Syringols		1.47%	0.49%	-66.6%	***0.001***
	2,6-dimethoxyphenol (C8H10O3)[e]	0.31%	0.16%	-48.7%	***0.004***
	2,6-dimethoxy-4-methylphenol (C9H12O3)[e]	0.22%	0.08%	-64.7%	***0.003***
	2,6-dimethoxy-4-ethylphenol (C10H14O3)*[e]	0.08%	0.02%	-70.0%	***0.002***
	2,6-dimethoxy-4-vinylphenol (C10H12O3)*[e]	0.19%	0.04%	-81.3%	***0.002***
	4-(2-propenyl)-2,6-dimethoxyphenol (C11H14O3)[e]	0.11%	0.02%	-85.8%	***0.002***
	4-(1-propenyl)-2,6-dimethoxyphenol (isomer 1) (C11H14O3)*[e]	0.07%	0.01%	-86.5%	***0.001***

		Red Oak Control	AAEM Passivated Red Oak	Change	P-value (2-tail)
		(wt. % of feedstock)	(wt. % of feedstock)	(Passivated-Control) / Control	
	4-(1-propenyl)-2,6-dimethoxyphenol (isomer 2) (C11H14O3)*[e]	0.24%	0.01%	-95.2%	***0.002***
	3,5-dimethoxy-4-hydroxybenzaldehyde (C9H10O4)[e]	0.05%	0.02%	-54.1%	***0.003***
	2-(4-hydroxy-3,5-dimethoxyphenyl)acetaldehyde (C9H10O3)*[e]	0.03%	0.05%	100.8%	***0.010***
	3,5-dimethoxy-4-hydroxyacetophenone (C10H12O4)[e]	0.08%	0.04%	-50.3%	***0.004***
	3,5-dimethoxy-4-hydroxyacetophenone (isomer) (C10H12O4)*[e]	0.03%	0.02%	-15.0%	***0.050***
	4-(3-hydroxy-1-propenyl)-2,6-dimethoxyphenol (C11H14O4)[e]	0.02%	0.00%	-78.6%	***0.002***
	3-(4-hydroxy-3,5-dimethoxyphenyl)-prop-2-enal (C11H12O4)[e]	0.05%	0.01%	-70.3%	***0.003***
Carbohydrate Products					
Sugars		6.08%	17.01%	179.6%	***0.032***
Anhydrosugars		5.20%	15.42%	196.4%	***0.035***
	Cellobiosan[c]	0.57%	0.98%	71.9%	0.233
	Galactose[c]	1.02%	2.17%	112.2%	0.114
	Levoglucosan[c]	2.64%	11.00%	316.0%	***0.036***
	Levoglucosan-Furanose[e]	0.02%	0.52%	2772.9%	*0.056*
	Xylosan[c]	0.94%	0.74%	-21.0%	0.335
Levoglucosan Dehydration Products		0.11%	0.33%	202.9%	***0.002***
	Levoglucosenone (C6H6O3)[e]	0.03%	0.01%	-51.6%	***0.002***

	Red Oak Control	AAEM Passivated Red Oak	Change	P-value (2-tail)
	(wt. % of feedstock)	(wt. % of feedstock)	(Passivated-Control) / Control	
1,4:3,6-dianhydro-a-D-glucopyranose (C6H8O4)[e]	0.08%	0.31%	301.2%	***0.002***
Unknown Anhydrosugar Derivatives	0.77%	1.26%	63.4%	***0.002***
Carbohydrate Derivative 2 (C5H8O3)**[e]	0.14%	0.01%	-92.7%	***0.001***
Carbohydrate Derivative 3 (C5H6O3)**[e]	0.08%	0.02%	-77.5%	***0.002***
Carbohydrate Derivative 4 (C6H8O3)**[e]	0.06%	0.03%	-56.0%	***0.008***
Carbohydrate Derivative 5 (C6H8O4)**[e]	0.06%	0.01%	-87.2%	***0.002***
Carbohydrate Derivative 6 (C6H8O4)**[e]	0.03%	0.01%	-55.0%	***0.013***
Carbohydrate Derivative 7 (C6H8O3)**[e]	0.10%	0.03%	-68.3%	***0.003***
Carbohydrate Derivative 8 (C7H10O5)**[e]	0.01%	0.26%	4782.7%	***0.003***
Carbohydrate Derivative 9 (C7H10O5)**[e]	0.09%	0.49%	449.5%	***0.002***
Carbohydrate Derivative 10 (C6H8O4)**[e]	0.11%	0.11%	-4.8%	***0.040***
Carbohydrate Derivative 11 (C9H12O6)**[e]	0.02%	0.18%	666.6%	***0.002***
Carbohydrate Derivative 12 (C8H12O6)**[e]	0.01%	0.03%	179.8%	***0.006***
Carbohydrate Derivative 13 (C6H12O6)**[e]	0.06%	0.08%	40.2%	***0.011***
Carbohydrate Dehydration Products	**2.93%**	**1.55%**	**-47.0%**	***0.001***
Cyclopentanes	0.66%	0.19%	-71.0%	***0.000***
2-methyl-2-cyclopenten-1-one (C6H8O)[e]	0.01%	0.00%	-95.2%	***0.008***
2-hydroxy-2-cyclopenten-1-one (C5H6O2)*[e]	0.44%	0.12%	-72.4%	***0.001***

		Red Oak Control	AAEM Passivated Red Oak	Change	P-value (2-tail)
		(wt. % of feedstock)	(wt. % of feedstock)	(Passivated-Control) / Control	
	3-methyl-2-cyclopenten-1-one (C6H8O)[e]	0.02%	0.01%	-23.9%	***0.003***
	3-methyl-1,2-cyclopentanedione (C6H8O2)[e]	0.19%	0.06%	-70.5%	***0.001***
Furans		0.79%	0.92%	16.3%	***0.008***
	2-methylfuran (C5H6O)[e]	0.10%	0.04%	-56.9%	***0.006***
	2-furaldehyde (C5H4O2)[e]	0.34%	0.58%	72.1%	***0.003***
	2-furanmethanol (C5H6O2)[e]	0.04%	0.06%	28.2%	***0.004***
	5-methyl-2-furaldehyde (C6H6O2)[e]	0.09%	0.04%	-50.4%	***0.005***
	3-furanmethanol (C5H6O2)[e]	0.05%	0.06%	37.1%	***0.023***
	5-(hydroxymethyl)-2-furaldehyde (C6H6O3)[e]	0.17%	0.12%	-26.9%	***0.004***
Lactones		0.54%	0.13%	-75.3%	***0.000***
	dihydro-2(3H)-Furanone (C4H6O2)*[e]	0.10%	0.03%	-71.0%	***0.002***
	2(5H)Furanone (C4H4O2)[e]	0.28%	0.05%	-82.0%	***0.000***
	5-methyl-2(5H)-Furanone (C5H6O2)*[e]	0.04%	0.02%	-52.4%	***0.002***
	3-methyl-2(5H)-furanone (C5H6O2)[e]	0.05%	0.01%	-74.4%	***0.001***
	4-hydroxy-5-methyl-3-furanone (C5H6O3)[e]	0.01%	0.01%	-27.8%	***0.004***
	4-methyl-5H-furan-2-one (C5H6O2)*[e]	0.06%	0.02%	-73.8%	***0.001***
Misc. Furans		0.38%	0.18%	-53.1%	***0.001***
	Furan Derivative 3 (C5H4O)**[e]	0.01%	0.00%	-72.9%	***0.006***

		Red Oak Control	AAEM Passivated Red Oak	Change	P-value (2-tail)
		(wt. % of feedstock)	(wt. % of feedstock)	(Passivated-Control) / Control	
	Furan Derivative 1 (C5H6O2)**[e]	0.02%	0.01%	-51.8%	***0.001***
	Furan Derivative 2 (C6H6O2)**[e]	0.03%	0.02%	-32.3%	***0.005***
	Furan Derivative 4 (C6H8O)**[e]	0.03%	0.01%	-70.7%	***0.002***
	Furan Derivative 16A (C5H6O3)**[e]	0.28%	0.13%	-53.4%	***0.002***
Pyrans		0.05%	0.05%	-8.0%	*0.050*
	Carbohydrate Derivative 1 (C5H8O3)**[e]	0.03%	0.03%	-2.0%	0.282
	2H-Pyran-2-one (C5H4O2)[e]	0.02%	0.01%	-19.0%	***0.009***
Tetrahydrofurans		0.52%	0.09%	-82.7%	***0.001***
	2,5-dimethoxytetrahydrofuran (isomer) (C6H12O3)[e]	0.22%	0.03%	-84.5%	***0.001***
	2,5-dimethoxytetrahydrofuran (isomer) (C6H12O3)[e]	0.25%	0.04%	-82.6%	***0.001***
	(S)-(+)-3-hydroxytetrahydrofuran (C4H8O2)[e]	0.06%	0.01%	-77.0%	***0.002***
Total Sugars		7.76%	15.88%	104.5%	***0.018***
Xylose Hydrolyzable Sugars[b]		1.26%	3.25%	157.3%	***0.033***
Glucose Hydrolyzable Sugars[b]		4.66%	12.63%	170.9%	***0.011***
Sorbitol Hydrolyzable Sugars[b]		1.84%	0.00%	-100.0%	*0.053*
Light Oxygenates		7.76%	4.21%	-45.8%	***0.039***
Alcohols		0.30%	0.34%	16.0%	***0.002***

		Red Oak Control	AAEM Passivated Red Oak	Change	P-value (2-tail)
		(wt. % of feedstock)	(wt. % of feedstock)	(Passivated-Control) / Control	
	Methanol (CH4O)[f]	0.24%	0.29%	20.4%	***0.002***
	Ethanol (C2H6O)[f]	0.04%	0.04%	-0.8%	***0.023***
	2-Propanol (C3H8O)[f]	0.01%	0.00%	-45.7%	***0.012***
	1-Propanol (C3H8O)[f]	0.01%	0.01%	3.1%	*0.076*
Aldehydes		1.06%	0.47%	-55.5%	***0.005***
	Acetaldehyde (C2H4O)[f]	0.02%	0.02%	-12.6%	***0.016***
	Glycolaldehyde (C2H4O2)*[e]	1.04%	0.45%	-56.5%	***0.005***
Carboxylic Acids		4.93%	3.08%	-37.5%	*0.075*
	Acetic Acid[g]	3.63%	2.57%	-29.3%	0.120
	Butanoic Acid[e]	0.06%	0.02%	-64.8%	0.217
	Formic Acid[g]	0.62%	0.17%	-72.0%	***0.034***
	Glycolic Acid[g]	0.39%	0.14%	-65.4%	0.183
	Proponoic Acid[g]	0.23%	0.18%	-20.4%	0.203
Misc. Light Oxygenates		1.47%	0.31%	-78.9%	***0.001***
	Acetone (C3H6O)[f]	0.03%	0.05%	110.8%	***0.003***
	2,3-butanedione (C4H6O2)[e]	0.09%	0.05%	-48.8%	***0.005***
	Hydroxyacetone (C3H6O2)[e]	0.81%	0.12%	-84.8%	***0.001***
	1-hydroxy-2-butanone (C4H8O2)[e]	0.08%	0.02%	-75.5%	***0.004***

	Red Oak Control	AAEM Passivated Red Oak	Change	P-value (2-tail)
	(wt. % of feedstock)	(wt. % of feedstock)	(Passivated-Control) / Control	
Light Oxygenate 1 (C4H6O3)**[e]	0.20%	0.03%	-87.4%	***0.003***
Light Oxygenate 2 (C4H6O3)**[e]	0.12%	0.01%	-87.7%	***0.001***
Light Oxygenate 3 (C6H10O2)**[e]	0.06%	0.01%	-89.3%	***0.002***
Acetoxyacetone (C5H8O3)[e]	0.07%	0.02%	-73.2%	***0.001***
Reaction Water[a]	12.78%	15.52%	21.5%	0.164
Total Bio-oil Accounted	68.78%	82.15%		

*- Identified via GC/MS

** - Molecular formula determine via GC-TOF

[a] - Karl Fischer Titration

[b] - Acid Hydrolysis - HPLC

[c] - Water Soluble Sugar Analysis

[d] - Water Insoluble Analysis

[e] - GC/FID

[f] - GC/FID Low Boiling Compounds Method

[g] - Ion Chromatography

APPENDIX B

INDIVIDUAL COMPOUND SUMMARY FOR CONTROL AND AAEM PASSIVATED SWITCHGRASS

The data in the *Appendix B* is a summary of all the compounds investigated for switchgrass experiments in *Chapter 2.* Please note that all yields are given in mass percentage of dry feedstock.

		Switchgrass Control	AAEM Passivated Switchgrass	Change	P-value (2-tail)
		(wt. % of feedstock)	(wt. % of feedstock)	(Passivated-Control) / Control	
Mass Balance					
Bio-oil		54.29%	56.70%	4.4%	0.266
Biochar		21.20%	27.58%	30.1%	0.123
	Sieved	96.88%	50.32%	-48.1%	***0.017***
	Combusted	3.13%	49.68%	1489.8%	***0.017***
Non-Condensable Gas		13.20%	7.19%	-45.6%	***0.040***
	Carbon Dioxide	8.28%	4.90%	-40.8%	*0.094*
	Carbon Monoxide	4.10%	1.92%	-53.1%	***0.048***
	Light Hydrocarbons (CH4, C2H6, C2H4)	0.82%	0.36%	-55.8%	0.121
Bio-oil Composition					
Lignin Products		11.42%	8.96%	-21.6%	*0.087*
Water Insoluble Content[d]		9.00%	7.73%	-14.1%	0.167
Phenols		1.06%	0.39%	-63.5%	***0.001***
	Anisole (C7H8O)[e]	0.01%	0.00%	-78.0%	***0.005***
	Phenol (C6H6O)[e]	0.10%	0.05%	-49.3%	***0.001***
	2-methylphenol (C7H8O)[e]	0.05%	0.01%	-81.0%	***0.001***
	2,6-dimethylphenol (C8H10O)[e]	0.06%	0.02%	-67.3%	***0.001***
	4-methylphenol (C7H8O)[e]	0.10%	0.03%	-71.8%	***0.001***

		Switchgrass Control	AAEM Passivated Switchgrass	Change	P-value (2-tail)
		(wt. % of feedstock)	(wt. % of feedstock)	(Passivated-Control) / Control	
	2,5-dimethylphenol (C8H10O)[e]	0.03%	0.01%	-69.5%	***0.001***
	2,3-dimethylphenol (C8H10O)[e]	0.03%	0.02%	-33.3%	***0.006***
	3,5-dimethylphenol (C8H10O)[e]	0.01%	0.00%	-58.4%	***0.003***
	3-ethylphenol (C8H10O)[e]	0.10%	0.04%	-62.2%	***0.001***
	4-ethylphenol (C8H10O)[e]	0.00%	0.01%	239.3%	***0.006***
	3,4-dimethylphenol (C8H10O)[e]	0.06%	0.01%	-88.1%	***0.001***
	Phenolic Derivative 1 (C9H8O)**[e]	0.02%	0.02%	0.7%	0.238
	4-vinylphenol (C8H8O)[e]	0.40%	0.11%	-72.0%	***0.001***
	1,2-dihydroxybenzene (C6H6O2)[e]	0.03%	0.02%	-30.2%	***0.009***
	1,4-dihydroxybenzene (C6H6O2)[e]	0.05%	0.04%	-35.1%	***0.002***
	1,3-dihydroxybenzene (C6H6O2)[e]	0.01%	0.00%	-69.5%	***0.000***
Guaiacols		0.90%	0.57%	-36.4%	***0.002***
	2-methoxyphenol (C7H8O2)[e]	0.14%	0.08%	-38.7%	***0.002***
	2-methoxy-4-methylphenol (C8H10O2)[e]	0.08%	0.09%	18.0%	***0.015***
	4-ethyl-2-methoxyphenol (C9H12O2)[e]	0.04%	0.02%	-39.9%	***0.002***
	2-methoxy-4-vinylphenol (C9H10O2)[e]	0.29%	0.16%	-44.8%	***0.003***
	4-(2-propenyl)-2-methoxyphenol (C10H12O2)[e]	0.03%	0.01%	-77.5%	***0.002***
	2-methoxy-4-propylphenol (C10H14O2)[e]	0.02%	0.00%	-70.9%	***0.001***

		Switchgrass Control	AAEM Passivated Switchgrass	Change	P-value (2-tail)
		(wt. % of feedstock)	(wt. % of feedstock)	(Passivated-Control) / Control	
	4-(1-propenyl)-2-methoxyphenol (isomer) (C10H12O2)[e]	0.02%	0.03%	36.5%	***0.036***
	3-methoxy-5-methylphenol (C8H10O2)[e]	0.01%	0.00%	-42.6%	***0.005***
	4-(1-propenyl)-2-methoxyphenol (isomer)(C10H12O2)[e]	0.08%	0.01%	-84.0%	***0.001***
	4-hydroxy-3-methoxybenzaldehyde (C8H8O3)[e]	0.06%	0.04%	-40.5%	***0.002***
	2-methoxy-4-methyl-6-propenylphenol (C11H14O2)*[e]	0.01%	0.00%	-72.1%	***0.006***
	2-(4-hydroxy-3-methoxyphenyl)acetaldehyde (C9H10O3)*[e]	0.01%	0.02%	30.1%	***0.003***
	1-(4-hydroxy-3-methoxyphenyl)ethanone (C9H10O3)*[e]	0.06%	0.02%	-66.3%	***0.000***
	4-hydroxy-3-methoxyphenylacetone (C10H12O3)[e]	0.03%	0.04%	45.8%	***0.001***
	4-(3-hydroxy-1-propenyl)-2-methoxyphenol (C10H12O3)[e]	0.00%	0.01%	106.2%	***0.000***
	4-hydroxy-3-methoxycinnamaldehyde (C10H10O3)[e]	0.02%	0.03%	71.6%	***0.001***
	3-(4-hydroxy-3-methoxyphenyl)-2-propenal (isomer) (C10H10O3)*[e]	0.01%	0.00%	-100.0%	***0.004***
Syringols		0.45%	0.26%	-41.8%	***0.001***
	2,6-dimethoxyphenol (C8H10O3)[e]	0.12%	0.08%	-30.7%	***0.001***
	2,6-dimethoxy-4-methylphenol (C9H12O3)[e]	0.05%	0.04%	-16.4%	***0.008***
	2,6-dimethoxy-4-ethylphenol (C10H14O3)*[e]	0.03%	0.01%	-60.3%	***0.001***
	2,6-dimethoxy-4-vinylphenol (C10H12O3)*[e]	0.06%	0.01%	-88.6%	***0.000***
	4-(2-propenyl)-2,6-dimethoxyphenol (C11H14O3)[e]	0.03%	0.01%	-62.5%	***0.001***
	4-(1-propenyl)-2,6-dimethoxyphenol (isomer 1) (C11H14O3)*[e]	0.02%	0.02%	-23.7%	***0.002***

		Switchgrass Control	AAEM Passivated Switchgrass	Change	P-value (2-tail)
		(wt. % of feedstock)	(wt. % of feedstock)	(Passivated-Control) / Control	
	4-(1-propenyl)-2,6-dimethoxyphenol (isomer 2) (C11H14O3)*[e]	0.07%	0.02%	-78.1%	***0.001***
	3,5-dimethoxy-4-hydroxybenzaldehyde (C9H10O4)[e]	0.02%	0.03%	33.3%	***0.031***
	2-(4-hydroxy-3,5-dimethoxyphenyl)acetaldehyde (C9H10O3)*[e]	0.00%	0.01%	206.8%	***0.013***
	3,5-dimethoxy-4-hydroxyacetophenone (C10H12O4)[e]	0.02%	0.02%	-16.0%	***0.004***
	3,5-dimethoxy-4-hydroxyacetophenone (isomer) (C10H12O4)*[e]	0.01%	0.01%	28.1%	***0.018***
	4-(3-hydroxy-1-propenyl)-2,6-dimethoxyphenol (C11H14O4)[e]	0.01%	0.00%	-72.5%	***0.002***
	3-(4-hydroxy-3,5-dimethoxyphenyl)-prop-2-enal (C11H12O4)[e]	0.01%	0.00%	-48.5%	***0.010***
Carbohydrate Products					
Sugars		4.37%	13.05%	198.5%	***0.047***
Anhydrosugars		3.49%	11.75%	236.4%	***0.050***
	Cellobiosan[c]	0.25%	0.93%	271.1%	*0.051*
	Galactose[c]	0.60%	1.64%	170.5%	0.138
	Levoglucosan[c]	1.70%	8.30%	388.2%	*0.057*
	Levoglucosan-Furanose[e]	0.02%	0.33%	1260.3%	*0.067*
	Xylosan[c]	0.91%	0.55%	-39.4%	0.169
Levoglucosan Dehydration Products		0.13%	0.67%	414.9%	***0.001***
	Levoglucosenone (C6H6O3)[e]	0.02%	0.11%	385.3%	***0.003***

	Switchgrass Control	AAEM Passivated Switchgrass	Change	P-value (2-tail)
	(wt. % of feedstock)	(wt. % of feedstock)	(Passivated-Control) / Control	
1,4:3,6-dianhydro-a-D-glucopyranose (C6H8O4)[e]	0.11%	0.55%	421.5%	***0.000***
Unknown Anhydrosugar Derivatives	0.75%	0.63%	-16.2%	***0.004***
Carbohydrate Derivative 2 (C5H8O3)**[e]	0.17%	0.06%	-64.0%	***0.003***
Carbohydrate Derivative 3 (C5H6O3)**[e]	0.07%	0.01%	-90.1%	***0.001***
Carbohydrate Derivative 4 (C6H8O3)**[e]	0.05%	0.05%	5.5%	*0.063*
Carbohydrate Derivative 5 (C6H8O4)**[e]	0.04%	0.00%	-93.5%	***0.001***
Carbohydrate Derivative 6 (C6H8O4)**[e]	0.06%	0.07%	24.7%	***0.008***
Carbohydrate Derivative 7 (C6H8O3)**[e]	0.11%	0.01%	-94.8%	***0.002***
Carbohydrate Derivative 8 (C7H10O5)**[e]	0.02%	0.00%	-80.9%	***0.005***
Carbohydrate Derivative 9 (C7H10O5)**[e]	0.09%	0.08%	-12.2%	***0.018***
Carbohydrate Derivative 10 (C6H8O4)**[e]	0.06%	0.25%	292.6%	***0.001***
Carbohydrate Derivative 11 (C9H12O6)**[e]	0.01%	0.01%	-21.5%	***0.004***
Carbohydrate Derivative 12 (C8H12O6)**[e]	0.01%	0.02%	83.4%	***0.001***
Carbohydrate Derivative 13 (C6H12O6)**[e]	0.03%	0.05%	54.0%	***0.001***
Carbohydrate Dehydration Products	**3.30%**	**2.63%**	**-20.2%**	***0.002***
Cyclopentanes	0.68%	0.21%	-68.8%	***0.001***
2-methyl-2-cyclopenten-1-one (C6H8O)[e]	0.01%	0.00%	-100.0%	***0.003***
2-hydroxy-2-cyclopenten-1-one (C5H6O2)*[e]	0.45%	0.14%	-69.0%	***0.001***

		Switchgrass Control	AAEM Passivated Switchgrass	Change	P-value (2-tail)
		(wt. % of feedstock)	(wt. % of feedstock)	(Passivated-Control) / Control	
	3-methyl-2-cyclopenten-1-one (C6H8O)[e]	0.02%	0.01%	-68.0%	***0.005***
	3-methyl-1,2-cyclopentanedione (C6H8O2)[e]	0.20%	0.07%	-66.3%	***0.000***
Furans		0.98%	1.67%	71.0%	***0.001***
	2-methylfuran (C5H6O)[e]	0.10%	0.02%	-77.2%	***0.003***
	2-furaldehyde (C5H4O2)[e]	0.54%	1.23%	127.9%	***0.001***
	2-furanmethanol (C5H6O2)[e]	0.05%	0.11%	108.4%	***0.001***
	5-methyl-2-furaldehyde (C6H6O2)[e]	0.10%	0.07%	-29.8%	***0.004***
	3-furanmethanol (C5H6O2)[e]	0.04%	0.09%	147.8%	***0.003***
	5-(hydroxymethyl)-2-furaldehyde (C6H6O3)[e]	0.15%	0.15%	1.1%	0.112
Lactones		0.51%	0.19%	-63.0%	***0.001***
	dihydro-2(3H)-Furanone (C4H6O2)*[e]	0.09%	0.02%	-80.7%	***0.001***
	2(5H)Furanone (C4H4O2)[e]	0.27%	0.06%	-77.5%	***0.001***
	5-methyl-2(5H)-Furanone (C5H6O2)*[e]	0.04%	0.02%	-38.3%	***0.002***
	3-methyl-2(5H)-furanone (C5H6O2)[e]	0.05%	0.02%	-66.5%	***0.002***
	4-hydroxy-5-methyl-3-furanone (C5H6O3)[e]	0.01%	0.04%	202.3%	***0.000***
	4-methyl-5H-furan-2-one (C5H6O2)*[e]	0.04%	0.03%	-39.6%	***0.007***
Misc. Furans		0.59%	0.47%	-20.4%	***0.006***
	Furan Derivative 3 (C5H4O)**[e]	0.00%	0.00%	-82.4%	***0.008***

	Switchgrass Control	AAEM Passivated Switchgrass	Change	P-value (2-tail)
	(wt. % of feedstock)	(wt. % of feedstock)	(Passivated-Control) / Control	
Furan Derivative 1 (C5H6O2)**[e]	0.02%	0.01%	-59.9%	***0.004***
Furan Derivative 2 (C6H6O2)**[e]	0.05%	0.13%	188.5%	***0.001***
Furan Derivative 4 (C6H8O)**[e]	0.03%	0.01%	-73.1%	***0.002***
Furan Derivative 16A (C5H6O3)**[e]	0.49%	0.32%	-34.4%	***0.004***
Pyrans	0.05%	0.05%	-5.7%	***0.018***
Carbohydrate Derivative 1 (C5H8O3)**[e]	0.03%	0.03%	-22.1%	***0.006***
2H-Pyran-2-one (C5H4O2)[e]	0.01%	0.02%	33.7%	***0.004***
Tetrahydrofurans	0.49%	0.04%	-91.3%	***0.000***
2,5-dimethoxytetrahydrofuran (isomer) (C6H12O3)[e]	0.20%	0.02%	-89.9%	***0.001***
2,5-dimethoxytetrahydrofuran (isomer) (C6H12O3)[e]	0.24%	0.01%	-94.9%	***0.000***
(S)-(+)-3-hydroxytetrahydrofuran (C4H8O2)[e]	0.05%	0.01%	-80.7%	***0.003***
Total Sugars	4.50%	16.15%	258.9%	***0.017***
Xylose Hydrolyzable Sugars[b]	1.31%	3.20%	144.9%	*0.074*
Glucose Hydrolyzable Sugars[b]	2.55%	12.95%	408.0%	***0.013***
Sorbitol Hydrolyzable Sugars[b]	0.64%	0.00%	-100.0%	*0.054*
Light Oxygenates	6.84%	3.26%	-52.4%	***0.043***
Alcohols	0.18%	0.13%	-29.1%	***0.001***

		Switchgrass Control	AAEM Passivated Switchgrass	Change	P-value (2-tail)
		(wt. % of feedstock)	(wt. % of feedstock)	(Passivated-Control) / Control	
	Methanol (CH4O)[f]	0.14%	0.10%	-28.3%	***0.001***
	Ethanol (C2H6O)[f]	0.03%	0.02%	-40.4%	***0.003***
	2-Propanol (C3H8O)[f]	0.01%	0.00%	-38.0%	***0.000***
	1-Propanol (C3H8O)[f]	0.00%	0.01%	23.3%	***0.028***
Aldehydes		0.74%	0.50%	-32.4%	***0.004***
	Acetaldehyde (C2H4O)[f]	0.02%	0.01%	-33.8%	***0.000***
	Glycolaldehyde (C2H4O2)*[e]	0.73%	0.49%	-32.4%	***0.004***
Carboxylic Acids		4.17%	2.36%	-43.5%	*0.084*
	Acetic Acid[g]	3.02%	1.71%	-43.3%	0.110
	Butanoic Acid[e]	0.05%	0.01%	-79.5%	0.117
	Formic Acid[g]	0.52%	0.26%	-50.3%	0.163
	Glycolic Acid[g]	0.37%	0.23%	-37.9%	0.140
	Proponoic Acid[g]	0.21%	0.15%	-30.5%	0.180
Misc. Light Oxygenates		1.75%	0.27%	-84.5%	***0.000***
	Acetone (C3H6O)[f]	0.02%	0.04%	62.4%	***0.000***
	2,3-butanedione (C4H6O2)[e]	0.10%	0.05%	-51.3%	***0.001***
	Hydroxyacetone (C3H6O2)[e]	1.00%	0.11%	-88.9%	***0.000***
	1-hydroxy-2-butanone (C4H8O2)[e]	0.10%	0.02%	-82.7%	***0.000***

	Switchgrass Control	AAEM Passivated Switchgrass	Change	P-value (2-tail)
	(wt. % of feedstock)	(wt. % of feedstock)	(Passivated-Control) / Control	
Light Oxygenate 1 (C4H6O3)**[e]	0.25%	0.03%	-88.5%	***0.000***
Light Oxygenate 2 (C4H6O3)**[e]	0.10%	0.01%	-90.7%	***0.001***
Light Oxygenate 3 (C6H10O2)**[e]	0.05%	0.01%	-89.8%	***0.003***
Acetoxyacetone (C5H8O3)[e]	0.13%	0.01%	-89.4%	***0.001***
Reaction Water[a]	14.65%	16.44%	12.2%	0.198
Total Bio-oil Accounted	72.26%	76.71%		

*- Identified via GC/MS

** - Molecular formula determine via GC-TOF

[a] - Karl Fischer Titration

[b] - Acid Hydrolysis – HPLC

[c] - Water Soluble Sugar Analysis

[d] - Water Insoluble Analysis

[e] - GC/FID

[f] - GC/FID Low Boiling Compounds Method

[g] - Ion Chromatography

APPENDIX C

LITERATURE REVIEW ON THE EFFECT OF ALKALI AND ALKALINE EARTH METALS ON LIGNIN FAST PYROLYSIS

Abstract

Lignin makes up a large portion of lignocellulosic biomass and remains mostly unconverted during biological upgrading of lignocellulose to biofuels. Thermochemical conversion offers advantages since it is capable of converting the entirety of the biomass into valuable products with minimal pretreatment and cleanup prior to processing. The effect of alkali and alkaline earth metals (AAEMs) on holocellulose has been thoroughly investigated by other researchers; however there is much less literature covering the effect of these inherit catalysts on lignin pyrolysis. Some evidence suggests that alkali and alkaline earth metals have the potential to assist lignin depolymerization during pyrolysis to produce phenolic monomers. Using a catalyst already present in biomass and exploiting its catalytic mechanism has the potential to produce a higher value bio-oil at a lower cost than some of the more expensive upgrading technologies. The goal of this review is to summarize previous research on the subject of the AAEM catalyst effects on lignin pyrolysis and offer conclusions and recommendation for further research.

Introduction

Biomass consists of three major components: cellulose, hemicellulose, and lignin. Cellulose and hemicellulose are commonly collectively called holocellulose and

the collection of all three components is commonly referred to as lignocellulose. Lignin is the only non-carbohydrate portion of biomass and can represent up to 30% of the biomass feedstock [1]. The aromatic character of lignin gives it a much higher carbon-to-oxygen ratio than holocellulose, which gives it an energy content similar to that of certain bituminous coals [2]. Conversion of the lignin in biomass to chemicals and fuels is thus vital to achieving economic feasibility of biofuels.

Both biochemical and thermochemical pathways exist for conversion of biomass to fuels and chemicals. The biochemical pathway employees the use of microorganisms for the key conversion step whereas the thermochemical pathway utilizes heat, chemicals and/or catalysts for the key conversion process. Lignin in the plant cell wall is important for protecting holocellulose from microbial attack while the plant is living and growing [3]. The protection lignin offers however makes the lignin very recalcitrant toward conversion to fuels and chemicals. A key step in the biochemical pathway, known as saccharification, involves the use enzymes or acids to depolymerize the holocellulose to monosaccharides that are susceptible to fermentation. Pretreatment is however required to break apart the lignin and increase the porosity of the biomass particle in order to make the holocellulose accessible to enzymes or acids [4]. The pretreatment required to efficiently convert cellulosic biomass into ethanol leads to production costs of cellulosic ethanol that are nearly twice that of grain ethanol [5]. Biochemical conversion of cellulosic feedstocks also leaves all of the lignin unconverted [6] where it is commonly used for low value applications such as combustion for process heat.

Several thermochemical processes have been developed that can make use of the entirety of lignocellulosic feedstocks. One such pathway is gasification which takes place at high temperatures (750-850^{o}C) in a partially oxidative environment. Gasification converts the solid fuel into a mixture of carbon monoxide, hydrogen, methane, nitrogen, carbon dioxide, water, and small concentrations of larger hydrocarbons [7]. The mixture of gases resulting from gasification is collectively known as producer gas if air is used as the oxidizer or syngas if oxygen and steam are used as the oxidizer. Syngas or producer gas can then be converted to hydrocarbons through a variety of gas-to-liquids (GTL) processes such as Fischer-Tropsch synthesis. Many other catalytic routes also exist that produce hydrogen, methanol, ethanol, ethers, or a variety of other chemicals from syngas or producer gas and are discussed elsewhere [8]. Alternatively synthesis gas can be fed to microorganisms designed to produce hydrocarbons via fermentation in a process known as hybrid processing [9]. Syngas or producer gas commonly require extensive cleaning prior to upgrading in order to eliminate contaminants such as particulate matter, tar, sulfur, chlorine, and ammonia which poison catalysts and microorganisms [10]. Extensive gas cleaning increases production and maintenance costs which can quickly negatively affect process economics.

Another thermochemical pathway is fast pyrolysis in which the biomass is depolymerized by rapidly heating to moderate temperatures (400-600°C) in the absence of oxygen to produce solids, liquids and gases. The liquid, known as bio-oil, can account for up to 78% of the total mass for short residence times (0.5-2.0s) and rapid

quenching at the end of the process [7]. The solid, known as biochar, has potential value as a soil amendment. Biochar retains most of the mineral content of the original biomass and can be reapplied to the field to decrease fertilizer needs and increase crop yields. Soil application of biochar is subject of several researchers and is discussed elsewhere [11-14]. Biochar also has many other applications such as fuel, a sorbent, or in carbon sequestration [15].

Non-condensable gases resulting from fast pyrolysis are made up of mostly carbon monoxide and carbon dioxide, along with lesser quantities of hydrogen, methane, and other light hydrocarbons. Absence of oxygen during fast pyrolysis prevents non-condensable gases from becoming oxidized and they therefore retain some heating value that can be recovered via combustion of the non-condensable gases for process heat. Non-condensable gases or their combustion products can also provide an oxidizer free stream for recycling during the fast pyrolysis process which eliminates the need to separate oxygen from air or having large reservoirs of non-reactive gas to provide the oxygen free atmosphere.

Liquid products from fast pyrolysis

Fast pyrolysis of holocellulose produces predominately anhydrosugars, furans, and light oxygenates, whereas lignin depolymerizes to a mixture of phenolic compounds. Separation of the considerably different products of holocellulose and lignin during collection of the bio-oil has been subject of several researchers [16]. Fractions containing carbohydrate products and fractions containing phenolic compounds would

most likely be upgraded separately and hold more value as separated compounds rather than a mixture.

Ideal biomass would contain only cellulose, hemicellulose, and lignin; however actual biomass contains many extractives such as proteins, lipids, non-structural sugars, nitrogenous materials, chlorophyll, waxes, and inorganic species [17]. Inorganics include fertilizer and soil picked up from the field as well as inherit mineral content of the plant. Of the inorganic species, alkali and alkaline earth metals (AAEMs) are especially known for their catalytic activity during biomass depolymerization. The AAEM cations form coordinate bonds with hydroxyl groups of sugar moieties in the holocellulose structure which then fragment the ring structures of the sugar moieties; forming light oxygenates rather than depolymerizing to anhydrosugars [18-21]. Kuzhiyil et al. [22] found that catalytic activity of AAEMs can be passivated by titration with sulfuric or phosphoric acids to form thermally stable sulfate or phosphate salts, respectively. Levoglucosan yields increased by more than fivefold from several feedstocks as a result of AAEM passivation [22]. An increase in char and decrease in bio-oil lignin content with AAEM passivation led to suspicions that the AAEMs in their active form may also play a significant role during lignin pyrolysis. Therefore it would be advantageous to develop a better understanding of the role of AAEMs during lignin pyrolysis. The goal of this review is to summarize results from the literature pertaining to the role of AAEMs on lignin pyrolysis and to investigate methods of exploiting mechanisms leading to increased yields of more valuable volatile aromatics.

Literature Review – Effects of AAEMs on Lignin Pyrolysis

Effects of AAEMs on carbohydrate pyrolysis have been fairly well investigated and are discussed elsewhere [21, 23-24]. The effects of these catalysts inherit to biomass on lignin pyrolysis has however provided mixed results. This review will highlight some of the main points of the available literature.

Patwardhan et al. [8] doped organosolv cornstover lignin with 1 wt. % sodium, potassium, magnesium, and calcium chloride and noticed no significant differences in the volatile products of pyrolysis. Infusion of the AAEM chlorides only led to an approximate 1 wt. % increase in char attributed to the presence of the non-volatile minerals. No temperature data for the pyrolysis was given. Patwardhan et al. suggests the drastic differences between effects of AAEMs on the carbohydrate versus lignin portion may be due to aromatic rings in lignin which would not readily form coordinate bonds with the minerals.

Gray et al. [25] pyrolyzed ground woodex pellets subject to either: no treatment, acid-washing to remove minerals, or calcium ion-exchange. The calcium exchanged samples were prepared by soaking the untreated material in a calcium acetate solution and buffering the solution to achieve a final calcium content of 1.24 wt. % (0.62 meq/g sample). Gray found the calcium exchanged wood to give approximately the same yield of guaiacols as the untreated wood at 330°C (1.73 wt. % from untreated samples vs. 1.61 wt. % from calcium exchanged) and approximately a threefold increase in guaiacols at 460°C (1.37 wt. % from untreated vs. 3.99 wt. % from calcium exchanged). The acid washed samples reduced the yield of guaiacols to approximately 80% of the yield from

the untreated sample at 330°C (1.38 wt. % for acid washed samples vs. 1.73 wt. % for untreated) and to about 55% of the guaiacols yield at 460°C (0.74 wt. % for acid washed vs. 1.37 wt. % for untreated). Guaiacols were the only products listed coming from lignin, however the drastic changes in guaiacols yield suggests calcium and inherit mineral content both have some effect on the lignin portion of the wood pellets during pyrolysis.

Evans et al. [26] used direct mass-spectrometric methods to study the primary pyrolysis of lignin and found lignin to largely pyrolyze to its monolignols precursors. Addition of 1 wt. % basic catalyst (potassium hydroxide) to degraded pine wood consisting largely of lignin was shown to have no effect on primary product distribution. Addition of an acid catalyst (zinc chloride) to the same pine lignin sample reduced the overall yield of monolignols and increased the abundance of guaiacol and 4-methylguaiacol; however no quantitative data was given. Temperature data and overall mass balance were not listed either. Evans et al. proposes that the acid is catalyzing dehydration of the primary alcohol on the gamma-carbon of the alkyl side chain of the monolignols within the lignin structure. This prevents devolatilization of the precursor monomer from the lignin and eliminates a potential source of transferable hydrogen.

Jakab et al. [27] added sodium chloride to milled wood lignin and noticed significant effects on thermal decomposition. Sodium added to milled wood lignin was shown to facilitate cleavage of functional groups. Char increased which led to a decrease in organic volatiles. Jakab et al. noted that the catalytic effect of the sodium

chloride increased with increasing sodium concentration in the range tested from 0-4.9 wt. % sodium. Milled wood lignin mixed with sodium chloride had less catalytic effect than milled wood lignin treated with sodium hydroxide even though they had the same sodium concentration. Jakab et al. explains this by the sodium hydroxide solution making closer contact with the lignin structure and most likely forming phenolic sodium salts. The overall effect exhibited on lignin by sodium was to decrease monomer and oligomer formation while promoting fragmentation to water, carbon dioxide, methanol, and methane. Jakab et al. used a thermogravimetric system and mass spectrometer where the samples were heated from 30 to 900°C at 20°C/min in an argon atmosphere. Heating rates therefore do not represent the heating rates experienced during fast pyrolysis and may be expected to produce slightly different results.

Pan and Richards [28] investigated the effects of untreated wood, acid washed wood, calcium exchanged wood, and potassium exchanged wood from 500 to 700 K under a nitrogen atmosphere. In general the potassium exchanged wood behaved similar to the untreated wood and the calcium treated wood behaved similar to the acid washed wood. Treating wood with potassium increased the char yield substantially compared to the other wood samples.

Scott et al. [29] used hot water to wash mineral content from poplar wood and pyrolyzed the wood at 500°C. Scott et al. found nearly all of the potassium could be washed from the sample with water, however much of the calcium would remain in the wood sample. This indicates that most of the calcium is likely bound organically to the biomass constituents whereas potassium more likely exists as soluble salts.

Deionization of poplar prior to pyrolysis led to an increase in pyrolytic lignin to 22.4 wt. % vs. 16.2 wt. % from the control.

Di Blasi et al. [30] impregnated fir wood with approximately 0.40 wt. % potassium or sodium in the forms of sodium hydroxide, potassium hydroxide, sodium carbonate, potassium carbonate, potassium acetate, and sodium chloride. The samples were pyrolyzed at approximately 800 K under nitrogen in a fixed bed reactor. Impregnation of hydroxide salts increased the yield of phenols most significantly; increasing from 2.10 wt. % for the control, to 4.19 wt. % with addition of sodium hydroxide, and to 3.83 wt. % with addition of potassium hydroxide. Carbonates increased the yield of phenols the next most significantly at 2.89 wt. % from sodium carbonate and 2.34 wt. % with potassium carbonate. Potassium acetate increased the yield of phenols marginally up to 2.50 wt. %. Sodium chloride reduced yield of phenols to 1.70 wt. %. Further investigation of the listed individual phenolic compounds suggests that both potassium and sodium hydroxide increased overall yield of phenols and several functional groups including: propyl groups, methoxy groups, hydroxyl groups, and unsaturated propenyl groups (isoeugenol). Both potassium hydroxide and sodium carbonate increased the saturated ethyl functionalities while potassium carbonate had little effect. Sodium hydroxide significantly reduced the ethyl functionalities. Both of the potassium compounds decreased the aldehyde functionality (in the form of vanillin) by more than half, while sodium compounds only reduced it slightly. Di Blasi et al. suggest that the basicity of the additive is the dominant factor effecting catalytic activity during pyrolysis. Di Blasi et al. conclude that AAEM catalyzed reactions in

lignin generally promote carbonization (char production), dehydration, decarboxylation, and demethoxylation leading to a modified carbonaceous structure that is more stable.

Wang et al. [31] researched the catalytic effects of four sodium compounds (hydroxide, carbonate, silicate, and chloride) on pyrolysis of pine wood, cotton stalk, and fir wood at an approximate 10 wt. % concentration of additive. It should be noted that experiments by Wang et al. were conducted at a heating rate of 10 K/min which may produce different results than the higher heating rates used for fast pyrolysis. The slower heating rate should however serve to get a basic understanding of the effect of AAEMs on lignin during pyrolysis. Wang et al. found the temperature of maximum weight loss decreased with compound basicity. Wang et al. also noticed an increase in exothermicity of pyrolysis from 250-400°C with sodium hydroxide and sodium carbonate which is attributed to char formation. Each of the sodium compounds increased the yield of net char, and the increase correlated with compound basicity. Differences due to basicity may be attributed to increased dehydration by basic compounds that results in more condensation and char formation. As a possible explanation to why sodium appears to have a much more pronounced catalytic effect than other metals, Wang et al. suggests the size of sodium atom (being physically smaller than the rest of the AAEMs in the experiments) allows it to penetrate deeper into the biomass texture and break the intermolecular hydrogen bridges under swelling or heating.

Chen et al. [32] performed a similar investigation as Wang et al. on lignin with the same salts and concentration; however used microwave pyrolysis rather than a TGA

to achieve the heating. Each of the sodium salts (hydroxide, carbonate, silicate, and chloride) nearly doubled the yield of char compared to the control; increasing from 17.3 wt. % for the control to 36 wt. % with sodium hydroxide, 33.3 wt. % with sodium carbonate, 34.0 wt. % with sodium silicate, and 34.7 wt. % with sodium chloride. The liquid yield was not significantly affected where the untreated sample produced 22.7 wt. % liquid, sodium hydroxide 20.0 wt. %, sodium carbonate 22 wt. %, sodium silicate 16.0 wt. % and sodium chloride increased liquid yield to 26.0 wt. %. Gas decreased with sodium salts for all cases; from 60 wt. % for untreated to 44.0 wt. % with sodium hydroxide, 44.7 wt. % with sodium carbonate, 50.0 wt. % with sodium silicate, and 39.3 wt. % with sodium chloride. Mass yield of water remained constant at around 30 wt. % for each sample. Guaiacol and 4-methylwere the only two phenolic species quantified. Each sodium salt decreased response of 4-methylguaiacol compared the control and all except sodium silicate increased guaiacol. It should however be noted that the data given for guaiacol and 4-methylguaiacol were in area % and may not reflect the true mass comparison between samples.

Nowakowski et al. [33] experimented with uncatalyzed and potassium catalyzed pyrolysis of individual lignocellulose components as well as model compounds. Potassium had a profound effect on lignin pyrolysis; however the mechanisms were not clear. Addition of 1 wt. % potassium (from potassium acetate) to organosolv lignin decreased the temperature of maximum conversion by over 70 K. Polymerization reactions were catalyzed by the potassium and resulted in additional char. The control produced around 37 wt. % char and the potassium impregnated sample produced over

50 wt. % char. Nowakowski et al. also noted the Py-GC-MS fingerprints were similar between the washed lignin sample and the potassium impregnated samples. Individual compounds were not quantified, however differences in intensity of certain species were observed.

In a second paper Nowakowski et al. [34] performed a similar experiment with short rotation willow coppice and synthetic biomass. The synthetic biomass consisted of a mixture of each of the lignocellulosic components blended at 50 wt. % cellulose, 15 wt. % alkali lignin, 15 wt. % organosolv lignin, and 20 wt. % xylan. Potassium impregnation of willow increased yields of several phenols including: phenol, 2-methoxyphenol, 2,6-dimethoxyphenol, and isoeugenol; similar to the increase observed from organosolv lignin. The synthetic biomass however produced different results indicating the separation techniques play a crucial role in the end pyrolysis products. The bonds of cellulose and lignin in raw biomass likely prevent the release of many phenolics and instead result in increased char yield.

Conclusions and Recommendations

As shown in the reviewed literature, there is no consensus on which metals or in what form act as catalysts during lignin pyrolysis. Of the reviewed resources many used different forms of salts, different temperatures, different heating rates, and looked at different products.

In general the addition of neutral and thermally stable salts, such as chlorides, resulted in little change in the overall product distribution. Addition of sodium and

potassium in more basic forms and thermally unstable forms, such as acetates, hydroxides, or carbonates, promotes charring of the lignin and had major influences on the liquid product yield and composition. The basicity of the salts is expected to promote the dehydration. Alkaline metal compounds, such as calcium exchanged samples, in general had less effect on the lignin pyrolysis than did the alkali metal samples. Potassium, being the more active metal, would also be expected to be the more active catalyst; however sodium was more active in production of phenols from lignin pyrolysis. Wang et al. [31] explains this by the sodium ion being much smaller than the rest of the AAEMs investigated, however offers little evidence. To test this hypothesis lignin samples could be impregnated with salts of both smaller ions, such as lithium, and larger ions, such as rubidium or cesium, at similar concentrations with the same anion attached and identical operating conditions for comparison.

As shown by several of the researchers, the temperature of the pyrolysis with the metal catalysts also plays a significant role on the end product distribution and composition. A more systematic investigation with various AAEMs in various forms at different temperatures could provide more insight to the mechanism responsible for AAEM catalysis on lignin pyrolysis.

References

1. U.S. Department of Energy, *Biomass Feedstock Composition and Property Database*, 2006, Energy Efficiency and Renewable Energy - Biomass Program.

2. Boateng, A.A., P.J. Weimer, H.G. Jung, and J.F.S. Lamb, *Response of Thermochemical and Biochemical Conversion Processes to Lignin Concentration in Alfalfa Stems †.* Energy & Fuels, 2008. **22**(4): p. 2810-2815.

3. Vance, C.P., T.K. Kirk, and R.T. Sherwood, *Lignification as a Mechanism of Disease Resistance.* Annual Review of Phytopathology, 1980. **18**(1): p. 259-288.

4. Carroll, A. and C. Somerville, *Cellulosic Biofuels*, in *Annual Review of Plant Biology*2009, Annual Reviews: Palo Alto. p. 165-182.

5. Regalbuto, J.R., *Cellulosic Biofuels—Got Gasoline?* Science, 2009. **325**(5942): p. 822-824.

6. Wyman, C.E., *What is (and is not) vital to advancing cellulosic ethanol.* Trends in Biotechnology, 2007. **25**(4): p. 153-157.

7. Brown, R.C., *Biorenewable resources : engineering new products from agriculture*. 1st ed2003, Ames, Iowa: Iowa State Press. xii, 286 p.

8. Patwardhan, P.R., R.C. Brown, and B.H. Shanks, *Understanding the Fast Pyrolysis of Lignin.* ChemSusChem, 2011. **4**(11): p. 1629-1636.

9. Choi, D., A.A. Dispirito, D.C. Chipman, and R.C. Brown, *Hybrid Processing*, in *Thermochemical Processing of Biomass*2011, John Wiley & Sons, Ltd. p. 280-306.

10. Woolcock, P.J. and R.C. Brown, *A review of cleaning technologies for biomass-derived syngas.* Biomass and Bioenergy, 2013. **52**: p. 54-84.

11. Brewer, C., R. Unger, K. Schmidt-Rohr, and R. Brown, *Criteria to Select Biochars for Field Studies based on Biochar Chemical Properties.* BioEnergy Research, 2011. **4**(4): p. 312-323.

12. Brewer, C.E., K. Schmidt-Rohr, J.A. Satrio, and R.C. Brown, *Characterization of biochar from fast pyrolysis and gasification systems.* Environmental Progress & Sustainable Energy, 2009. **28**(3): p. 386-396.

13. Deal, C., C.E. Brewer, R.C. Brown, M.A.E. Okure, and A. Amoding, *Comparison of kiln-derived and gasifier-derived biochars as soil amendments in the humid tropics.* Biomass and Bioenergy, 2012. **37**: p. 161-168.

14. Unger, R., R. Killorn, and C. Brewer, *Effects of Soil Application of Different Biochars on Selected Soil Chemical Properties.* Communications in Soil Science and Plant Analysis, 2011. **42**(19): p. 2310-2321.

15. Lehmann, J. and S. Joseph, *Biochar for environmental management : science and technology*2009, London ; Sterling, VA: Earthscan. xxxii, 416 p.

16. Pollard, A.S., M.R. Rover, and R.C. Brown, *Characterization of bio-oil recovered as stage fractions with unique chemical and physical properties.* Journal of Analytical and Applied Pyrolysis, 2012. **93**: p. 129-138.

17. A. Sluiter, R.R., C. Scarlata, J. Sluiter, and D. Templeton, *Determination of Extractives in Biomass*, 2008, National Renewable Energy Laboratory: Golden, Colorado.

18. Ponder, G.R. and G.N. Richards, *A review of some recent studies on mechanisms of pyrolysis of polysaccharides.* Biomass and Bioenergy, 1994. **7**(1–6): p. 1-24.

19. Ponder, G.R. and G.N. Richards, *Pyrolysis of inulin, glucose and fructose.* Carbohydrate Research, 1983. **244**(2): p. 341-359.

20. Richards, G.N. and F. Shafizadeh, *Formation of "Glucometasaccharinolactones" in the pyrolysis of curdlan, A (1→3)-β-d-glucan.* Carbohydrate Research, 1982. **106**(1): p. 83-91.

21. Patwardhan, P.R., J.A. Satrio, R.C. Brown, and B.H. Shanks, *Influence of inorganic salts on the primary pyrolysis products of cellulose.* Bioresource Technology, 2010. **101**(12): p. 4646-4655.

22. Kuzhiyil, N., D. Dalluge, X. Bai, K.H. Kim, and R.C. Brown, *Pyrolytic Sugars from Cellulosic Biomass.* ChemSusChem, 2012. **5**(11): p. 2228-2236.

23. Patwardhan, P.R., R.C. Brown, and B.H. Shanks, *Product Distribution from the Fast Pyrolysis of Hemicellulose.* ChemSusChem, 2011. **4**(5): p. 636-643.

24. Patwardhan, P.R., J.A. Satrio, R.C. Brown, and B.H. Shanks, *Product distribution from fast pyrolysis of glucose-based carbohydrates.* Journal of Analytical and Applied Pyrolysis, 2009. **86**(2): p. 323-330.

25. Gray, M.R., W.H. Corcoran, and G.R. Gavalas, *Pyrolysis of a wood-derived material. Effects of moisture and ash content.* Journal Name: Ind. Eng. Chem. Process Des. Dev.; (United States); Journal Volume: 24:3, 1985: p. Medium: X; Size: Pages: 646-651.

26. Evans, R.J., T.A. Milne, and M.N. Soltys, *Direct mass-spectrometric studies of the pyrolysis of carbonaceous fuels: III. Primary pyrolysis of lignin.* Journal of Analytical and Applied Pyrolysis, 1986. **9**(3): p. 207-236.

27. Jakab, E., O. Faix, F. Till, and T. Székely, *The effect of cations on the thermal decomposition of lignins.* Journal of Analytical and Applied Pyrolysis, 1993. **25**: p. 185-194.

28. Pan, W.-P. and G.N. Richards, *Influence of metal ions on volatile products of pyrolysis of wood.* Journal of Analytical and Applied Pyrolysis, 1989. **16**(2): p. 117-126.

29. Scott, D.S., L. Paterson, J. Piskorz, and D. Radlein, *Pretreatment of poplar wood for fast pyrolysis: rate of cation removal.* Journal of Analytical and Applied Pyrolysis, 2001. **57**(2): p. 169-176.

30. Di Blasi, C., A. Galgano, and C. Branca, *Influences of the Chemical State of Alkaline Compounds and the Nature of Alkali Metal on Wood Pyrolysis.* Industrial & Engineering Chemistry Research, 2009. **48**(7): p. 3359-3369.

31. Wang, J., M. Zhang, M. Chen, F. Min, S. Zhang, Z. Ren, and Y. Yan, *Catalytic effects of six inorganic compounds on pyrolysis of three kinds of biomass.* Thermochimica Acta, 2006. **444**(1): p. 110-114.

32. Chen, M.-q., J. Wang, M.-x. Zhang, M.-g. Chen, X.-f. Zhu, F.-f. Min, and Z.-c. Tan, *Catalytic effects of eight inorganic additives on pyrolysis of pine wood sawdust by microwave heating.* Journal of Analytical and Applied Pyrolysis, 2008. **82**(1): p. 145-150.

33. Nowakowski, D.J. and J.M. Jones, *Uncatalysed and potassium-catalysed pyrolysis of the cell-wall constituents of biomass and their model compounds.* Journal of Analytical and Applied Pyrolysis, 2008. **83**(1): p. 12-25.

34. Nowakowski, D.J., J.M. Jones, R.M.D. Brydson, and A.B. Ross, *Potassium catalysis in the pyrolysis behaviour of short rotation willow coppice.* Fuel, 2007. **86**(15): p. 2389-2402.

APPENDIX D

BIO-OIL CALCULATION AND CONVERSIONS SUMMARY

Throughout the course of analyzing bio-oil samples from several projects it was found to be time consuming to derive equations necessary to normalize yields to a moisture free biomass basis. This short summary was put together to serve as a reference for calculations used in this dissertation and to provide a general reference for others.

Mass Balance Data Definitions	
$Wet\ Char\ Yield = \frac{g\ wet\ char}{g\ wet\ biomass}$	Char yield reported in mass balance worksheet.
$Wet\ Bio-Oil\ Yield = \frac{g\ wet\ bio-oil}{g\ wet\ biomass}$	Bio-oil yield reported in mass balance worksheet.
$Wet\ NC\ Gas\ Yield = \frac{g\ NC\ gas}{g\ wet\ biomass}$	Non-condensable (NC) gas yield reported in mass balance worksheet.

TGA Data Definitions	
$Biomass\ Moisture = \frac{g\ water_{moisture}}{g\ wet\ biomass}$	Moisture reported from TGA analysis on biomass.
$Char\ Moisture = \frac{g\ char\ moisture}{g\ wet\ char}$	Moisture reported from TGA analysis on char.

$Ash_{Biomass} = \frac{g\ ash_{biomass}}{g\ wet\ biomass}$	Ash or residue reported from TGA analysis on biomass. (the terms "ash" and "inorganics" can be used interchangeably)
$Ash_{Char} = \frac{g\ ash_{char}}{g\ wet\ char}$	Ash or residue reported from TGA analysis on char. (the terms "ash" and "inorganics" can be used interchangeably)
$Ash_{Bio-oil} = \frac{g\ ash_{bio-oil}}{g\ wet\ bio-oil}$	Ash or residue reported from TGA analysis on bio-oil. (the terms "ash" and "inorganics" can be used interchangeably)

Karl-Fischer Data Definitions	
$Bio-oil\ Moisture = \frac{g\ water_{total}}{g\ wet\ bio-oil}$	Moisture reported from Karl-Fischer analysis on bio-oil.

CHNSO Data Definitions	
$Element\ Fraction_{Biomass} = \frac{g\ Element_{biomass}}{g\ wet\ biomass}$	Any element reported from CHNSO data for biomass. ("Element" can be replaced with carbon, hydrogen, oxygen nitrogen or sulfur).

$Element\ Fraction_{Char} = \frac{g\ Element_{char}}{g\ wet\ char}$	Any element reported from CHNSO data for char. ("Element" can be replaced with carbon, hydrogen, oxygen nitrogen or sulfur).
$Element\ Fraction_{Bio-oil} = \frac{g\ Element_{bio-oil}}{g\ wet\ oil}$	Any element reported from CHNSO data for bio-oil. ("Element" can be replaced with carbon, hydrogen, oxygen nitrogen or sulfur).

Carried Water/Reaction Water Data Definitions	
$g\ water_{total} = g\ water_{moisture} + g\ water_{reaction}$	Total water found by Karl-Fischer analysis on bio-oil.
$g\ wet\ bio-oil = g\ organics_{bio-oil} + g\ water_{total} + g\ ash_{bio-oil}$	Wet bio-oil collected from the reactor contains both carried water and reaction water.
$g\ bio-oil_{m.f.biomass} = g\ organics_{bio-oil} + g\ water_{reaction} + g\ ash_{bio-oil}$	Dry bio-oil contains all of the condensable components (and ash) produced during pyrolysis, thus still contains reaction water. Carried water is subtracted as it may inflate wet oil yield for a high moisture feedstock.

Conversion to Moisture Free (m.f.) Biomass Basis	
$$Char\ Yield_{m.f.Biomass} = \frac{g\ dry\ char}{g\ dry\ biomass}$$ $$= \frac{(Wet\ Char\ Yield\ ) * (1 - (Char\ Moisture))}{1 - (Biomass\ Moisture)}$$	Char is assumed to be moisture free immediately following the reaction, however absorbs moisture from the air during cool down. The moisture char absorbs from the air must be subtracted from the overall mass balance. See data definitions for Mass Balance and TGA.
$$Bio - oil\ Yield_{m.f.Biomass} = \frac{g\ bio - oil\ (m.f.biomass)}{g\ dry\ biomass}$$ $$= \frac{(Wet\ Bio - Oil\ Yield) - (Biomass\ Moisture)}{1 - (Biomass\ Moisture)}$$	Moisture contained in the original feedstock is assumed to condense into the bio-oil; this water is known as moisture water or carried water. Water is also released during the pyrolysis reactions and also condenses into the bio-oil; this water is known as reaction water. Dry bio-oil refers to the oil yield after carried water is subtracted however reaction water remains in the bio-oil. For removal of both sources of water see:"Separation of Carried Water and Reaction Water" below. See data definitions for Mass Balance and TGA.

$$NC\ Gas\ Yield\ (m.f.Biomass) = \frac{g\ NC\ gas}{g\ dry\ biomass}$$ $$= \frac{(Wet\ NC\ Gas\ Yield)}{1 - (Biomass\ Moisture)}$$	Non-condensable gas yield normalized to dry biomass. See data definitions for Mass Balance and TGA.

Separation of Carried Water and Reaction Water	
$$Bio - oil\ Reaction\ Water\ Fraction = \frac{g\ water_{reaction}}{g\ dry\ biomass}$$ $$= \frac{(Bio - oil\ Moisture) * (Wet\ Bio - Oil\ Yield) - (Biomass\ Moisture)}{1 - (Biomass\ Moisture)}$$	Used to calculate the mass fraction of water produced during the pyrolysis reaction which may be influenced by feedstock properties. See data definitions for Karl-Fischer, Mass Balance, TGA, and Carried Water/Reaction Water.
$$Bio - oil\ Organic\ Fraction = \frac{g\ organics_{bio-oil}}{g\ dry\ biomass}$$ $$= \frac{(Wet\ Bio - Oil\ Yield) * (1 - (Bio - oil\ Moisture) - (Ash_{Bio-oil}))}{1 - (Biomass\ Moisture)}$$	Used to calculate the mass fraction of organic compounds produced and collected in the bio-oil. See data definitions for Karl-Fischer, Mass Balance, TGA, and Carried Water/Reaction Water.

Elemental Conversion to per Dry Biomass Basis	
$$\frac{g\ Element_{char}}{g\ dry\ biomass} = \frac{(Element\ Fraction_{Char}) * (Wet\ Char\ Yield)}{1 - (Biomass\ Moisture)}$$	Used to calculate the mass fraction of an element that is distributed in the char. ("Element" can be substituted by: carbon, nitrogen or sulfur).
$$\frac{g\ Element_{bio-oil}}{g\ dry\ biomass} = \frac{(Element\ Fraction_{Bio-oil}) * (Wet\ Bio-Oil\ Yield)}{1 - (Biomass\ Moisture)}$$	Used to calculate the mass fraction of nitrogen that is distributed in the bio-oil. ("Element" can be substituted by: carbon, nitrogen or sulfur).
$$\frac{g\ hydrogen_{bio-oil\ organics}}{g\ dry\ biomass} = \frac{[(Hydrogen_{Bio-oil}) - ((Bio-oil\ Moisture) * 0.112)] * (Wet\ Bio-oil\ Yield)}{1 - (Biomass\ Moisture)}$$	Used to subtract hydrogen contributed from bio-oil water content. See definitions for Karl-Fischer and CHNSO.

$$\frac{g\ oxygen_{bio-oil\ organics}}{g\ dry\ biomass} = \frac{[(Oxygen_{Bio-oil}) - ((Bio-oil\ Moisture) * 0.888)] * (Wet\ Bio-oil\ Yield)}{1-(Biomass\ Moisture)}$$	Used to subtract oxygen contributed from bio-oil water content. See definitions for Karl-Fischer and CHNSO.

Conversion to Ash per Dry Biomass	
$$\frac{g\ ash_{biomass}}{g\ dry\ biomass} = \frac{(Ash_{Biomass})}{1-(Biomass\ Moisture})$$	Used to calculate the mass fraction of ash in dry biomass.
$$\frac{g\ ash_{char}}{g\ dry\ biomass} = \frac{(Ash_{Char}) * (Wet\ Char\ Yield)}{1-(Biomass\ Moisture)}$$	Used to calculate the mass fraction of ash that is distributed in the char.
$$\frac{g\ ash_{bio-oil}}{g\ dry\ biomass} = \frac{(Ash_{Bio-oil}) * (Wet\ Bio-Oil\ Yield)}{1-(Biomass\ Moisture)}$$	Used to calculate the mass fraction of ash that is distributed in the bio-oil.

$$C_{\left[\frac{C\ Fraction_{Product}}{12.011}\right]} H_{\left[\frac{H\ Fraction_{Product}}{1.008}\right]} O_{\left[\frac{O\ Fraction_{Product}}{15.999}\right]} N_{\left[\frac{N\ Fraction_{Product}}{14.007}\right]} S_{\left[\frac{S\ Fraction_{Product}}{32.065}\right]}$$
Note: This will be normalized to wet product when used directly from CHNSO data.